University of South Florida
Scholar Commons

Graduate Theses and Dissertations | Graduate School

2007

# Process optimization and consumable development for Chemical Mechanical Planarization (CMP) processes

Subrahmanya R. Mudhivarthi
*University of South Florida*

Follow this and additional works at: http://scholarcommons.usf.edu/etd

Part of the American Studies Commons

Scholar Commons Citation
Mudhivarthi, Subrahmanya R., "Process optimization and consumable development for Chemical Mechanical Planarization (CMP) processes" (2007). *Graduate Theses and Dissertations.*
http://scholarcommons.usf.edu/etd/2295

This Dissertation is brought to you for free and open access by the Graduate School at Scholar Commons. It has been accepted for inclusion in Graduate Theses and Dissertations by an authorized administrator of Scholar Commons. For more information, please contact scholarcommons@usf.edu.

www.manaraa.com

# Process Optimization and Consumable Development for Chemical Mechanical Planarization (CMP) Processes

by

Subrahmanya R. Mudhivarthi

A dissertation submitted in partial fulfillment
of the requirements for the degree of
Doctor of Philosophy
Department of Mechanical Engineering
College of Engineering
University of South Florida

Major Professor: Ashok Kumar, Ph.D.
Mohammad Rahman, Ph.D.
Daniel Hess, Ph.D.
Vinay Gupta, Ph.D.
Qiang Huang, Ph.D.
Pritish Mukherjee, Ph.D.

Date of Approval:
November 2, 2007

Keywords: temperature, tribology, slurry, electrochemistry, abrasive particles, scratches, pad conditioning, coefficient of friction

© Copyright 2007 , Subrahmanya R. Mudhivarthi

المنارة للاستشارات

www.manaraa.com

## DEDICATION

This dissertation is dedicated to Lord Sri Shirdi Saibaba, Guru Sri Ammula Sambasiva Rao and my Parents, Mr. Subba Rao and Mrs. Parvatha Vardhani

للاستشارات
www.manaraa.com

## ACKNOWLEDGMENTS

Firstly I would like to thank my advisor Prof. Ashok Kumar for giving me an opportunity to pursue research under his guidance and support throughout my doctoral studies. I would like to thank Dr. Vinay Gupta for his constant encouragement and guidance in several aspects of my dissertaion. I would like to Dr. Yaw Obeng for his invaluable help in sharing technical know how all along the course of my research during his tenure earlier at Texas Instruments, Inc and presently at NIST. I would like to acknowledge the help of Dr. Mohammed Rahman whose guidance in the areas of heat transfer and thermal modeling was crucial for the completion of this dissertation. I thank Dr. Daniel Hess, Dr. Qiang Huang and Dr. Pritish Mukherjee for being a part of my dissertation committee and for their valuable suggestions to improve this work. I would like to acknowledge the financial support for this research from NSF GOALI grant #DMII 0218141. I would like to thank Dr. Norm Gitis of CETR Inc. and Dr. Anthony Kim of Intel Corporation for providing me with Internship opportunities which helped me to gain industry experience and better perspective of my research.

I owe every achievement of my life to my parents and all the members of my family. I am extremely grateful for their continuous encouragement and love throughout my life. Special thanks go to all my friends for their love and affection which helped me survive the most difficult times of my life during this work. I would also like to thank the former and present colleagues of Dr. Ashok Kumar's research group who have been very helpful during the course of this work.

www.manaraa.com

## TABLE OF CONTENTS

LIST OF TABLES.....vi

LIST OF FIGURES..... vii

ABSTRACT..... xiii

CHAPTER 1: INTRODUCTION..... 1

1.1 Semiconductor manufacturing trends ..... 1

1.2 Need for planarization..... 4

1.3 Damascene architecture for MLM using metal CMP ..... 5

1.4 Other CMP applications..... 7

1.5 Outline of the thesis ..... 8

CHAPTER 2: BACKGROUND OF CMP PROCESS..... 11

2.1 CMP process ..... 11

2.1.1 Material removal mechanism..... 12

2.1.1.1 Mechanical aspects of CMP..... 13

2.1.1.2 Chemical aspects of CMP process ..... 14

2.1.2 Governing factors of CMP process..... 15

2.1.2.1 Process parameters..... 17

2.1.2.2 Consumable characteristics..... 17

2.2 Tribology of CMP process..... 19

2.2.1 Tribology during CMP process..... 19



المنارة للاستشارات

www.manaraa.com

2.2.2 Tribo-metrology of CMP ... 20
2.3 Thermal studies during CMP process ... 25
2.4 Challenges during CMP process ... 27
2.4.1 Non-planarity ... 28
2.4.2 Surface scratches ... 30
2.4.3 Delamination during cu/low-k CMP ... 31
2.5 Research objectives ... 32
2.5.1 Process optimization: effect of temperature ... 33
2.5.2 Thermal model ... 33
2.5.3 Low defect slurry development ... 34
CHAPTER 3: EFFECT OF TEMPERATURE ON COPPER CMP PROCESS ... 35
3.1 Introduction ... 35
3.2 Materials and techniques ... 36
3.2.1 CMP bench top tester ... 36
3.2.2 Nanoindentation ... 39
3.2.3 Electrochemistry and x-ray photoelectron spectroscopy ... 40
3.3 Results and discussion ... 42
3.3.1 Effect of temperature on CMP tribology ... 42
3.3.2 Effect of temperature on electrochemistry ... 44
3.3.3 Effect of temperature on surface chemical compounds ... 45
3.3.4 Effect of temperature on polished copper surface ... 51
3.3.4.1 Surface roughness ... 51
3.3.4.2 Non-uniformity ... 52



المنارة للاستشارات
www.manaraa.com

3.3.4.3 Mechanical properties ... 54

3.5 Conclusions ... 59

CHAPTER 4: EFFECT OF TEMPERATURE ON TRIBOLOGY DURING CMP ... 60

4.1 Introduction ... 60

4.1.1 Effect of polishing pad characteristics on CMP tribology ... 60

4.1.2 Effect of slurry characteristics on CMP tribology ... 61

4.1.3 Effect of wafer contour characteristics on CMP tribology ... 62

4.2 Experimental methods and materials ... 64

4.3 Results and discussion ... 66

4.3.1 Effect of process parameters and slurry temperature ... 66

4.3.2 Effect of oxidizer on CMP tribology ... 71

4.3.3 Effect of slurry chemistry on CMP tribology ... 73

4.3.4 Effect of temperature on pad conditioning process ... 76

4.3.4.1 Pad conditioning process ... 76

4.3.4.2 Pad conditioning experiments ... 78

4.3.4.3 Results and discussion ... 79

4.4 Summary ... 87

CHAPTER 5: THERMAL MODEL – STEADY STATE HEAT CONDUCTION ... 89

5.1 Introduction ... 89

5.2 Thermal model development ... 91

5.3 Temperature contours on wafer surface ... 94

5.4 Slurry flow rate experiments ... 97

5.4.1 Materials and techniques ... 100



المنارة للاستشارات
www.manaraa.com

5.4.2 Experimental procedures and samples ... 101

5.4.3 Results and discussion for flow rate experiments ... 104

5.5 Summary ... 108

CHAPTER 6: NOVEL SLURRY DEVELOPMENT TO REDUCE CMP DEFECTS ... 110

6.1 Introduction ... 110

6.2 Silica hybrid particles ... 112

6.2.1 Hybrid particle synthesis ... 112

6.2.2 Particle characterization ... 113

6.2.3 Post CMP surface characterization ... 113

6.2.4 Experimental conditions for silica hybrid particle slurry testing ... 114

6.2.5 Results and discussion – silica hybrid particles ... 115

6.3 Ceria composite particles ... 120

6.3.1 Composite particle synthesis ... 121

6.3.2 Experimental conditions for composite particle slurry testing ... 122

6.3.3 Results and discussion – composite particles ... 122

6.3.4 Post CMP surface characterization ... 126

6.4 Summary ... 129

CHAPTER 7: SUMMARY AND FUTURE WORK ... 130

7.1 Effect of temperature on CMP process ... 130

7.2 Effect of slurry flow rate on CMP process ... 132

7.3 Novel slurry development to reduce CMP defects ... 132

7.4 Future work ... 133



المنارة للاستشارات

www.manaraa.com

7.4.1 Thermal model ... 133

7.4.2 Electrochemistry and impedance spectroscopy ... 134

7.4.3 Low defect slurry development ... 134

REFERENCES ... 135

ABOUT THE AUTHOR ... 143



المنارة للاستشارات

www.manaraa.com

## LIST OF TABLES

Table 2.1 Factors that govern the output of CMP process………………………….16

Table 3.1 Mechanical properties of copper thin films before and after polishing........................................................................................ 58

Table 4.1 Process parameter conditions for the study of effect of temperature........ 64

Table 4.2 Process parameter conditions for slurry chemical experiments................ 65

Table 4.3 Corrosion potential and current density from polzarization experiments........................................................................................ ..75

Table 4.4 Consumables and process parameters in polishing experiments………... 78

Table 4.5 Process parameter set for patterned CMP experiments…………………..84

Table 5.1 Consumables and process parameters in slurry flow rate experiments........................................................................................ 102

Table 6.1 Details of the slurry samples made out of hybrid and silica particles........................................................................................ 115

Table 6.2 Experimental conditions for slurry testing............................................ 115

Table 6.3 Surface roughness of wafer after CMP using various abrasive particles ........................................................................................ 119

Table 6.4 Numerical values for coefficient of friction, surface roughness and removal rate ........................................................................................ 125



المنارة للاستشارات
www.manaraa.com

## LIST OF FIGURES

Figure 1.1 Increase in transistors per die with years of technology advancement....... 1

Figure 1.2 Schematic of a basic MOS capacitor with contact metallization................ 2

Figure 1.3 Cross section SEM images of the multilevel metallization stack............... 4

Figure 1.4 Roughness resulting out of metallization without CMP............................. 5

Figure 1.5 Conventional and damascene approaches to fabricate MLM structure. ...... 7

Figure 2.1 Schematic of CMP process as simulated on the bench top tester............. 12

Figure 2.2 A close up view of the polishing interface............................................... 14

Figure 2.3 Stribeck Curves generated using coefficient of friction data.................... 22

Figure 2.4 Pattern dependent non-planarity resulting due to CMP process............... 28

Figure 2.5 Post polish surface anomalies due to pattern deviations resulting in wafer surface non-planarity ................................................................... 29

Figure 2.6 Optical microscopy of scratches and pitting on wafer surface ................. 30

Figure 2.7 Delaminated interface during CMP process ............................................ 31

Figure 2.8 Delamination at via layer and a) copper dielectric cap interface b) the trench layer stress point ................................................................ 32

Figure 3.1 Bench top CMP tester that can simulate real time CMP process ............. 37

Figure 3.2 MIT 854 mask lay out with varying pattern line widths and densities..... 38

Figure 3.3 Nanoindenter XP used for the mechanical characterization of thin films ......................................................................................................... 39



www.manaraa.com

Figure 3.4 Schematic of the electrochemical cell for the polarization experiments. ........................................................................................ 41

Figure 3.5 Increase in removal rate and coefficient of friction with change in temperature ........................................................................................ 43

Figure3.6 Change in corrosion current density and corrosion potential with change in slurry temperature.................................................................. 44

Figure 3.7 Comparision of cu ($2P^{3/2}$) spectra for as-received and slurry treated samples at different temperatures ........................................................... 46

Figure 3.8 Increase in dissolution rate with an increase in slurry temperature. ......... 47

Figure 3.9 Curve fitted cu ($2P^{3/2}$) spectra for as-received and slurry treated samples at different temperatures ........................................................... 48

Figure 3.10 Comparison of oxygen (O1(s)) spectra for as-received and slurry treated samples at different temperatures ................................................ 49

Figure 3.11 Concentration ratio of oxide/metal on copper surface treated at different temperatures ..................................................................... 50

Figure 3.12 AFM images of the blanket copper sample after CMP at (a) 18.5$^{o}$C (b) 21.5$^{o}$C (c) 27$^{o}$C (d) 31$^{o}$C.................................................................... 51

Figure 3.13 (a) AFM images and schematic of the pattern describing the analysis for non-uniformity measurement (b) non-uniformity with-in die versus the temperature of polishing....................................... 51

Figure 3.14 Load versus displacement curve ............................................................ 55

Figure 3.15 Load versus displacement for polished copper samples at different slurry temperatures.......................................................................... 57



المنارة للاستشارات

www.manaraa.com

Figure 3.16 Hardness versus displacement for unpolished and polished copper samples........ 57

Figure 3.17 Modulus versus displacement for polished and unpolished copper samples........ 58

Figure 4.1 Effect of pressure and velocity on coefficient of friction during copper CMP ........ 67

Figure 4.2 COF versus p*v during copper CMP using commercial copper slurry ........ 69

Figure 4.3 COF versus p*v during glass polishing using de-ionized water.............. 69

Figure 4.4 Dependence of coefficient of friction with slurry temperature at different process conditions. ........ 70

Figure 4.5 Effect of % concentration of hydrogen peroxide on coefficient of friction at different p*v values........ 71

Figure 4.6 Effect of slurry chemistry on the coefficient of friction during CMP ...... 73

Figure 4.7 Potentiodynamic polarization scans for copper-slurry systems using various slurry chemistries. ........ 74

Figure 4.8 Effect of substrate (polished with 5 % $NH_4OH$ + 5 % $H_2O_2$ + 5 mM BTA) on COF during CMP........ 75

Figure 4.9 Pad surface temperature during conditioning at different temperatures........ 79

Figure 4.10 Pad coefficient of friction measured in-situ during pad conditioning at different temperatures ........ 80



المنارة للاستشارات

www.manaraa.com

Figure 4.11 Coefficient of friction curves during pad conditioning at different temperatures ........ 81
Figure 4.12 Carriage position during conditioning tests plotted versus time ........ 82
Figure 4.13 Pad wear rate versus temperature during conditioning. ........ 83
Figure 4.14 Removal Rate and Coefficient of friction measured during copper polishing after pad conditioning at different temperatures ........ 85
Figure 4.15 Dishing depth measured at 50 μm features for samples polished after pad conditioning at different temperatures ........ 86
Figure 5.1 Local polishing interface temperature for a silicon wafer at different flow rates of alumina as the slurry (b=0.075mm, Ω=100 rpm, q=455W/$m^2$) ........ 95
Figure 5.2 Polishing interface temperature for a silicon wafer at different coefficient of friction (q = 455 to 593W/$m^2$, b = 0.075mm, Ω = 100 rpm) ........ 95
Figure 5.3 Local polishing interface temperature for a silicon wafer at different (Ω) spinning rates and alumina as the slurry (Q=65 mL/min, b= 0.075mm, q =1364W/$m^2$) ........ 96
Figure 5.4 Cross sectional temperature within the wafer during CMP at a rotation speed of Ω=200 rpm (Q = 65 mL/min, b = 0.075 mm, q=1049W/$m^2$) ........ 97
Figure 5.5 Bench top CMP tester mod. CP-4 ........ 100
Figure 5.6 Coefficient of friction real-time graphs for three slurry flow rates ....... 103



المنارة للاستشارات
www.manaraa.com

Figure 5.7 Coefficient of friction and copper removal rate versus slurry flow rate ........ 104

Figure 5.8 Effects of slurry flow rate on (a) dishing, (b) erosion and (c) metal loss ........ 105

Figure 5.9 AFM images of dishing profiles of a 50 µm wafer feature at a) 20 ml/min b) 30 ml/min c) 45 ml/min d) 55 ml/min and e) 75 ml/min slurry flow rates........ 107

Figure 5.10 Measured temperature rise on the pad surface during copper polish at different slurry flow rates........ 108

Figure 6.1 TEM images of the Hybrid particles and silica particles........ 116

Figure 6.2 COF data measured in-situ during CMP of thermal oxide wafers using various kinds of abrasive particles. ........ 116

Figure 6.3 Removal rate measurements during CMP of thermal oxide wafers using various kinds of abrasive particles. ........ 117

Figure 6.4 FTIR spectroscopy on thermal oxide wafer before and after CMP. ........ 118

Figure 6.5 AFM images of the thermal oxide wafer surfaces polished with (a) 300 nm hybrid (b) 500 nm hybrid (c) 50 nm silica and (d) 150 nm silica ........ 119

Figure 6.6 TEM image of the composite particle - dark spots indicate $CeO_2$........ 123

Figure 6.7 DLS of microgels where the particle phase separates at nearly 32°C. ... 123

Figure 6.8 FTIR characterization of silica removal from the wafer surface. ........ 124



المنارة للاستشارات

www.manaraa.com

Figure 6.9 Optical microscopy (5X magnification) images of wafers polished with (a) ceria composite particles, (b) 0.5wt% $CeO_2$, (c) 0.25wt% $CeO_2$ nanoparticles ............................................................ 127

Figure 6.10 AFM images of wafers polished with (a) 0.25wt% $CeO_2$, (b) 0.5wt% $CeO_2$ nanoparticles and (c) composite particles ................. 128



المنارة للاستشارات
www.manaraa.com

# PROCESS OPTIMIZATION AND CONSUMABLE DEVELOPMENT FOR CHEMICAL MECHANICAL PLANARIZATION (CMP) PROCESS

Subrahmanya R. Mudhivarthi

## ABSTRACT

Chemical Mechanical Planarization (CMP) is one of the most critical processing steps that enables fabrication of multilevel interconnects. The success of CMP process is limited by the implementation of an optimized process and reduction of process generated defects along with post CMP surface characteristics such as dishing and erosion. This thesis investigates to identify various sources of defects and studies the effect of factors that can be used to optimize the process. The major contributions of this work are: Understanding the effect of temperature rise on surface tribology, electrochemistry and post CMP pattern effects during the CMP process; investigating the effect of pad conditioning temperature and slurry flow rate on tribology and post CMP characteristics; development of novel slurries using polymer hybrid particles and improvement in slurry metrology to reduce surface damage during CMP.

From the current research, it was shown that the effect of temperature on CMP tribology is predominantly affected by the polishing parameters and the polishing pad characteristics more than the chemical nature of the slurry. The effect of temperature is



للاستشارات المنارة

www.manaraa.com

minimal on the resulting surface roughness but the with-in die non-uniformity is significantly affected by the temperature at the interface. Secondly, in this research it was shown that the effectiveness and aggressiveness of the pad conditioning process is highly influenced by the conditioning temperature. This aspect can be utilized to optimize the parameters for the pad conditioning process. Further, post CMP characteristics such as dishing, erosion and metal loss on patterned samples were shown to decrease with increase in slurry flow rate.

This research then concentrates on the development of novel low defect slurry using polymer hybrid abrasive particles. Several varieties of surface functionalized polymer particles were employed to make oxide CMP slurries. These novel slurries proved to be potential candidates to reduce surface damage during CMP as they resulted in low coefficient of friction and much less surface scratches as compared to conventional abrasives. Thus, this research helps to reduce defects and non-planarity issues during CMP process thereby improving yield and reducing the cost of ownership.



المنارة للاستشارات
www.manaraa.com

## CHAPTER 1: INTRODUCTION

### 1.1 Semiconductor manufacturing trends

According to “Moore’s Law” [1] the demand in the semiconductor industry with respect to the number of transistors per chip will be doubled every 1.5 to 2 years. Another observation as per Moore is that the microprocessor performance in terms of millions of instructions per second (MIPS) will also double in the same 1.5 to 2 years [2]. Figure 1.1 below compares the trend in microprocessors according to the semiconductor industry performance in the past [3].

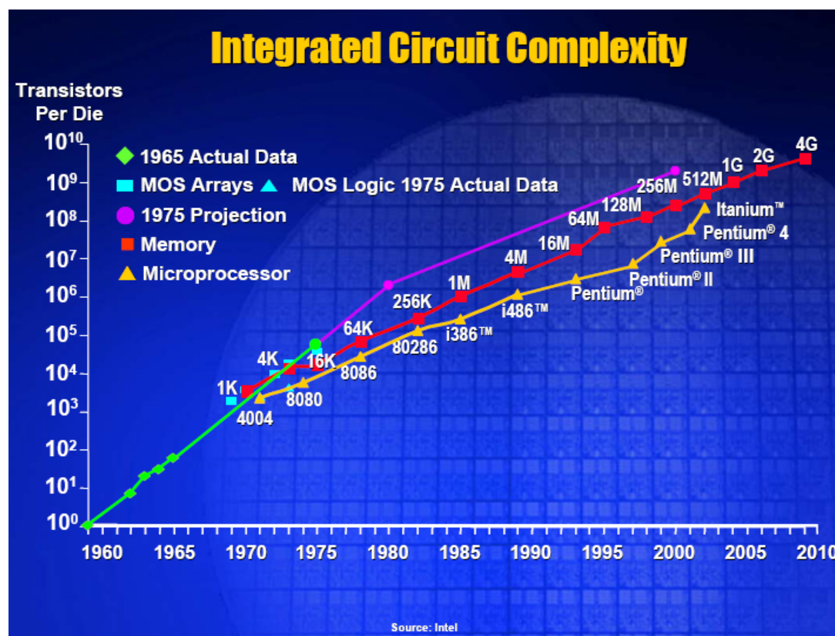


Figure 1.1 Increase in transistors per die with years of technology advancement [3]

Entire research in semiconductor device manufacturing is focused to implement such an increase in device density, which marks the advancement in technology to the



المنارة للاستشارات
www.manaraa.com

next level. A transistor, one of the millions of devices that constitute an Integrated Chip (IC), is typically a MOSFET (metal-oxide-semiconductor Field Effect Transistor), which consists of a source, gate and a drain. These devices can be made to operate faster by reducing the size of the devices and to have the devices packed densely onto a given chip area thereby decreasing the distance the carriers have to travel [4, 5]. The minimum feature size decreases with the size of the device itself and this also translates into reduction in intermediate pitch or spacing between the features. Figure 1.2 below shows the schematic of a MOS capacitor with first-level of metallization.

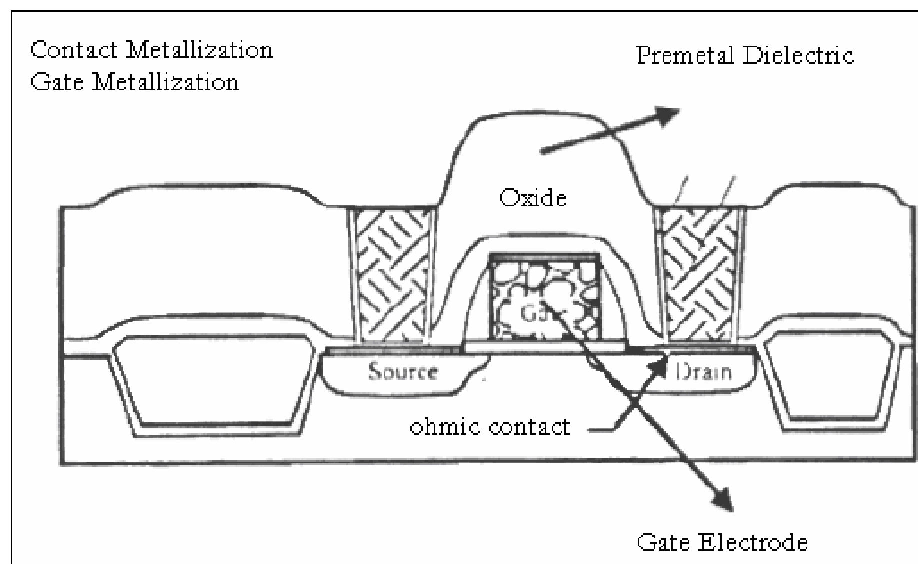


Figure 1.2 Schematic of a basic MOS capacitor with contact metallization [4, 5].

Shrinking of device dimensions is crucial for the IC performance because the transit time ($T_r$) of the electrons with a velocity (V) in a device is directly proportional to the length of the gate ($L_g$) (transit time is the ratio of gate length to velocity of the electron), and the transit times in turn dictate the frequency of operation [5, 6]. Thus, we can understand the efforts of the semiconductor industry to reduce the gate length of the devices. As the



www.manaraa.com

devices become smaller and smaller, their fabrication (otherwise called semiconductor device processing) faces several design, manufacturing and process control challenges. Once the devices are fabricated on the silicon substrate, they need to be connected to form a device network and at the same time need to be connected to the outside world using interconnect materials. The metallization connecting the devices at the silicon level is called contact or first-level metallization and the metallization that connects the devices to the outer world is the second-level metallization [4, 5]. The materials required for metallization need to be selected based on their electrical, chemical and mechanical characteristics since the properties of these materials dictate the frequency of flow of charge. The time delay ($T_{RC}$) in seconds or the frequency of charge flow associated with the interconnect materials is computed as a product of resistance (R) of the metal lines and the capacitance (C) of the insulating interconnects. Substituting for resistance in terms of wiring dimensions and material properties, RC time delay can be written as [7]:

$$T_{RC} = R * C = 2\rho\kappa\varepsilon_0 L^2 \left[ \frac{4}{P^2} + \frac{1}{T^2} \right]$$

where ρ is the resistivity of the metallic interconnect, k is the dielectric constant of the insulator, $\varepsilon_0$ is the permittivity of vacuum, L is the length of the interconnect line, P is the pitch between interconnect lines, and T is the thickness of the line [7]. The RC delay has to be reduced in order to achieve better performance of the Integrated Chip. To reduce RC delay from the dimension point of view, the length of interconnect wiring needs to be reduced, which explains the trend of increasing the number of metallization layers. As per the International Technology Roadmap for Semiconductors (ITRS) the minimum and maximum number of metallization layers in 2007 and beyond need to be 13 and 17



المنارة للاستشارات
www.manaraa.com

respectively [2]. Figures 1.3 below shows the cross section SEM micrograph of multilevel metallization scheme, which uses 7 layers of metallization.

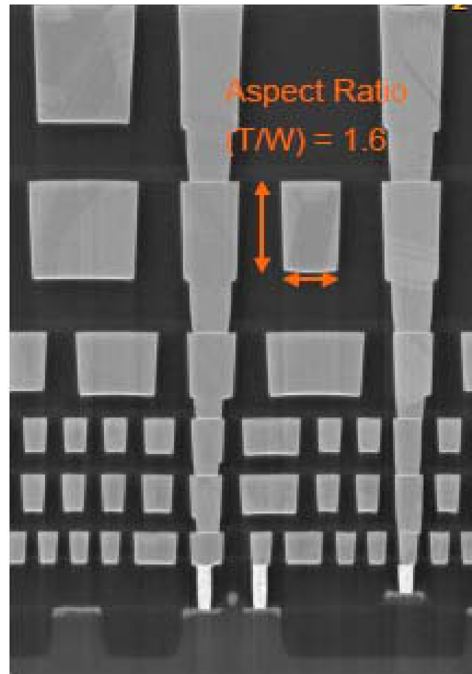


Figure 1.3 Cross section SEM images of the multilevel metallization stack [6]

## 1.2 Need for planarization

In order to successfully manufacture such an MLM structure as shown in the figures above, the topmost layer of the previous metallization level has to be optically flat with minimal surface roughness. This is because if there exists any residual roughness at the previous layer, it will get compounded as the layers increase and soon after a couple of metallization layers, the roughness will be so significantly high that lithography (patterning) experiences issues with the depth of focus and any further processing is not possible. It has been proven [7, 8] that Chemical Mechanical Planarization (CMP) process is the method of choice among other planarization techniques to achieve local



المنارة للاستشارات
www.manaraa.com

and global planarization across the wafer surface. The figure 1.4 below shows an SEM image of an interconnect structure without planarization [9].

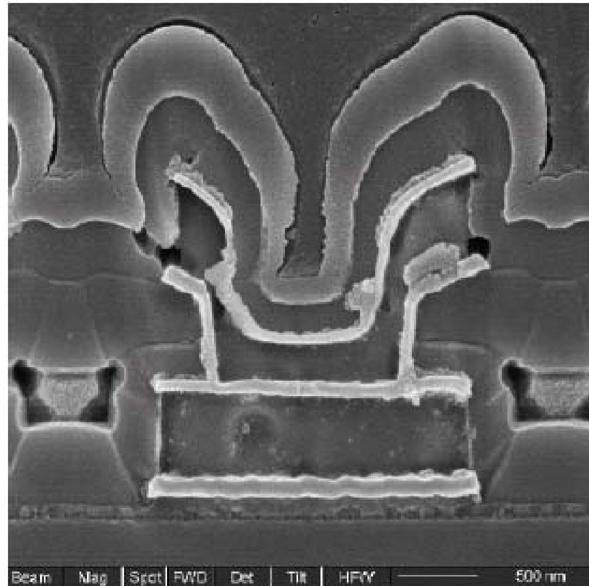


Figure 1.4 Roughness resulting out of metallization without CMP [9]

It can be seen from the above figure that it is not possible to proceed with further processing steps as depth of focus issues come up during photolithography and several other subsequent processing challenges, such as voids with in interconnect layers due to compounded roughness, occur. Thus, CMP process becomes a crucial processing step in device fabrication in order to achieve successful fabrication of MLM structure.

## 1.3 Damascene architecture for MLM using metal CMP

Besides increasing the number of metallization layers, reducing the resistance of the metal interconnects and the capacitance of the dielectric layer reduces the RC delay. Hence, it can be said that choosing the interconnect materials with optimum electrical



المنارة للاستشارات
www.manaraa.com

properties would reduce RC time delay. The desired optimum properties of the materials that can find application as interconnect materials are listed below [5].

- Low Resistivity
- Easy to form
- Easy to etch for pattern generations
- Should be stable in oxidizing ambients, oxidizeable
- Mechanical Stability, good adherence, low stress
- Surface smoothness
- Stability throughout processing, including high temperature sinter, dry or wet oxidation, gettering, phosphorous glass (or any other material) passivation, metallization.
- No reaction with final metal, aluminum/copper
- Should not contaminate devices, wafers, or working apparatus.
- Good device characteristics and lifetimes.
- For window contacts – low contact resistance, minimal junction penetration, low electromigration.

Following the above properties as guide-lines, copper has been chosen to replace aluminum as the material for metallic interconnects to reduce RC delay [10, 11]. However, choosing electrically superior copper over aluminum comes with an inherent drawback that an etchant to precisely pattern copper is not available and an alternate or a 'damascene' approach to make the metallization layers was eventually developed [7].



المنارة للاستشارات
www.manaraa.com

Figure 1.5 below compares the processing step variation between conventional and damascene approaches.

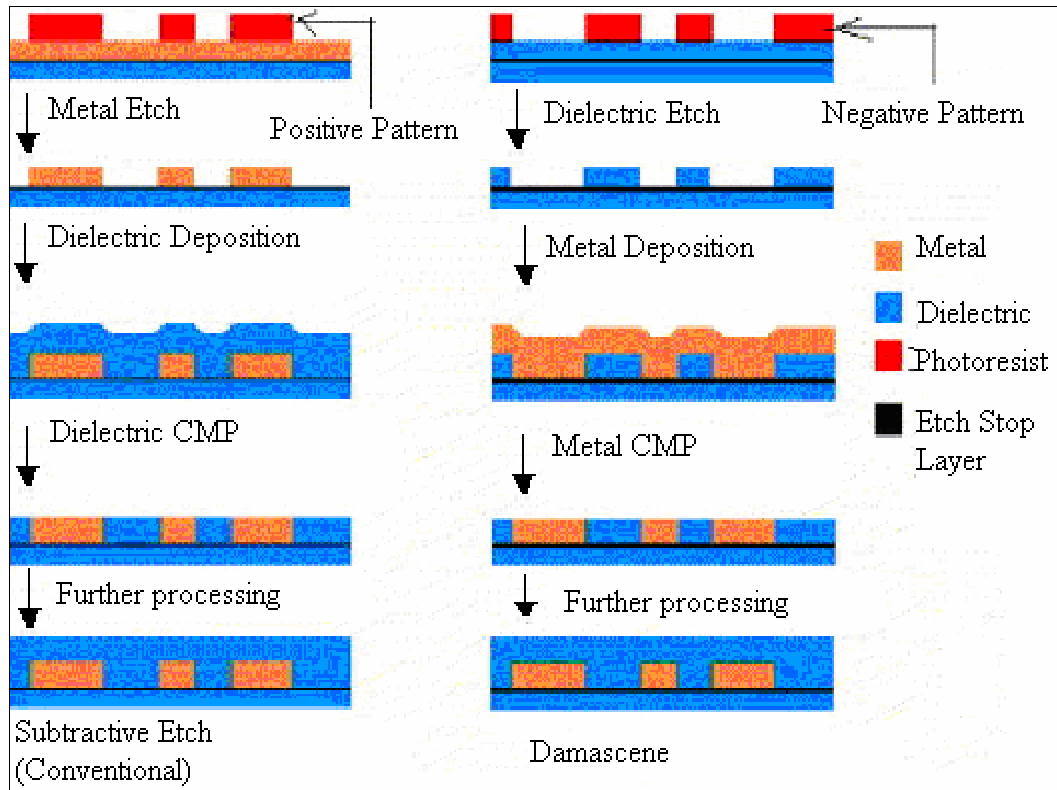


Figure 1.5 Conventional and damascene approaches to fabricate MLM structure [7].

In the damascene approach, the dielectric is patterned instead of the metal layer and then copper is deposited onto the patterned dielectric material. The excess copper or the copper over burden over the patterned dielectric is removed using CMP process.

## 1.4 Other CMP applications

Besides traditional CMP of dielectrics and copper or tungsten (metal) CMP, there are many other avenues and applications for CMP process. CMP finds its application not



www.manaraa.com

only in CMOS applications but also in Micro Electro Mechanical Systems (MEMS) applications [12]. CMP is also being developed for Integrated Optical elements, phase change memory materials, magnetic materials, and advanced substrates [9, 13]. Typical MEMS devices that involve CMP in their fabrication are accelerometers, torque sensors, and microfluidic processors; and typical materials involved are oxides, polymers, doped oxides, oxynitrides, polysilicon and certain metals for specific reflective surface applications. Of course, significant process understanding still needs to be developed for these new processes, which have many challenges like process stability, enhanced removal rates on the order of microns as compared to the nanometers in conventional CMP to achieve acceptable throughput, and novel chemistries for several different layers that do not usually find place in CMOS fabrication.

### 1.5 Outline of the thesis

This dissertation is broadly divided into two parts, the first half dealing with the effect of temperature and slurry flow rate on CMP, pad conditioning, and post CMP results. The second half deals with the development of novel soft abrasive particles, which offer a superior surface finish by reducing surface damage and scratches as compared to conventional abrasive particles.

Chapter 2 explains the basic mechanism of CMP process in both mechanical and chemical aspects and presents in detail the surface tribology during CMP and the various factors affecting the CMP tribology. Further, the chapter provides background into the thermal aspects of CMP, thermal modeling efforts in the recent past, and the



المنارة للاستشارات
www.manaraa.com

challenges involved with the process. Objectives of the present research are then listed towards the end of the chapter.

Chapter 3 presents the experimental details and analytical techniques to study the effect of temperature on CMP process with respect to the coefficient of friction, removal rate, post CMP surface quality, and non-uniformity. Further in the chapter, results from electrochemical and surface chemical studies are presented and discussed. Chapter 4 provides details about the tribological studies with varying temperature and the effect of process parameters on the role of temperature on tribology. It also presents the research on the effect of temperature on pad conditioning process and the subsequent CMP process on patterned samples. This part of the research is particularly important for the process optimization of CMP.

Further, Chapter 5 elucidates the development of thermal model for estimation of temperature on the surface of the wafer as a function of radius and thickness. It also presents the slurry flow effects on CMP. In this research a viable solution to reduce post CMP surface anomalies such as dishing, erosion, and metal loss has been proposed. It was shown that usage of higher flow rate is highly beneficial for CMP. However, it is suggested that cost of production should be taken into consideration in relation to the defect severity. Chapter 6 presents the development of slurries containing hybrid abrasive particles, which are softer as compared to the conventional particles, to reduce scratching and prevent severe surface damage during CMP. Polymer abrasives with silica and silica-ceria composite as the surface oxide are developed and used for oxide CMP, and



المنارة للاستشارات
www.manaraa.com

resulting friction and surface finish are compared to the polishing done by conventional particles. This provides another solution to reduce defects during CMP, which is the main goal of this dissertation. Finally, the major findings of this dissertation are summarized in chapter 7 of this report.



المنارة للاستشارات
www.manaraa.com

# CHAPTER 2: BACKGROUND OF CMP PROCESS

## 2.1 CMP process

CMP is the process of reducing the non-planarity both with in the die and as well as across the wafer surface [7]. In a CMP process, the wafer being planarized is pressed (facing down) onto a polymer polishing pad and is abraded in the presence of slurry, which contains active chemicals and abrasive particles. Thus, CMP can be described as a process which uses the combination of mechanical energy from the pad and abrasives and chemical energy from the slurry chemicals to polish and remove material from the wafer surface. The schematic of the CMP process that is simulated in this research on a bench top tester is presented in the figure 2.1.

The application of CMP in electronic device fabrication is significant in both memory and logic (Microprocessor) device fabrication [2]. It is being further introduced into many other modern applications such as MEMS [9] and other electronic device fabrication. As the device and interconnect wiring dimensions continuously shrink with the technology advancement in device manufacturing, the output specifications of the CMP process have become and are becoming much more stringent. For example, the allowable dish depth has come down to less than 15 nm and many such process specifications change as the industry progresses into integrating much weaker low K dielectric materials with copper [2, 14].



المنارة للاستشارات
www.manaraa.com

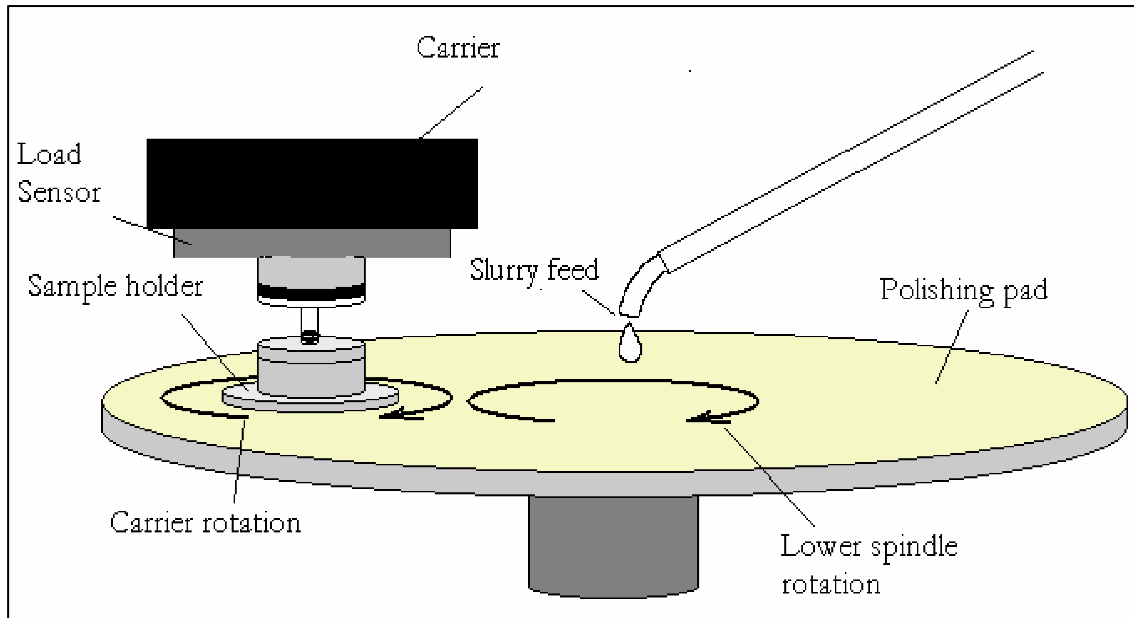


Figure 2.1 Schematic of CMP process as simulated on the bench top tester

The process induced defects such as micro-scratches and particle residue significantly hamper the device yield. These defects along with post CMP characteristics such as dishing and erosion need to be minimized if a successful implementation of the process is to be achieved. Yield and throughput of the polishing process is highly dependent on the process parameters and consumable characteristics.

### 2.1.1 Material removal mechanism

As mentioned above, CMP process involves both chemical and mechanical components acting in synergy to bring about removal of overburden and at the same time achieve planarization. In this context, it is important to understand the mechanism of material removal during CMP. The following sections provide an insight into the



المنارة للاستشارات
www.manaraa.com

mechanical and chemical aspects of CMP, which are responsible for effective material removal from the wafer surface.

#### 2.1.1.1 Mechanical aspects of CMP

CMP is inherently an abrasion process with two body and three body abrasion occurring simultaneously at the interface. Two body abrasion occurs when the abrasive particles from the slurry interact with the wafer surface, and also when the pad surface asperities slide against the wafer surface. As the roughness of the pad is in the order of microns and the size of the abrasive particles is in the order of nanometers, a significant amount of two body abrasion takes place across the wafer involving the interaction between only the wafer and pad surface asperities. However, the contact is more complicated at times when the wafer, pad, and abrasive surfaces come in contact, constituting a three-body abrasion. In this case, the contact involves abrasive particles that come in contact with the wafer, which are held in place under a given pressure by the pad asperities. As the abrasive particles are dragged across the wafer surface under pressure applied using the polishing pad, ploughing and cutting processes occur simultaneously, resulting in the material removal from the wafer surface. Figure 2.2 below shows the close up view of the interface [7], which presents the details of various mechanisms at the interface.



المنارة للاستشارات
www.manaraa.com

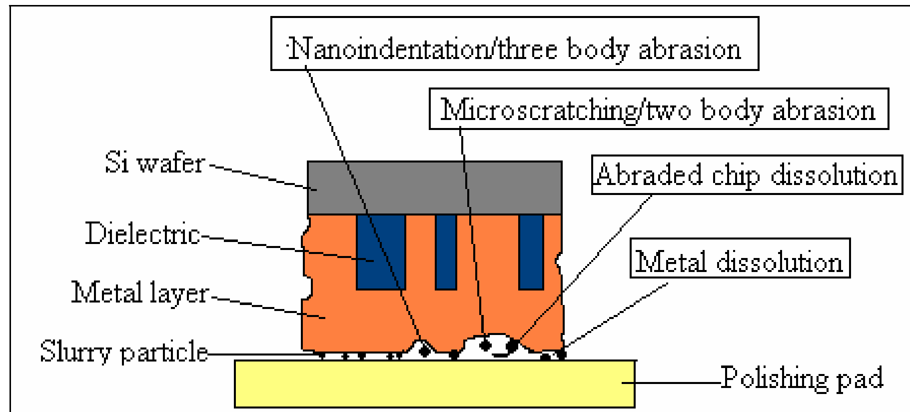


Figure 2.2 A close up view of the polishing interface [7].

The lubrication at the polishing interface is provided by the fluid (water based chemicals) in the slurry. The type of contact between the pad-slurry-wafer and the intensity of abrasion during polishing is dictated by the thickness of the fluid film at the interface. Thus, the dynamics at the contact involves several mechanical interactions.

#### 2.1.1.2 Chemical aspects of CMP process

CMP process, as the name suggests, has an active chemical component along with the mechanical component, where the wafer surface is modified by the chemicals in the slurry before getting abraded. Another important feature of the slurry is to dissolve the abraded material, thereby avoiding re-deposition of the removed material onto the wafer surface. In case of oxide CMP, the oxide surface is first hydrolyzed by various chemicals of the slurry and the abrasive particles abrade the surface. Besides providing the mechanical component, the abrasive particles while in contact with the wafer bond themselves chemically and remove the material as they separate from the surface [7, 16]. Thus, along with the chemicals in the slurry, the chemical nature of the abrasive particles



المنارة للاستشارات
www.manaraa.com

also has a significant role to play in oxide CMP process. In case of copper CMP, the slurries can be both acidic and alkaline in nature [15-20].

The metallic copper surface is modified by the active ingredients and the pH of the slurry, following the above mentioned reactions, to form dissolvable copper oxides and hydroxides [8, 15, 21]. The rate of oxidation of copper depends on the particular formulation of slurry and the concentration of oxidizers and complexing agents of the slurry. The formed surface copper compounds will then be abraded off the surface by the abrasive particles and the pad asperities. In the case of copper CMP, abrasive particles only provide mechanical action and the chemical nature of the particles does not play any role. The abraded copper compounds are then dissolved into the slurry and are carried away along with the dispensed slurry. This dissolution is very crucial to the removal process, as it avoids the re-deposition of the material onto the wafer surface. Thus, the material removal rate depends equally on the mechanical as well as chemical aspects, justifying the name given to the process as chemical mechanical planarization.

### 2.1.2 Governing factors of CMP process

CMP is a process involving many disciplines with several factors that affect the final output. These governing factors can be categorized broadly into a) process parameters and b) consumable characteristics. Table 2.1 below gives an overall list of aspects that govern the output of CMP process.



المنارة للاستشارات
www.manaraa.com

Table 2.1 Factors that govern the output of CMP process

| Process parameters | Consumable characteristics |
|---|---|
| 1. Load (psi)<br>2. Angular velocity (RPM) of polishing pad and wafer carrier<br>3. Slurry flow rate (ml/min) | 1. Wafer :<br>• Contour and size<br>• Pattern density<br>• Pattern dimensions<br>• Characteristics of inter-level dielectric layer<br>• Chemical compatibility of underlying layers to the slurry components<br>2. Pad:<br>• Bulk characteristics<br>• Surface characteristics<br>• Groove design<br>• Groove dimensions<br>3. Slurry<br>• pH of the slurry<br>• Particle size distribution<br>• Zeta potential<br>• Additives<br>• Oxidizer and its concentration |



المنارة للاستشارات
www.manaraa.com

#### 2.1.2.1 Process parameters

Pressure and relative velocity at the polishing interface are the most crucial process input variables which impact the CMP performance. As per Preston's Law [22] it can be easily seen that the pressure and the velocity during polishing dictate the removal rate during the process. Besides removal rate, pressure and velocity also determine the friction characteristics at the interface and also determine the regime of lubrication as per Stribeck Curve [23]. High pressures and velocities result in high shear forces applied on the wafer surface, which might induce delamination at the poorly adhering interfaces mainly involving dielectric materials [24]. Besides pressure and velocity, many other factors such as slurry flow rate and pad surface temperature significantly affect the removal rate and also have a pronounced effect on the overall process output.

#### 2.1.2.2 Consumable characteristics

The characteristics of the wafer being polished have a significant effect on CMP process. The size and contour of the wafer determines the contact area and the polishing uniformity across the wafer surface during polishing. The wafer contour also changes the interaction between the pad and the wafer at different pressure settings, resulting in a change in contact dynamics at the interface [25]. Looking at a die level, the pattern density and dimensions along with the layout of pattern in a die affects the uniformity with in the die, resulting in change in uniformity of polish and the generation of post CMP characteristics such as dishing and erosion [26, 27].



المنارة للاستشارات
www.manaraa.com

The polishing pad is another consumable of CMP, which provides a major part of the mechanical component to the polishing. Typically, a polishing pad is constituted of two sections: the top section of the polishing pad, which consists of grooves and surface asperities; and the bottom, or bulk portion of the pad, which supports the upper portion and helps in achieving polishing uniformity [8, 28]. These two sections of the pad can either be engineered separately, which is put together at the point of use or the bulk portion of the pad can be surface treated and grooved to suit a specific application of either metal or dielectric CMP. Another important characteristic of the polishing pad is the ability of the pad to transport slurry efficiently to the polishing interface [29]. The dimensions, such as width and depth of the pad groove, along with the groove pattern are also important to have a uniform slurry distribution on the pad surface. Along with the pad grooves, pad surface asperities or the texture are very crucial for CMP performance [30, 31]. A primary function of the pad asperities is to prevent the abrasive particles of the slurry from sliding off the pad due to centrifugal forces of rotation and to have an efficient pad-wafer contact [32]. The abrasive particles, which are held at the contact by the pad asperities, are the only particles available to provide active mechanical component during CMP.

Slurry constituted of oxidizers, complexing agents, abrasive particles, and dispersants is one of the major factors that affect CMP. Slurry plays a critical role in modifying the surface being planarized, abrading the modified surface, and also dissolving the abraded debris. The concentrations of its various constituents significantly influence the output of CMP. The characteristics of the abrasive particles, such as size



المنارة للاستشارات
www.manaraa.com

distribution, zeta potential, uniform dispersion, etc., need to be maintained and monitored continuously to avoid formation of agglomerated particles or chipped of particles with sharp edges. Failing to do so will result in the wafer surface being severely scratched, hampering the device yield and impacting the overall production line. Slurry also provides the chemical selectivity for different underlying layers (barrier and dielectric layers in case of Copper CMP) that are not supposed to be polished using suitable additives and pH conditions. Manufacturing the slurry so that it does not damage the underlying barrier and dielectric layers is critical to avoid yield and reliability issues. Successful implementation of CMP process significantly depends on optimizing the above mentioned factors for each process. Optimizing the process factors, selecting appropriate consumables, and ensuring consistent process performance are governed in turn by the cost involved, risk involved, and time lines for each technology cycle.

## 2.2 Tribology of CMP process

### 2.2.1 Tribology during CMP process

Tribology is the science dealing with friction, wear and lubrication during sliding of two surfaces. It is a Greek term which literally translates to "science of rubbing" in English. Studying various aspects of tribology helps in understanding various process mechanisms that happen at the rubbing interface. As mentioned previously in this chapter, CMP is an abrasion process which involves rubbing of wafer and pad surfaces in presence of chemical slurry and abrasive particles. Like many other industry specifications, during CMP lower friction and efficient lubrications are desirable. But at



المنارة للاستشارات
www.manaraa.com

the same time CMP process is aimed at obtaining higher wear (even though of the order of atomic layers) of the polished material to achieve considerable throughput.

The performance and the output of the CMP process depend on the nature of polishing, which in turn depends on the contact area and the frictional forces associated with it. Thus studying the frictional characteristics during CMP proves significant to understand and improve the process. There are numerous theoretical and analytical models that explain the frictional characteristics during a lubricating sliding contact [33, 34]. The interface of CMP is much more complicated as compared to conventional interfaces considered in these models and involves several additional factors such as the abrasive particles, chemical component of the slurry etc. Thus, these models find minimal application with respect to the CMP process. A better way of understanding the interface dynamics and mechanisms with respect to tribology is to study the frictional characteristics *in-situ* or during the process. The parameters that could prove useful to study the tribology at interface are coefficient of friction and acoustic emission signal [35].

### 2.2.2 Tribo-metrology of CMP

The above mentioned coefficient of friction and acoustic emission signal (AE) are crucial to characterize the friction characteristics of a system consisting of sliding surfaces irrespective of the nature of contact or the lubricating medium. These parameters along with other parameters such as wear rate of wafer surface and pad wear are termed as 'Tribo-metrology' [35].



المنارة للاستشارات
www.manaraa.com

Coefficient of friction, as defined by Leonardo Da Vinci in $14^{th}$ century [34], is the ratio of tangential force of friction (resisting motion) to the normal load. Such a coefficient representing the friction at the polishing interface reflects the nature of interaction of the wafer-abrasive-pad materials. Coefficient of friction is influenced by several factors including the material properties of the interacting surfaces. The shear force at the interface and the friction coefficient depend on many aspects, such as the pad's mechanical properties, the kinematic parameters of the polishing process, slurry viscosity, and chemical properties. A detailed description about the effect of various factors on coefficient of friction is presented in the imminent sections and chapters of this dissertation. Taking the advantage of this aspect, changes in the wafer surface can be analyzed by monitoring the coefficient of friction data either *in-situ* or *ex-situ*.

Another parameter that can be monitored during the CMP process is the acoustic emission or the AE signal. The AE signal is an estimate of the acoustic energy dissipated at the interface due to mechanical interactions of sliding surfaces and abrasive particles at the interface. Higher AE signal indicates intense mechanical interactions or aggressive abrasion at the interface and lower signal indicates a smooth, mild polishing resulting in lower shear forces and less damaged wafer surface. A noisy signal could indicate the presence of agglomerates or occurance of delamination at the interface [35]. The wafer surface wear rate, pad conditioner friction and pad wear are the other parameters that need to be monitored to effectively conduct CMP performance. The wear rate of the surface being polished is aimed to be considerably high to maintain process throughput whereas minimum possible pad wear is desired. Pad surface needs to be conditioned in



المنارة للاستشارات
www.manaraa.com

order to maintain the surface roughness and to facilitate uniform slurry flow on the pad. Conditioning process helps to achieve minimal wafer to wafer non-uniformity and improves process optimization. Pad conditioner coefficient of friction during such a conditioning process should be monitored, which upon stabilizing indicates the end point of conditioning process [35].

The following sections in the context of tribo-metrology, the original contribution of this author, were recently published in the tribometrology chapter of text book called 'Microelectronic applications of Chemical Mechanical Planarization' edited by Dr. Yuzhuo Li [35]. Coefficient of friction used to generate Stribeck curves [23] offers an efficient means to monitor a tribological process. Stribeck curves as shown in Figure 2.3 are generated using coefficient of friction data and the Sommerfeld number. These are greatly useful in determining the lubrication regime at the polishing interface.

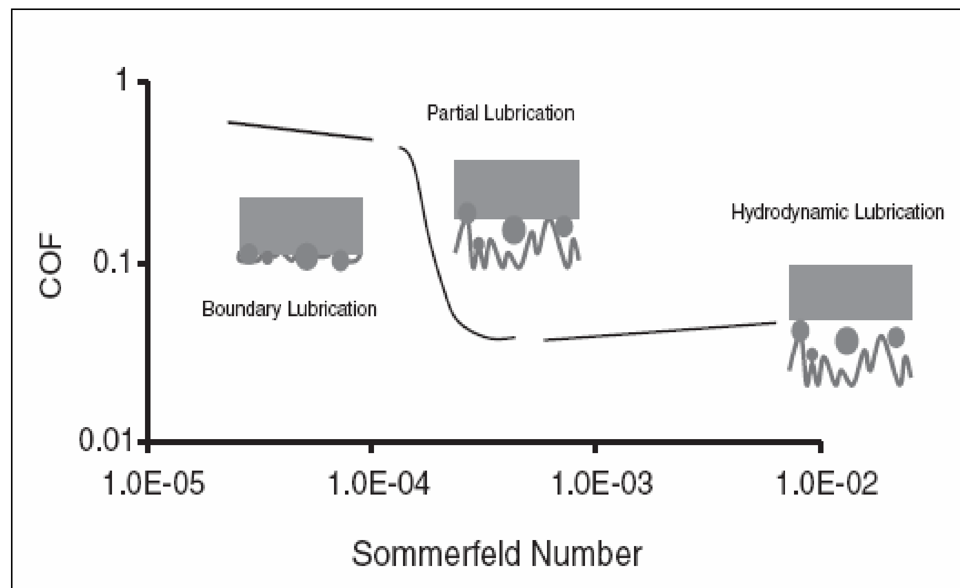


Figure 2.3 Stribeck curves generated using coefficient of friction data [36]



المنارة للاستشارات
www.manaraa.com

The Sommerfeld number is defined as $S_f = \frac{\mu U}{p\delta_{eff}}$, where $\mu$ is the viscosity of the lubricant, U is the relative velocity, p is the applied pressure, and $\delta$ eff is the effective lubricant film thickness. Applying the above formula to the CMP environment, $\mu$, (viscosity of the slurry) can be easily found, since pressure and velocity are known as they are the input process parameters. However, the fluid film thickness is the toughest to estimate. In recent research [37] the fluid film thickness was approximately estimated using the pad surface roughness. To account for the deviations of the slurry film thickness on different grooved pads, a dimensionless factor has also been suggested.

There are three main regimes of lubrication, namely a) boundary lubrication b) mixed lubrication, and c) hydrodynamic lubrication at a lubricated frictional interface; even though there are other minor regimes called hydrostatic and elastohydrodynamic lubrication regimes [33, 34]. During CMP, there exists solid-solid contact between the wafer and pad during boundary lubrication, where the removal process is dominated by surface abrasion. In this regime, polishing results in severe surface damage due to aggressive abrasion by slurry particles and the polishing pad. Also, the thermal energy dissipated in this case must be very high, resulting in a non uniform and inconsistent material removal rate. In the mixed lubrication regime there is a thin film of slurry which supports the applied pressure to an extent, and thus prevents aggressive abrasion. It is beneficial to ensure that the CMP process is conducted in this lubrication regime, as it would reduce the surface damage to a great extent. Hydrodynamic lubrication regime or hydroplaning mode of polishing results when the applied pressure is totally supported by



www.manaraa.com

the slurry film present at the interface. This may result in a very low coefficient of friction, but at the same time dramatically reduces the removal rate as there is practically no abrasion. Knowledge of the lubrication regime of polishing is thus highly beneficial to understand the polishing process in greater detail.

As mentioned earlier, the coefficient of friction (COF) and contact acoustic emission (AE) can be constantly monitored and recorded to determine the end point of the polishing process [7]. A change in coefficient of friction and AE signals can be observed as soon as the end point of the process occurs. This happens as the underlying thin film constituting the new polishing interface has different properties compared to the film that has been removed. Either *in-situ* or post CMP analysis of the friction coefficient data allows for calculations of the time to remove a particular layer, and thus the rate of material removal. These calculations can take place either during the process or after the entire layer has been removed. Such monitoring of coefficient of friction prevents over-polishing, thus avoiding defects such as dishing and erosion. Das *et al.,* [38] studied the coefficient of friction signal in order to determine the end-point detection more effectively. The raw COF data was analyzed and the noise levels were filtered out to more precisely determine the end point of the process. Variance sequential probability ratio test (SPRT) method was adopted to analyze and filter the raw data. Coefficient of friction signal can thus be processed and analyzed to detect the end point more effectively. Not only the removal rate or the end point detection of the process but also the uniformity of polish can be estimated from the coefficient of friction data. This can be done by monitoring the time taken for the coefficient of friction signal to change from



المنارة للاستشارات
www.manaraa.com

one level to another as the end point of the process is reached. This time for the change of signal can be termed as the transition time during end point. The longer the transition time, higher is the non-uniformity [39]. Similar analysis on AE signal can also be conducted to additionally determine process induced defects such as delamination and generation of micro-scratches.

From the above discussions it can be seen that tribology during CMP process significantly influences the mechanism of material removal and surface polishing. Moreover, the coefficient of friction and acoustic emission signal can provide valuable information regarding the nature of tribological interaction at the interface. In this research, investigation of coefficient of friction and factors influencing friction are studied in great detail to develop fundamental understanding of the CMP process mechanism and governing factors. Such an understanding is aimed at improving the process control and optimization

## 2.3 Thermal studies during CMP process

The thermal aspect of CMP, even though a significant factor affecting the process output as noted above, has not been researched as extensively as parameters like pressure, velocity, slurry flow rate, and other chemical aspects. Heat dissipation due to friction can result in a temperature rise at the interface and a rise of about 10 Kelvin at the polishing interface is high enough to double the removal rate during copper polishing [40]. Also, it has been noted that a change of 1 Kelvin can affect the process removal rate during polishing by 7 % [40]. This is attributed to the low activation energy of the copper



المنارة للاستشارات
www.manaraa.com

oxidation reaction in the slurry [41, 42]. Fractions of heat generated at the interface are either conducted to the wafer and pad, or convected away by the slurry which acts as a coolant at the interface.

Research work on temperature rise on the surface of the polishing pad during interlayer dielectric and metal polishing, removal rate dependence on temperature and its modeling, effect of slurry flow rate on pad temperature rise etc., has been carried out moderately in the recent past to understand the role of temperature on CMP performance [40, 43-45]. Borucki et al., [43, 44] have developed a thermal model for ILD polishing and then modified it slightly to get a model for copper (Metal) CMP which was validated by comparing with temperature measurements on the pad during metal CMP. They developed a theoretical understanding of the thermal aspects in their research and predicted temperature on the pad for the initial stages (first 60 sec) of polishing by evaluating the model based on transient heat transfer mechanism.

White et al., [45] have modeled dynamic thermal behavior which explains the energy exchange between the pad and slurry. Heat accumulation in the pad and the convection of heat to the slurry were explained in their research work. Also, a transient thermal model was proposed to explain the initial transient thermal behavior observed during CMP. Some other research works on thermal aspects such as using temperature change as end-point detection, experimental work involving the temperature rise on polishing pad [46-48], can also be found in the literature. These research works had modeling and experimental evidence of temperature rise only on the polishing pad. The



المنارة للاستشارات
www.manaraa.com

first attempt to measure the temperature on the silicon wafer was done by Sampurno et al. [49]. A direct temperature measurement set up was developed wherein a novel wafer carrier was designed such that the temperature on the back side of the wafer was measurable using a thermal imaging IR camera.

However, in all these research works the reported temperature rise is either the average temperature on the pad surface, a predicted average temperature on the wafer surface, or temperature rise at three isolated locations on the wafer. These works report the overall temperature rise but do not provide the information about the radial temperature distribution on the wafer surface. An analysis of the temperature distribution on the wafer surface after the polishing process reaches a steady state has not been researched to date, which forms the basis of another research objective of this research work. The temperature profile on the wafer surface as a function of radius and thickness will be developed for various input process variables. Since the material removal rate during copper CMP is highly sensitive to temperature, understanding the temperature profile will help in reducing the with-in-wafer non-uniformity, and thus improves yield by minimizing the number of faulty dies.

### 2.4 Challenges during CMP process

Besides being the unanimous choice for local and global planarization, CMP process has inherent challenges, particularly with the wide variety of materials being incorporated for Copper/Low K integration. Some of the critical challenges that are dealt with in this research are a) With in Die Non-Uniformity (WIDNU), b) dishing and



المنارة للاستشارات
www.manaraa.com

erosion due to non-uniformity in polish c) micro scratches on the surface and d) high friction resulting in delamination.

### 2.4.1 Non-planarity

Post polish non-planarity could be a result of several factors such as a) ,on-selective slurry, b) pad asperities reaching deep into the wide lines, both isolated and array, c) slurry with a high etch and dissolution rate, and d) non-uniform pressure distribution on patterns with varying line width and pattern densities [ 50-52].

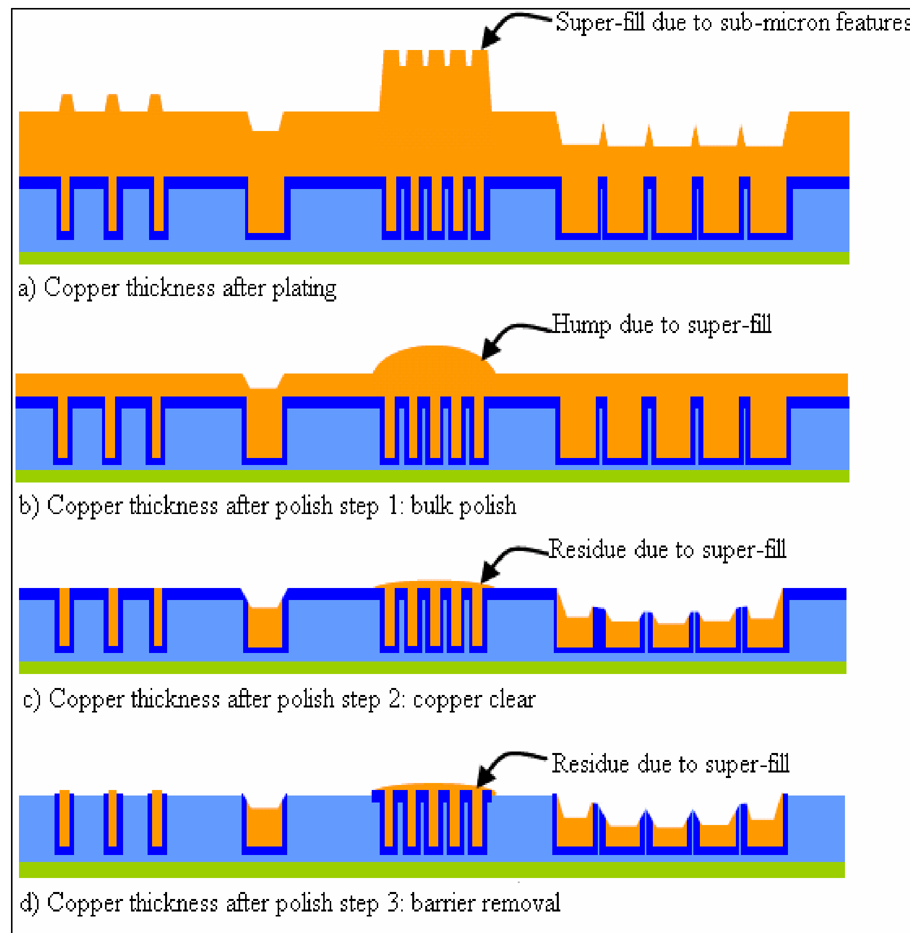


Figure 2.4 Pattern dependent non-planarity resulting due to CMP process [52]



المنارة للاستشارات
www.manaraa.com

Figure 2.4 above shows various post CMP surface characteristics [52] that result due to the above mentioned factors at different pattern densities and line widths. It can be seen that step 2 (copper clear) and step 3 (barrier removal) are more critical as compared to bulk removal in terms of pattern dependencies. Dishing, erosion, oxide and metal loss are the four types of post CMP pattern effects that result in deviation from achieving a planar surface. Dishing is the loss of metal from the wide metal lines, whereas erosion is the loss of oxide along with the narrow array of thin metal lines. Oxide loss is the loss of field oxide next to an array of thin metal lines separated by a wide oxide pattern and metal loss is the total loss of thickness of the metal lines separated by thin oxide pattern. Figure 2.5 below shows [52] the schematic of these pattern deviations. These post CMP characteristics affect the electrical properties of the interconnect structure and at the same time induce non-planarity over the wafer surface, causing lithography issues, which nullifies the primary purpose of CMP process [52]. Governing factors that would cause the deviation from non-planarity after CMP process need to be understood in detail to avoid reduction in device yield due to these characteristics.

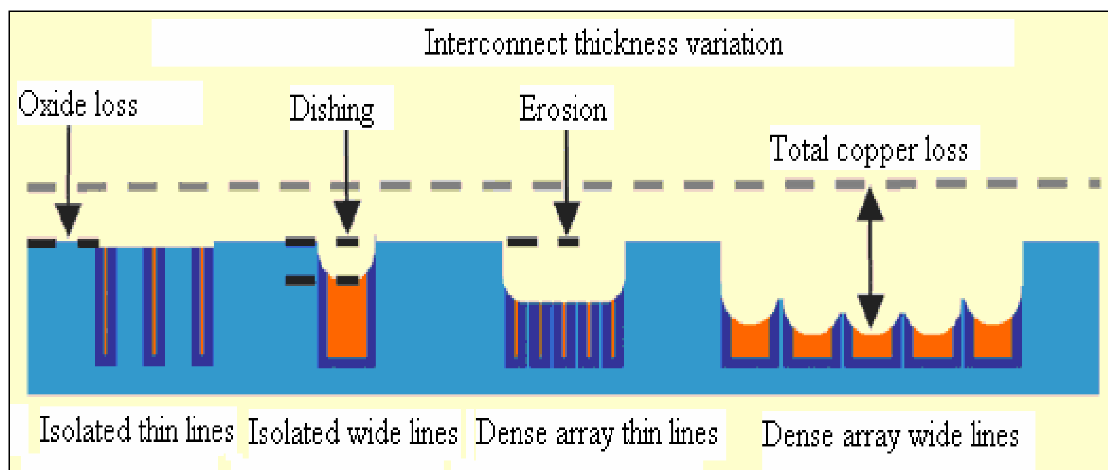


Figure 2.5 Post polish surface anomalies due to pattern deviations resulting in wafer surface non-planarity [52].



المنارة للاستشارات
www.manaraa.com

### 2.4.2 Surface scratches

Another source of defect that is generated due to the polishing process is the surface damage due to the mechanical interaction of abrasive particles with the wafer surface. Scratches, both macro and micro, form due to the deep indentation and dragging of the abrasive particles [53]. Many factors such as particle size distribution, presence of large particles in the slurry, formation of agglomerates due to slurry pH, which affects the surface charge on the particles causing them to bind to each other etc., could be the root cause of the surface scratches. Figure 2.6 shows some typical scratches that are formed on wafer surface during CMP process. Although some of these scratches can be removed during the final step of polishing called buffing (which eliminates shallow scratches), the more intense scratches are permanent and cannot be removed from the surface. Such a damaged surface will directly impact the electrical performance of the interconnect scheme and thus hampers the device yield. Thus, countering this kind of defect becomes a critical aspect of CMP process yield improvement. The third objective of developing new slurries to achieve reduced surface damage during CMP finds application in this context.

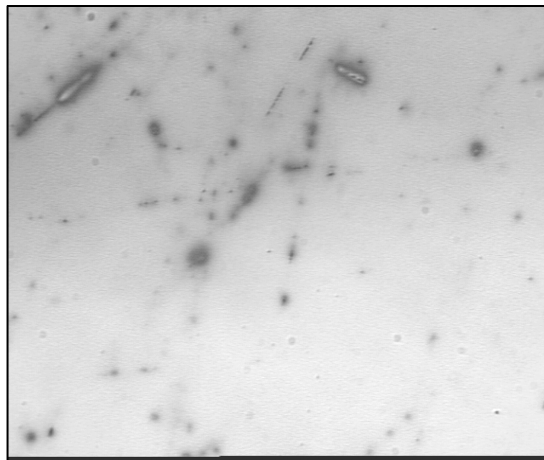

Figure 2.6 Optical microscopy of scratches and pitting on wafer surface [53].



المنارة للاستشارات
www.manaraa.com

### 2.4.3 Delamination during cu/low-k CMP

Besides replacing aluminum with copper, another way to reduce RC delay is the introduction of materials that have lower dielectric constant than $SiO_2$ as the inter-level dielectrics. The drawback of introducing such materials with low dielectric constant (low K) is that they are mechanically weak materials [54-60]. These mechanically weak materials cannot withstand the shear forces applied during CMP process. Moreover, their interfacial adhesion energies are so low [7, 61] that even moderate frictional forces can induce the failure of these interfaces. This will impact the reliability of the multilevel metallization stack. Several studies [24] have been conducted to determine the causes of delamination and how it could be prevented. Some of the major conclusions are that process development for CMP using low pressures and velocity is necessary to avoid such failures. They also suggested that slurries and polishing pads that result in less friction at the interface need to be developed. Less friction at the interface results in lower shear forces, thereby decreasing the occurrence of delamination. Figures 2.7 and 2.8 (a) and 2.8 (b) show the SEM images of the delaminated interfaces [7, 24].

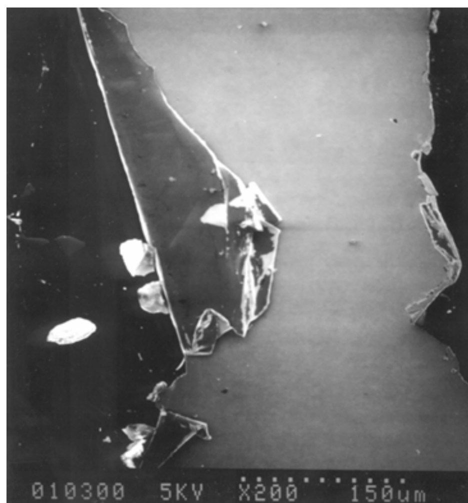


Figure 2.7 Delaminated interface during CMP process [7]



المنارة للاستشارات
www.manaraa.com

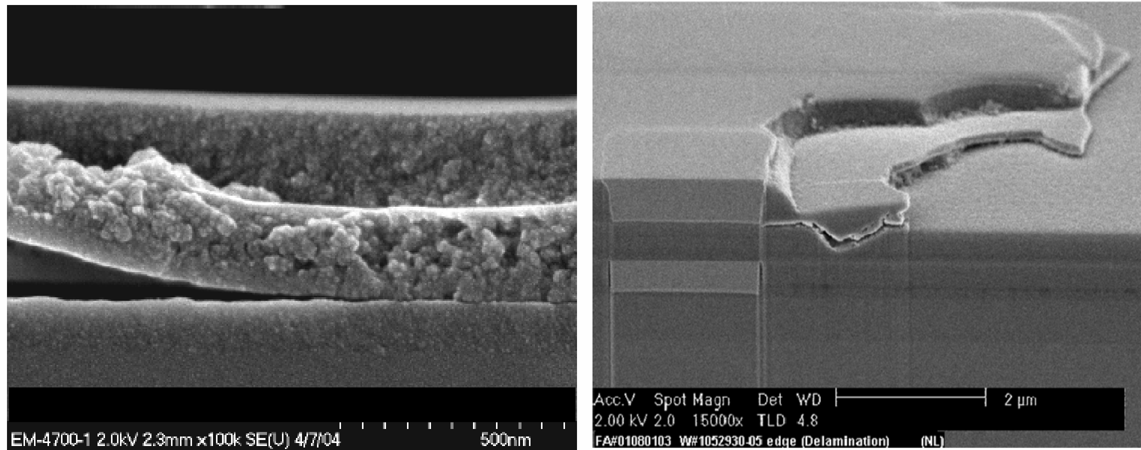


Figure 2.8 Delamination at via layer and a) copper dielectric cap interface b) the trench layer stress point [24]

These defects directly destroy the device, resulting in reduced yield and increased cost of production. The above discussion of generation of micro-scratches and the occurrence of delamination forms the basis for the final objective of this thesis, which is to develop slurries that reduce surface damage during CMP and at the same time reduce the friction at the polishing interface in order to avoid delamination.

## 2.5 Research objectives

There are mainly three objectives of this research work: a) Study the effect of temperature on CMP process including pad conditioning process, b) Develop a thermal model and accordingly study the effect of slurry flow rate on CMP process and post CMP surface characteristics, and c) Develop a slurry with novel 'soft' particles to achieve defect-free post CMP wafer surface. The objectives are explained in more detail in the following sections below.



المنارة للاستشارات
www.manaraa.com

### 2.5.1 Process optimization: effect of temperature

Every process needs to be optimized to minimize the defects and at the same time maximize the removal rate in order to achieve both yield and throughput. CMP has several variables and factors that affect its 'output', which in itself is constituted by several specifications with regard to removal rate, post polish surface quality, planarity, etc. One of the several factors affecting CMP that is least researched is the temperature, either be it operating or the temperature of the consumables. Even though there are few research works in the recent past, the entire effect of temperature on various facets of CMP is far from being understood in its entirety. The first objective of this research is to study the effect of temperature on the CMP process comprehensively and to conduct an in depth investigation into the causes of increased removal rate with an increase in temperature. This investigation is aimed at providing an insight into the various electrochemical and surface chemical aspects of copper-slurry interaction at different temperatures. An extension of this study will be to study the effect of temperature on pad conditioning process. Chapter 3 presents the result from temperature study and elucidates various mechanisms occurring at the interface. Since temperature affects the pad surface asperities, the contact area and the copper-slurry interaction, the effect of temperature on the coefficient of friction at various process parameters is studied in detail. Chapter 4 elucidates the results of the temperature effect on COF during CMP.

### 2.5.2 Thermal model

Another objective of this research is to model the conduction heat transfer mechanism at the interface after a steady state has been achieved by the polishing



المنارة للاستشارات
www.manaraa.com

process. By solving the model, this research presents the temperature profile on the wafer surface as a function of wafer radius and thickness. The analytical modeling effort is supported with the finite element analysis using FIDAP package which can handle both conduction and convection heat transfer environments effectively. The results from the model indicate a change in surface temperature due to a change in incoming slurry flow rate. Based on this result, a further study on the effect of slurry flow rate on the CMP process is conducted not only in the aspect of tribology but also with regard to post CMP surface asperities and pattern related characteristics such as dishing and erosion are studied.

### 2.5.3 Low defect slurry development

Another aspect of CMP process that gained a huge market in the recent past is the consumable market. The characteristics of the process consumables such as polishing pad material, slurry additives, slurry abrasive particles, dispersants, etc. influence the process output control. As observed in the previous section concerned with challenges during CMP, several defects such as micro-scratches and delamination occur during CMP. These defects can be countered effectively if a 'gentle' CMP process is developed, which results in fewer number of scratches and lower friction forces. Slurry with non-conventional soft abrasive particles could be a possible solution. This forms the third objective of this dissertation.



المنارة للاستشارات
www.manaraa.com

# CHAPTER 3: EFFECT OF TEMPERATURE ON COPPER CMP PROCESS

## 3.1 Introduction

Even though copper CMP process has been researched in the past [15, 62-66], certain factors of the process having significant effect on overall copper CMP process output need further investigation. Temperature rise at the polishing interface constituted by pad, film, and slurry abrasives is a significant factor that affects CMP, which has not been researched extensively nor been understood in its entirety. Thermal effects need to be thoroughly researched in order to better understand the resulting modifications in mechanisms during the process of copper CMP. Research based on thermal effects during Interlayer dielectric (ILD) polishing, friction induced heating, temperature increase on the polishing pad, removal rate dependence on temperature, and its modeling has been carried out in the recent past to understand the role of temperature at interface on CMP performance [40, 41, 45 ,67].

Present research deals with the changes in electrochemical aspects and surface modification mechanisms of copper with a variation in slurry temperature. Along with the electrochemical measurements, XPS studies, dissolution rate and pH variation with slurry temperature are monitored and their contribution towards the increase in removal rate are discussed. The effect of temperature during CMP on patterned samples is also conducted to understand the effect of temperature on with-in die non-uniformity. It is highly beneficial to understand the effect of temperature on CMP performance, in order



المنارة للاستشارات

www.manaraa.com

to achieve better removal rates without compromising any other planarization specifications.

## 3.2 Materials and techniques

### 3.2.1 CMP benchtop tester

Electroplated Copper blanket films of 15000 Å thick were polished using the CETR™ bench top CMP tester (see figure 3.1 below). Programmable forces, speeds and slurry flow rates allow one to closely imitate fabrication plant (fab) CMP processes on any production polisher and to understand the processes in detail. The tester holds a 6 inch polishing pad and can hold up to a 2 inch diameter silicon wafer. Real time coefficient of friction can be measured using a dual force sensor which measures lateral and normal forces. Lateral and normal forces are continuously monitored and recorded in-situ at a total sampling rate of 20 KHz. Features of the bench top tester are provided in detail in previous publication [68, 69]. A 6" diameter polishing pad coupon attached to the bottom platen was used to polish a 1" X 1" sample coupon placed face down onto the pad. Cabot iCue 5001 slurry and IC1000/Suba IV polyurethane perforated pads were used to polish the copper samples. The slurry temperature was varied from 18.5$^{o}$ C to 30$^{o}$ C. The slurry flowing at the interface is the only source to convect heat away from the interface. Hence, the variation of the slurry feed temperature directly decreases the amount of heat taken away from the interface, thus increasing the interfacial temperature. The slurry temperature was controlled for each experiment during the whole project by monitoring and maintaining the temperature at a specific value within a 0.5$^{o}$C variation. The experimental procedures dealing with the contact of wafer and the slurry were designed to be short in order to minimize thermal losses. Also, the slurry containers were



المنارة للاستشارات
www.manaraa.com

insulated with casing made of thermocol material to further reduce thermal losses. The coefficient of friction (COF) was monitored in-situ from the bench-top tester data acquisition system. This is made possible by using a dual load sensor attached above the wafer carrier which can measure the normal and lateral forces during the process, the ratio of which gives the coefficient of friction. The variation in COF upon removal of the copper film was used to determine removal rate.

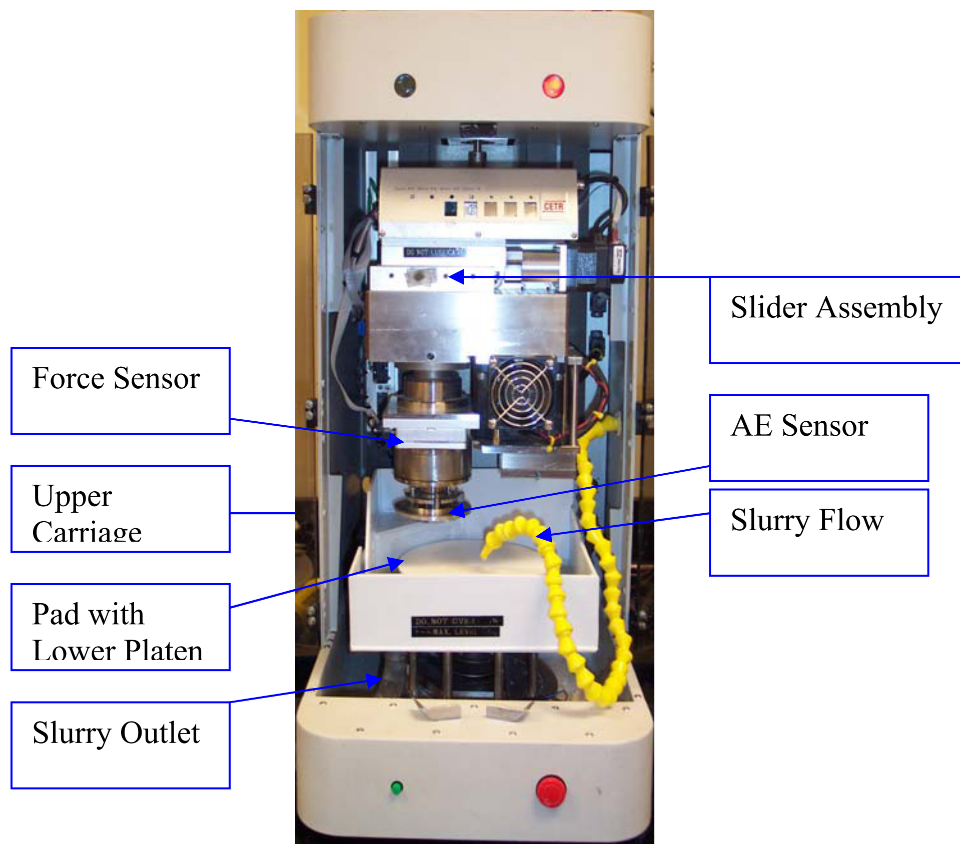


Figure 3.1 Bench top tester that can simulate real time CMP process

Polishing conditions were maintained at 3 PSI, 100 RPM bottom platen rotation, 95 RPM carrier rotation, slurry flow rate 50 ml/min. Patterned 0.8" (2 cm X 2 cm) square wafer coupons with 10 kÅ electroplated copper layers and an MIT 854 pattern were used



المنارة للاستشارات
www.manaraa.com

for non uniformity experiments [70]. The pattern consists of different line widths ranging from 0.18 µm to 100 µm and pattern densities ranging from 1% to 100%. The layout of the pattern is presented in Figure 3.2 below. Patterned wafer coupons were polished at 4 psi, 150 RPM bottom platen rotation, 145 RPM carrier rotation, and slurry flow rate was maintained at 75 ml/min.

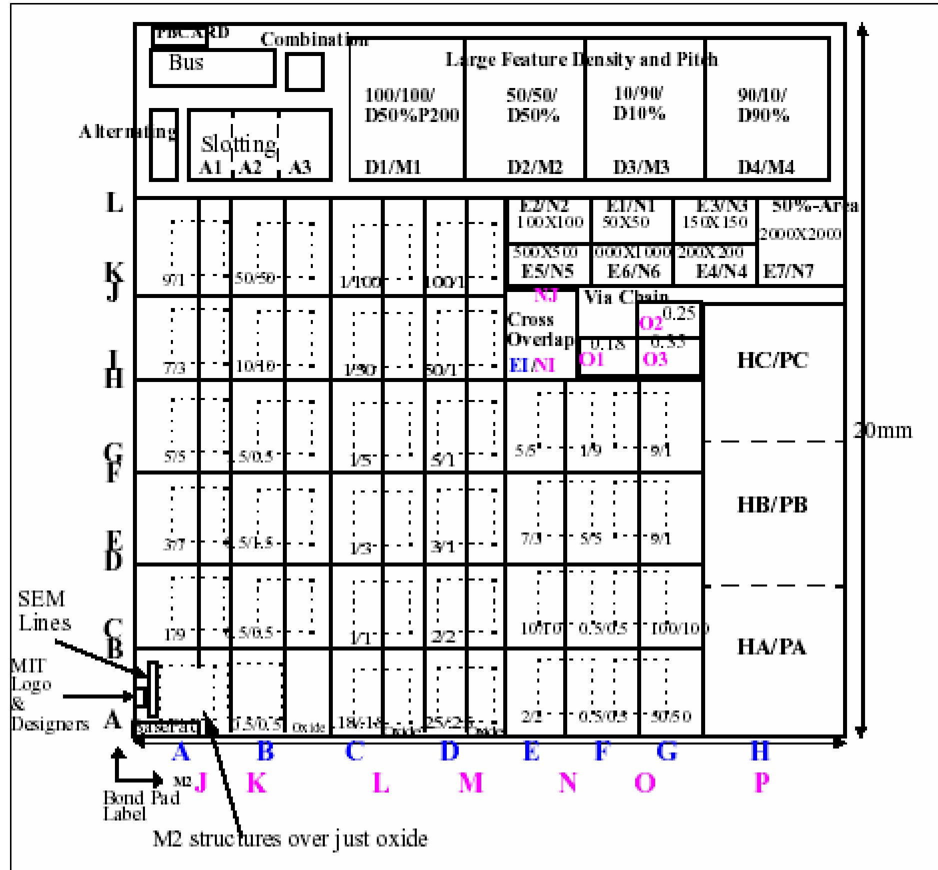


Figure 3.2 MIT 854 mask lay out with varying pattern line widths and densities

To understand the effect of temperature on copper surface due to polishing at different temperatures in terms of mechanical and surface properties, nanoindentation and atomic force microscopy (AFM) were conducted.



المنارة للاستشارات
www.manaraa.com

### 3.2.2 Nanoindentation

The evaluation of the mechanical properties of the Cu layer deposited on the top of the stack was performed using nanoindentation. The experiments were performed on a standard MTS nanoindentor (see figure 3.3) using a three sided Berkovich diamond tip. The hardness and Young's modulus of the candidate thin films were calculated. Experiments were performed in the continuous stiffness mode (CSM). Continuous stiffness mode enables one to conduct experiments while measuring the contact stiffness at each depth through out the indentation. Thus, a dynamic measurement is made possible and mechanical properties along the penetration depth are studied.

Figure 3.3 Nanoindenter used for the mechanical characterization of thin films

A Berkovich diamond indenter of radius 20 nm has been used as the indenter. The indentation depth was limited to the 150 nm (15 % of the total cu thickness) to avoid the effect of underlying thin film layers and the substrate. The calculation of hardness and modulus was performed from 70 to 140 nm of penetration depth. This range has been



المنارة للاستشارات
www.manaraa.com

chosen to minimize the substrate effects in calculation of mechanical properties of thin films and also to avoid getting data from the initial part where the indenter might not be totally stable and the minor variations present due to system vibrations and machine stiffness might influence the data. The values of hardness and Young's modulus as a function of indenter depth were plotted, and from these output parameters the effective hardness and modulus of the thin films was estimated. The effect of polishing temperature on the copper thin film has been elucidated from these illustrations. Post CMP Atomic Force Microscopy (AFM) was carried out to characterize the samples for surface roughness achieved after polish at different temperatures using a Digital Instruments Dimension$^{TM}$ 3100 AFM operated in tapping mode at 256 Hz frequency of the cantilever.

### 3.2.3 Electrochemistry and x-ray photoelectron spectroscopy

For electrochemical experiments, the constructed cell consisted of an Ag/AgCl/KCl saturated reference electrode with platinum strip as counter electrode and a diced strip of copper thin film coated silicon wafer as working electrode. The schematic of the electrochemical cell is presented in figure 3.4. The backside of the wafer was isolated from electrical and chemical contact by coating it with acrylate and polyester copolymer material. The electrodes were placed at least 10 mm apart from each other in the electrolyte. PARSTAT 2263 model advanced electrochemical system manufactured by Princeton Applied Research was used for polarizing experiments of the copper sample. Current density data was collected for an applied potential range of -0.9 Volts to 0.9 Volts scanned at a speed of 5mV/sec. The temperature of the electrolyte for each



المنارة للاستشارات
www.manaraa.com

experiment and the electrode-electrolyte contact area were maintained constant through out the experimentation.

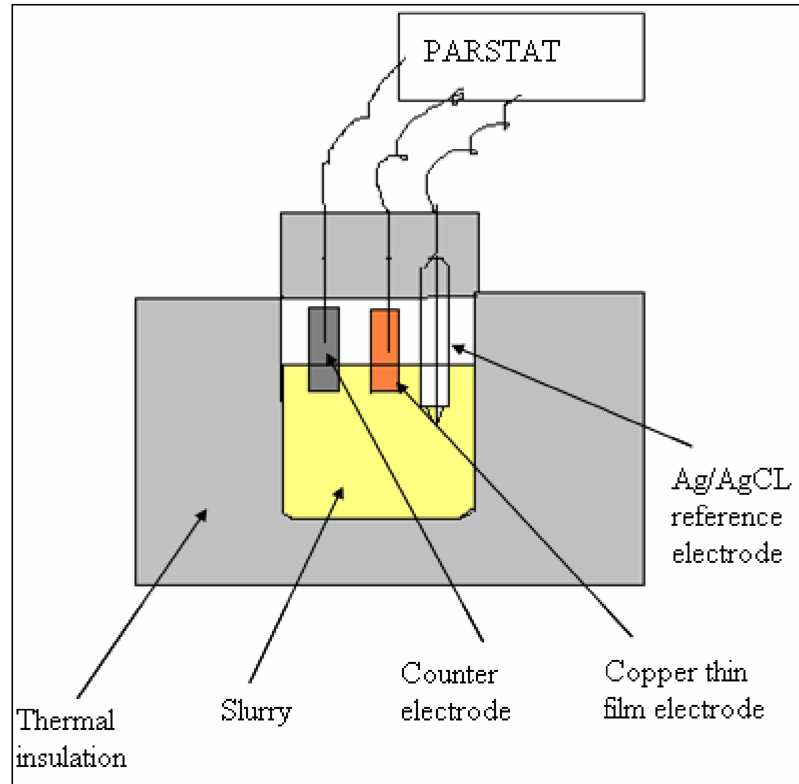


Figure 3.4 Schematic of the electrochemical cell for the polarization experiments.

Surface modifications were investigated by X-ray Photoelectron Spectroscopy (XPS) measurements performed using Al K$\alpha$ radiation on an as received copper film and a slurry treated copper film at four different temperatures. Ultraviolet Photoelectron Spectroscopy (UPS) was performed on the samples to estimate the work function to be used for XPS data. The samples were immersed in the slurry for 2 minutes, dried in an inert atmosphere, and then immediately transferred into the vacuum chamber for the collection of spectra. The peaks obtained were deconvoluted and were curve-fitted using



المنارة للاستشارات
www.manaraa.com

a combination of both Gaussian and Lorentzian profiles [71]. The copper samples were treated for 5 minutes in a temperature controlled environment, and gravimetric studies were performed to investigate the variation in dissolution rate with temperature. A precision balance (Sartorius R200D research model) was used for gravimetric studies with a sensitivity of 0.01 mg.

## 3.3 Results and discussion

### 3.3.1 Effect of temperature on CMP tribology

The temperature of the slurry was the only varying parameter during CMP of copper blanket samples performed on the CETR$^{TM}$ bench-top tester. The slurry was maintained at the predetermined temperature (both above and below room temperature) for the duration of the polishing experiment. Removal rates were calculated from the in-situ endpoint detection ability of the machine, which shows a change of the COF at the complete removal of the thin film. The time for removal was noted, which gives the removal rate information. The variation of the removal rate along with COF with change in slurry temperature is plotted in figure 3.5. An overall increase in the removal rate with temperature can be observed from the figure.



المنارة للاستشارات
www.manaraa.com

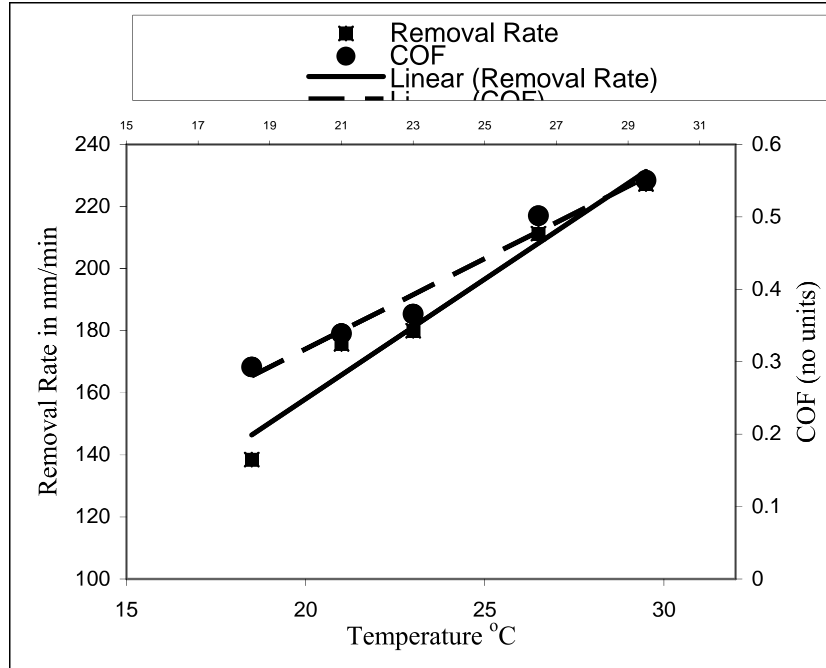


Figure 3.5 Increase in removal rate and coefficient of friction with change in temperature

This increase of the removal rate can be attributed to changes in both the mechanical and chemical nature of the polishing process. The change of the mechanical component of the process has two reasons. Firstly, as a result of polishing pad softening (change in mechanical properties of the pad due to the increase in temperature) the area of contact increases [72], thus increasing the number of abrasive particles coming in contact with the wafer surface. This is supported by the COF increase with increase in slurry temperature as shown in figure 3.5. These results are in agreement with the results from previous investigations by other authors [67]. Secondly, a decrease of the viscosity of the slurry occurs with increasing temperature, which increases the friction at the interface and hence increases shear resulting in higher removal rates [73].



المنارة للاستشارات
www.manaraa.com

### 3.3.2 Effect of temperature on electrochemistry

To investigate changes in the nature of the surface chemical reactions depending on slurry temperature, electrochemical studies were carried out. The applied potential is plotted against output current density in yielding potentiodynamic curves for samples treated at different temperatures. The concentration of $H_2O_2$ in the slurry at different temperatures in the specified temperature range was verified to be constant using titration methods. The variation in pH was noted to be constant for all practical purposes (7.6 – 7.4) within the specified temperature range. Figure 3.6 presents the corrosion potential and corrosion current density values derived from the potentiodynamic curves.

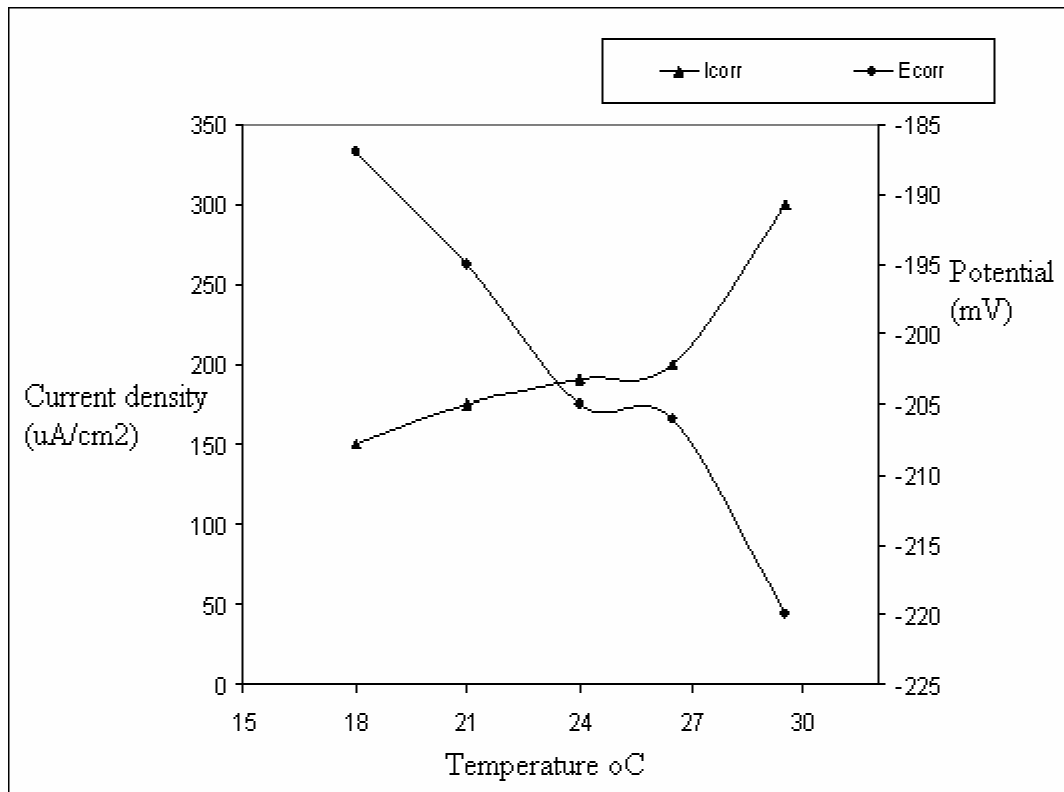


Figure3.6 Change in corrosion current density and corrosion potential with change in slurry temperature



المنارة للاستشارات
www.manaraa.com

Corrosion potential was directly obtained from the plotted E vs Log I curves. The potential at which both the anodic and cathodic current rates are equal is termed the corrosion potential by definition. The corrosion current was determined by extrapolating the cathodic and anodic curves, which approximately intersect on the line of corrosion potential (Ecorr), x-co-ordinate for the intersecting point gives the corrosion current density. The variation in corrosion current density is in agreement with the removal rate data provided in figure 3.5. The corrosion potential shifts towards more negative values with increasing temperature, indicating an enhanced anodic reaction. Changes in the anodic profile of the graph can be seen from the potentiodynamic curves, which give an estimate of the corrosion or the consumption of the metal. A continuous increase in the anodic current densities for higher temperature system at higher potentials can be noted from the figure 3.6 above. This indicates more corrosion and more anodic (metallic) dissolution observed at higher values of temperature.

### 3.3.3 Effect of temperature on surface chemical compounds

To further investigate the surface oxidation and modification, XPS was performed on as received and slurry treated samples at different temperatures. The work function as measured by UPS was found to be constant for samples treated with changing slurry temperature. Cu (2p) peaks were mainly analyzed to investigate changes in the oxidation state of Cu surface and relative intensities of oxides on copper surface. Figure 3.7 shows a comparison of the copper peaks for copper samples as received and treated with slurry at different temperatures.



المنارة للاستشارات
www.manaraa.com

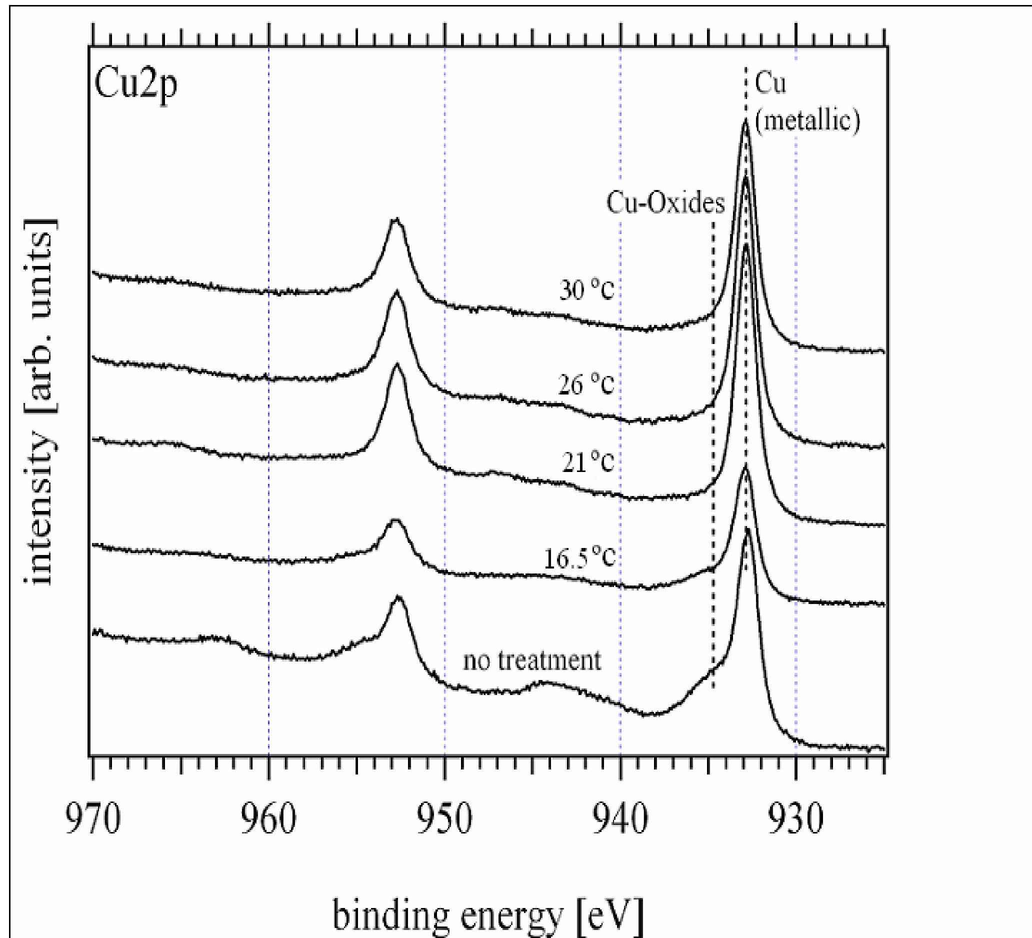


Figure 3.7 Comparision of cu ($2P^{3/2}$) spectra for as-received and slurry treated samples at different temperatures

From the spectra it can be seen that oxide peaks are relatively more intense, hence lowering the intensity of metallic copper for sample treated with slurry at 21°C (room temperature) as compared to the sample treated at 16.5°C. This indicates a higher oxidation rate. It can also be noted from the spectra that the shoulder of copper oxide is absent at higher temperatures. This is due to the increased dissolution rate of the surface oxides at higher temperatures. This hypothesis is supported by the chemical dissolution



المنارة للاستشارات
www.manaraa.com

data presented in figure 3.8, which shows a gradual increase in material loss at higher temperatures.

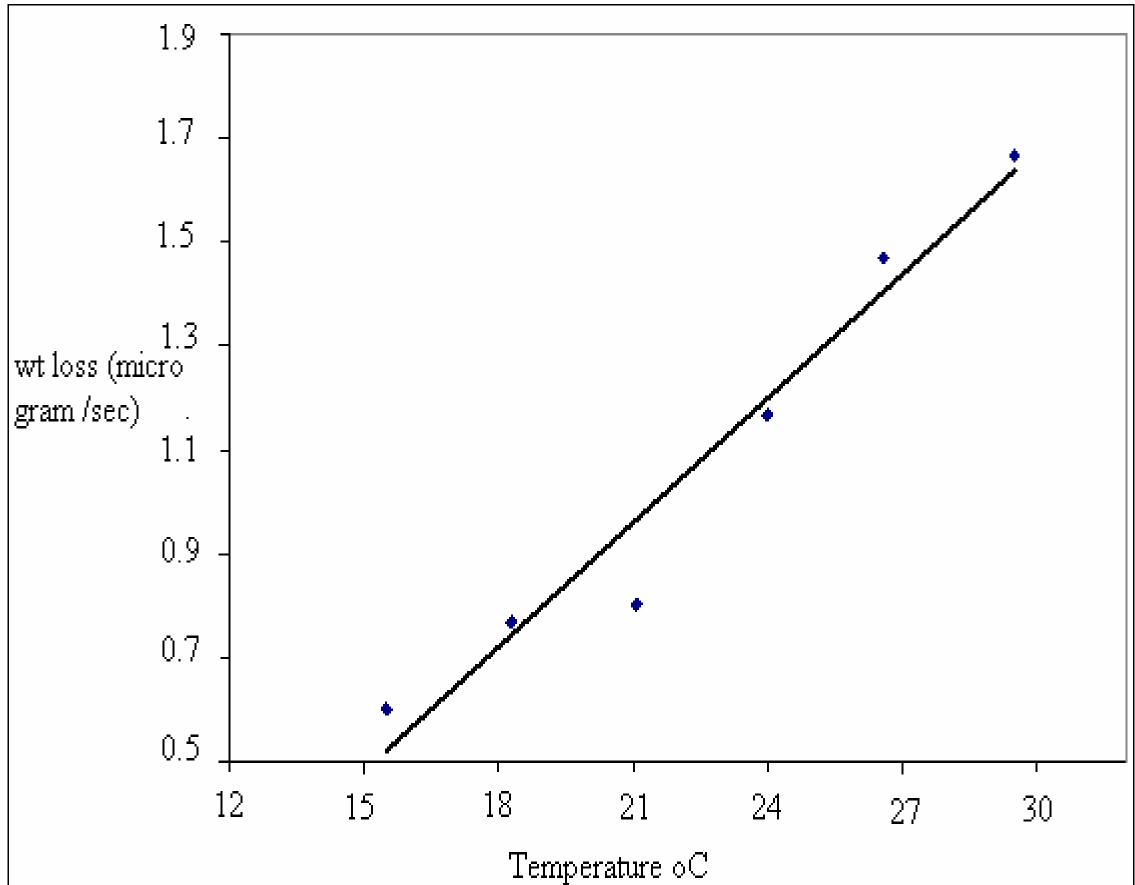


Figure 3.8 Increase in dissolution rate with an increase in slurry temperature.

A low shoulder can be seen from the as received copper sample, which can be attributed to the native surface oxides present on the sample before treatment. Figure 3.9 shows the curve fits of the spectra shown in figure 3.7.



المنارة للاستشارات
www.manaraa.com

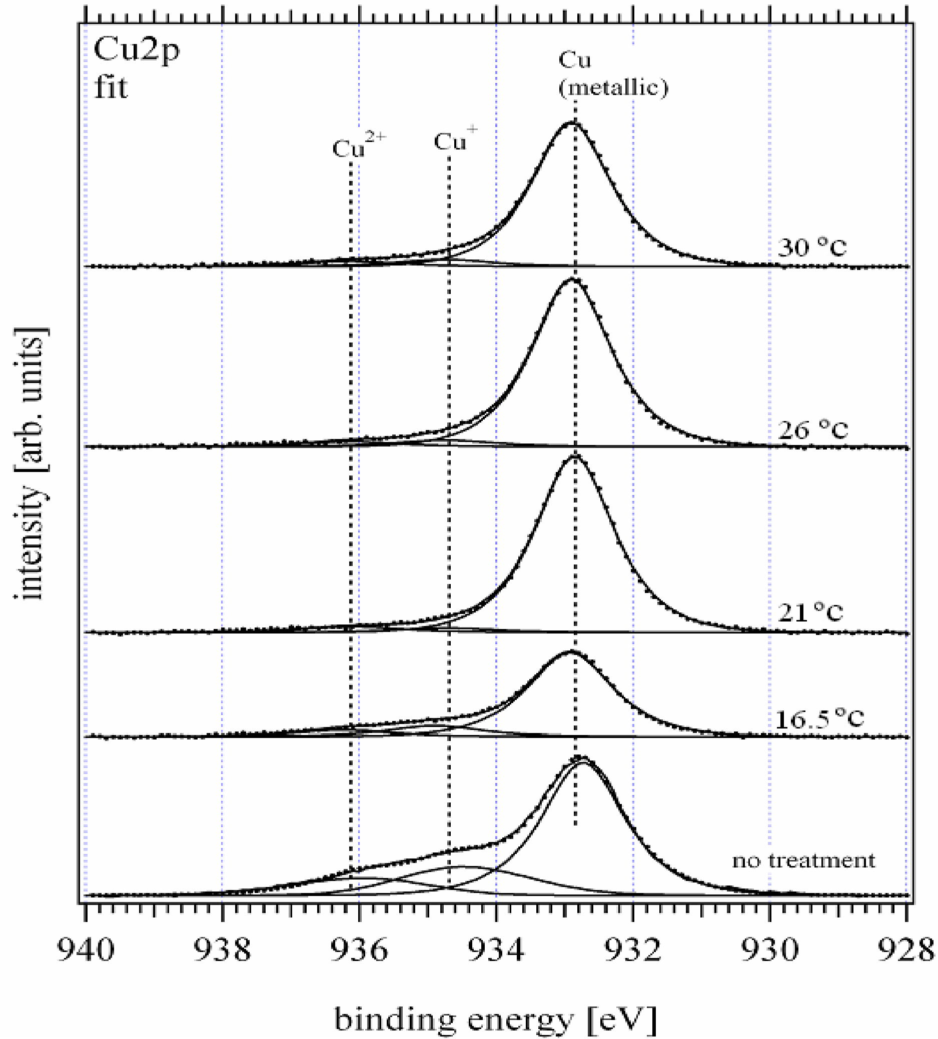


Figure 3.9 Curve fitted cu ($2P^{3/2}$) spectra for as-received and slurry treated samples at different temperatures

The oxide peaks (O (1s) spectra) studied for all the above samples are presented in figure 3.10. From the figure it can be noted that the copper oxide peaks are less intense than the alumina peaks (alumina particles are present in the slurry as abrasive). This is due to oxygen present in alumina deposited onto the sample surface being more sensitive to XPS as compared to the oxygen present in copper oxide. This is also the reason for



المنارة للاستشارات
www.manaraa.com

more intense copper oxide detection on the as-received sample as compared to the samples treated with the slurry as can be seen in figure 3.7.

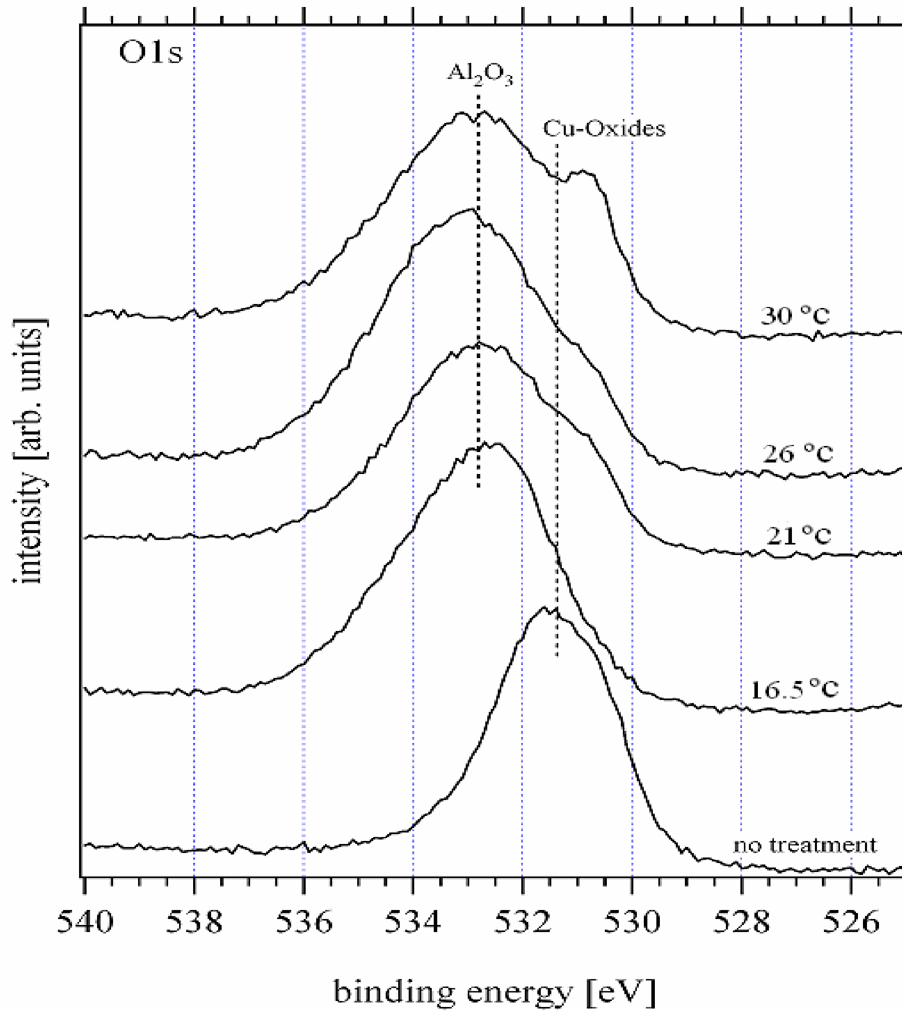


Figure 3.10 Comparison of oxygen (O1(s)) spectra for as-received and slurry treated samples at different temperatures

The relative concentrations of compounds on the surface were determined as a product of peak intensity and the full width at half maximum values. The ratio of copper oxide to copper metal depending on slurry temperature is shown in figure 3.11. The initial decrease in oxide to metal ratio from 16.5$^{o}$C till room temperature is due to



المنارة للاستشارات
www.manaraa.com

enhanced dissolution rate of copper in the slurry and not much increase in oxidation rate. The minor increase in the oxide to metal ratio above room temperature is due to increased oxidation rate, which is greater than the increase in dissolution rate. From these observations it can be reasoned that along with an increase in oxidation rate there occurs simultaneous dissolution of surface oxides into the slurry at a higher rate at elevated temperatures, contributing to an overall increase of the material removal rate during copper CMP.

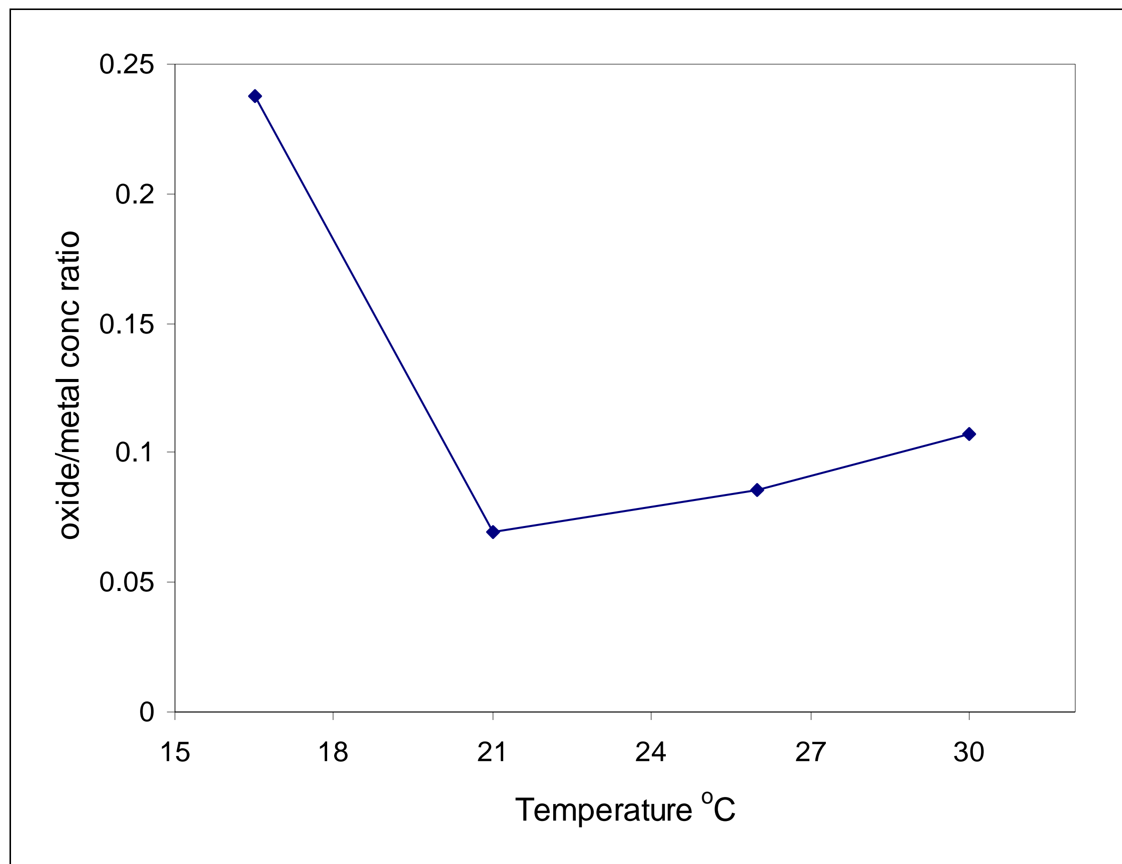


Figure 3.11 Concentration ratio of oxide/metal on copper surface treated at different temperatures



المنارة للاستشارات
www.manaraa.com

### 3.3.4 Effect of temperature on polished copper surface

#### 3.3.4.1 Surface roughness

Surface imaging post CMP samples polished at various slurry temperatures was performed using Atomic Force Microscopy. Surface images of 10 µm size at 200 nm vertical data scale were taken at five locations on the wafer surface and the value of the surface roughness was averaged. The three dimensional images of the surface that has the roughness closer to the average are presented in figure 3.12 (a-d).

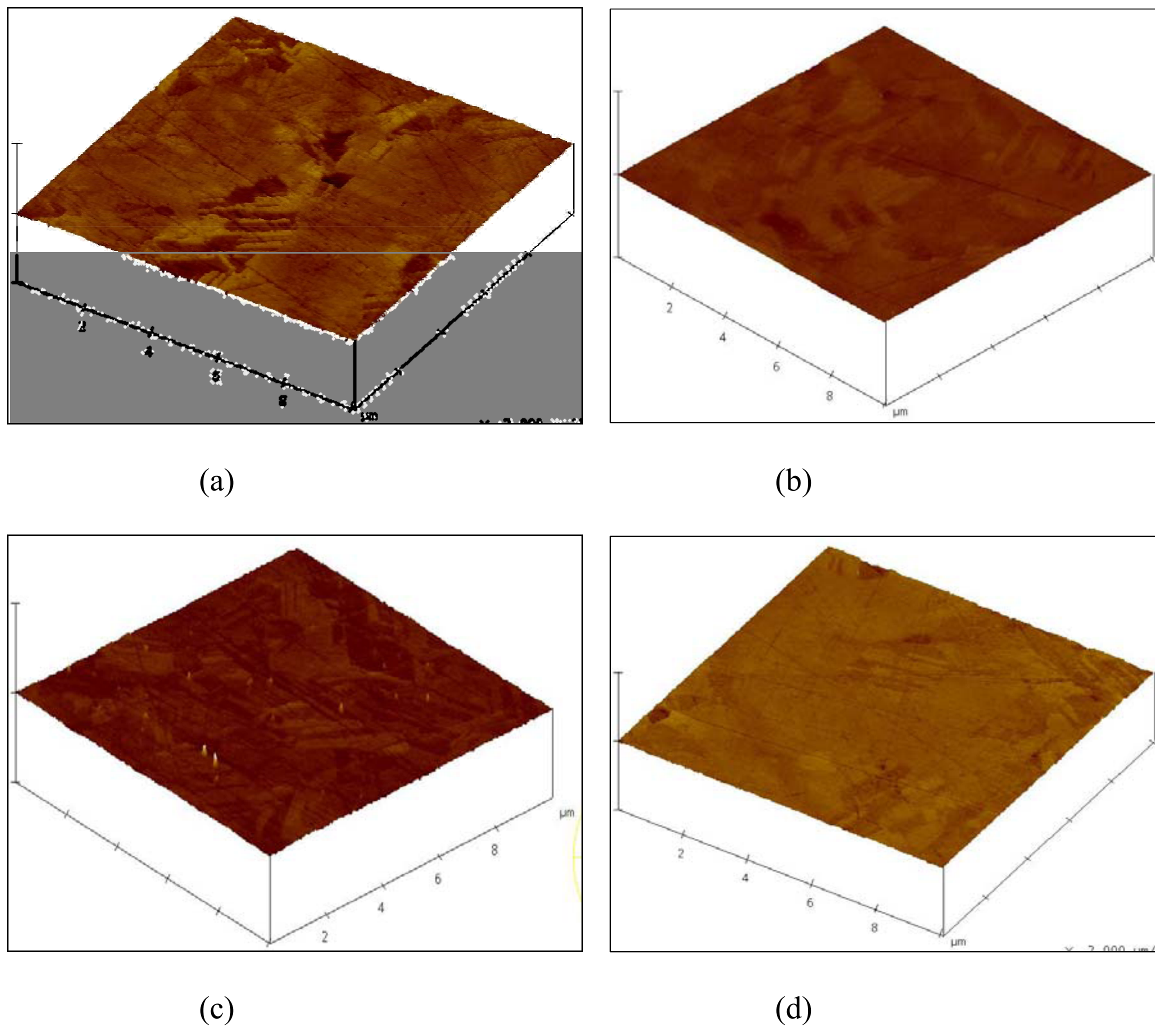

Figure 3.12 AFM images of the blanket copper sample after CMP at (a) 18.5$^{o}$C (b) 21.5$^{o}$C (c) 27$^{o}$C (d) 31$^{o}$C



المنارة للاستشارات
www.manaraa.com

It can be seen from the figures that the sample polished at 18.5°C has a relatively rougher surface. But for the sample polished at below room temperature, all the other samples had the similar roughness and no significant change has been observed. There was a minor increase in the depth of scratches for samples polished at higher temperatures. This increase in scratch depth might be due to two reasons: a) Changes in particle size distributions at higher temperatures as discussed by Kim et al [74], b) active dissolution of the modified surface layer exposing the underlying untreated copper surface to the particles. The change in depth of scratch is not found to be significant to change the overall surface roughness. In summary, the effect of temperature on the surface roughness generated during CMP was found to be insignificant.

#### 3.3.4.2 Non-uniformity

Patterned samples following the CMP at different temperatures were analyzed for the step height differences on isolated wide lines and narrow arrays. As was mentioned at the beginning of the chapter, the wafer samples contained MIT 854 mask pattern with a wide variety of feature sizes and densities. 9 μm wide isolated lines and 1 μm arrays were analyzed for step height differences. With-in die non uniformity was then computed as the difference in step height reduction at the isolated wide (9 μm) metal line and array of narrow (1 μm) features. The AFM images and the schematic presented in the figure 3.13 (a) elucidates the features being analyzed. The dependence of with in die non-uniformity on the polishing temperature is presented in figure 3.13 (b). From the figure it can be seen that the percentage difference in step height reduction decreases as the temperature



المنارة للاستشارات
www.manaraa.com

increases from below room temperatures until it reaches room temperature and then increases as the temperature increases above room temperature [75].

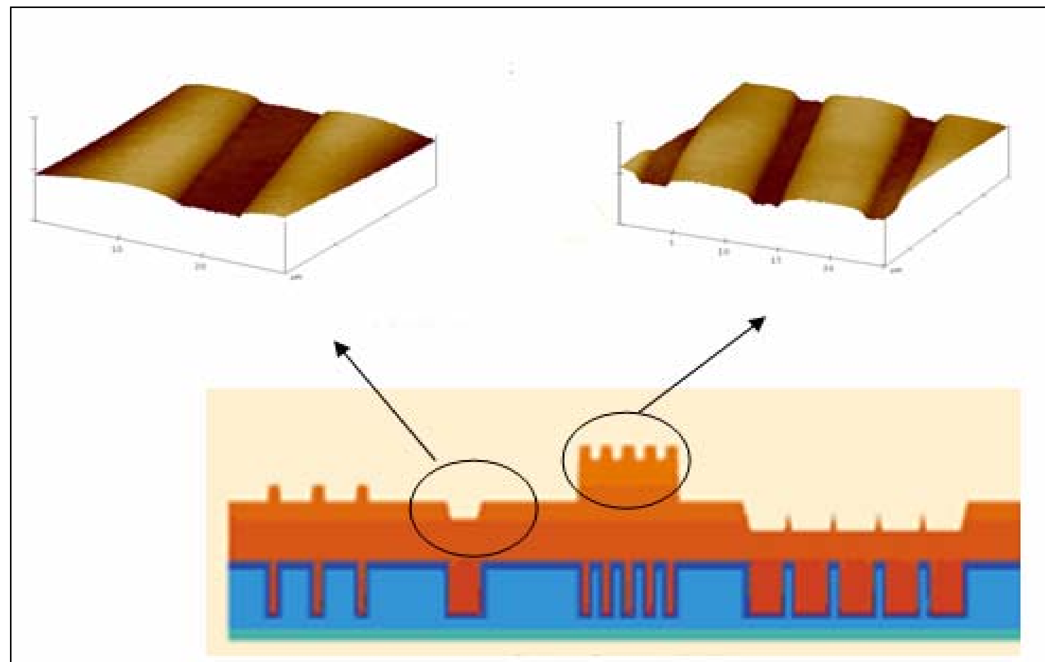

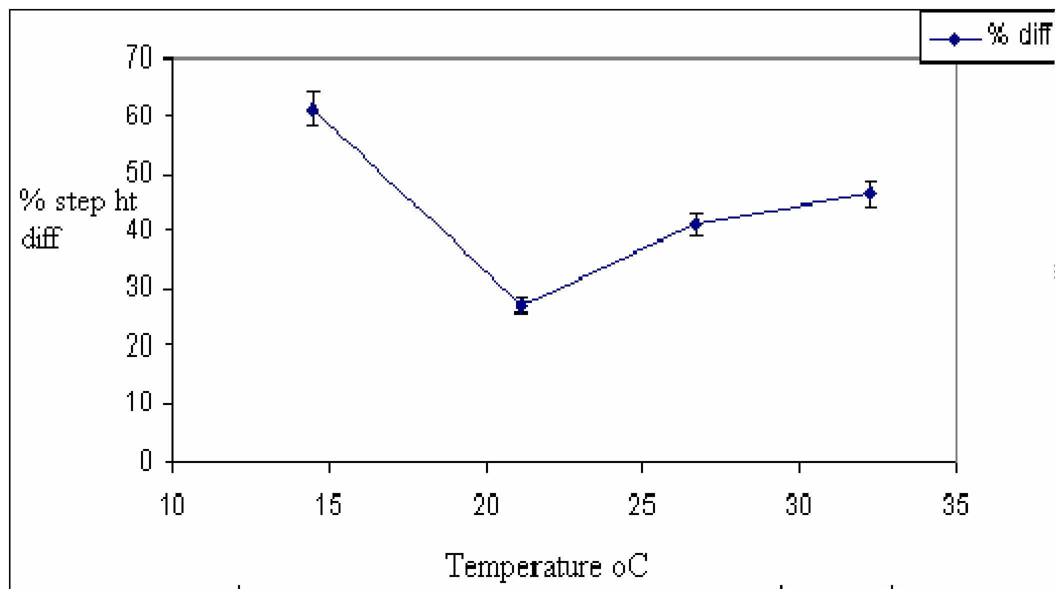


Figure 3.13 (a) AFM images and schematic of the pattern describing the analysis for non-uniformity measurement (b) non-uniformity with-in die versus the temperature of polishing.



المنارة للاستشارات
www.manaraa.com

A high level of non-uniformity at 15 $^{o}$C is attributed to the non-uniform chemical activity of the slurry and stiffened pad surface asperities, which result in predominant mechanical action. As the temperature increased the chemical activity increased, and a balance between the chemical and mechanical components of CMP is achieved resulting in least non–uniformity. At elevated temperatures soft pad asperities reached deeper into the wider lines but could not reach deep into the narrow isolated arrays causing differences in removal rates, resulting in increased non-uniformity. From these results, it can be understood that even though an increase in temperature increases the removal rate, it also increases non-uniformity with-in die during polishing. Such non-uniformity needs to be monitored more cautiously to prevent damage to the underlying features towards the end of the polishing step.

#### 3.3.4.3 Mechanical properties

To further investigate the changes in characteristics of the copper film with polishing process, nanoindentation studies were conducted on the pre-polished and post-polished copper samples. Mechanical properties of the thin film being polished play an important role during CMP. The surface scratches, being one of the critical aspects that determine the polishing performance, depend on the mechanical properties of the sliding surface. Mechanical properties of copper before and after polishing have been estimated as described below. The unloading curve of the load-displacement curve gives stiffness, which is used in the calculation of the modulus of elasticity. With the help of continuous stiffness measurement, hardness and elastic modulus can be measured along the depth of penetration [76, 77]. Figure 3.14 presents the typical load versus displacement curves



المنارة للاستشارات
www.manaraa.com

obtained during indentation. Stiffness is measured as slope of unloading curve as shown in equation 3.1

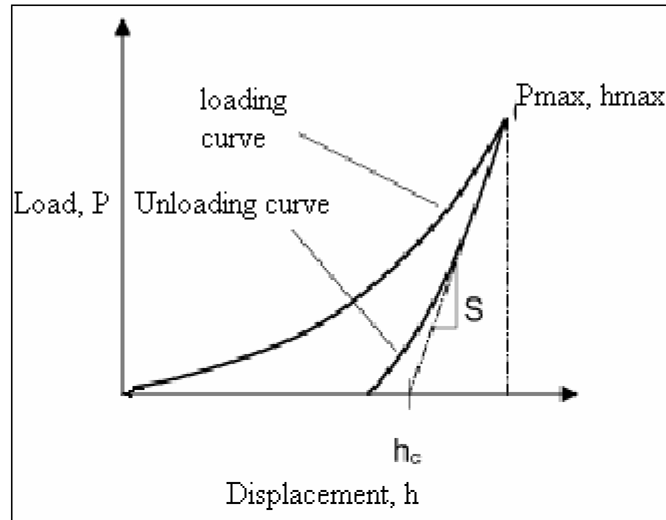


Figure 3.14 Load versus displacement curve

$$S = \frac{dP}{dh} = \frac{2\sqrt{A}}{\sqrt{\pi}} E_r \qquad (3.1)$$

Where 'S' is the contact stiffness and 'A' the contact area

The basic assumptions for the analysis are:

- Deformation upon unloading is purely elastic.
- The contact between a rigid indenter of defined shape and the sample is modeled using Sneddon's equation.

The deformation of the sample and of the indenter tip can be combined and given as reduced elastic modulus as shown in equation 3.2 as follows [76, 77]:

$$\frac{1}{E_r} = \frac{1 - \upsilon_i^2}{E_i} + \frac{1 - \upsilon_s^2}{E_s} \qquad (3.2)$$

Where $E_r$ is the "reduced modulus",$\upsilon$ is the Poisson ratio and 'i' and's' refer to the indenter and sample respectively.



المنارة للاستشارات
www.manaraa.com

Hardness of the thin film being indented can be determined as the ratio of maximum load and the area of contact (see equation 3.3). This area of contact is estimated as a function of indentation depth using area coefficients which depend on the shape of the indenter.

$$H = \frac{P}{A} \qquad (3.3)$$

Where 'P' is load and 'A' is contact area = fn ($h_c^2$)

Figure 3.14 shows the load versus displacement graph for the copper samples polished at different temperatures. The hardness and modulus of the copper samples is calculated according to the above mentioned procedure. Figure 3.15 presents the hardness of the unpolished film and for the films post CMP at different temperatures. From figure 3.16 it can be noted that the hardness of the polished copper surface increased with increasing slurry temperature. The unpolished sample had significantly lower hardness than the polished ones. This change can be attributed to the work hardening phenomenon during CMP. The work hardening phenomenon appears to be more influential at elevated temperatures. Similarly, the modulus of the polished and unpolished thin films along the penetration depth is presented in figure 3.17. It can be seen that the modulus of elasticity increases with increasing slurry temperature.



المنارة للاستشارات
www.manaraa.com

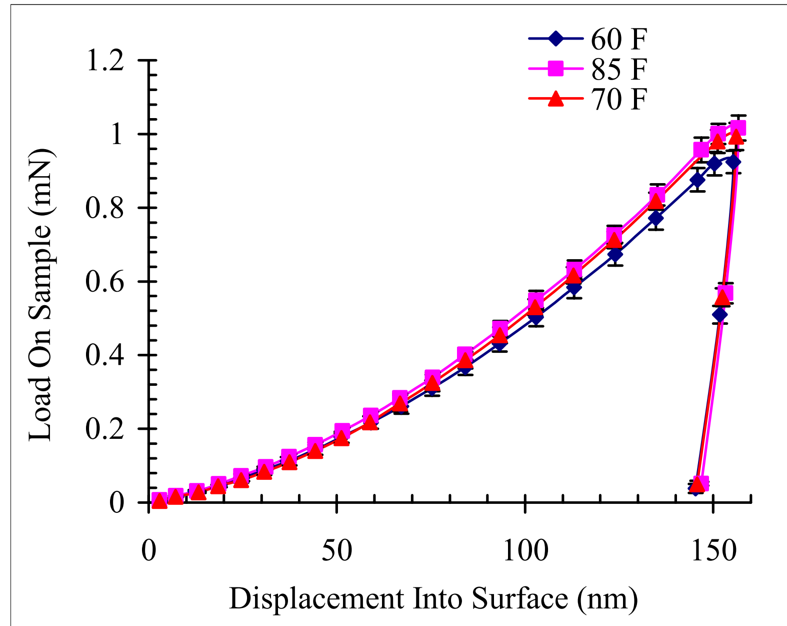


Figure 3.15 Load versus displacement for polished copper samples at different slurry temperatures

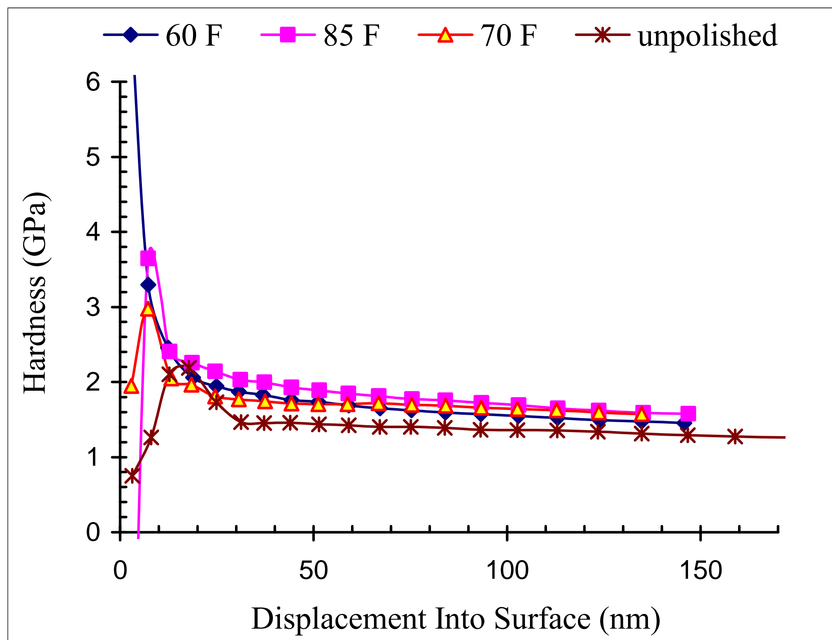


Figure 3.16 Hardness versus displacement for unpolished and polished copper samples



المنارة للاستشارات
www.manaraa.com

Also, the modulus of elasticity of the unpolished film is significantly lower than that of the polished samples. The numerical data from the nanoindentation experiments is tabulated below in Table 3.1 which presents in detail the change in mechanical properties of thin films with a change in slurry temperature.

Table 3.1 Mechanical properties of copper thin films before and after polishing.

| Sample | Modulus (Gpa) | Hardness (Gpa) |
|---|---|---|
| Unpolished Cu | 118.51 ± 3.72 | 1.22 ± 0.06 |
| Polished at 60 F | 136.38 ± 5.45 | 1.57 ± 0.087 |
| Polished at 70 F | 136.29 ± 4.77 | 1.66 ± 0.093 |
| Polished at 85 F | 143.45 ± 2.98 | 1.72 ± 0.068 |

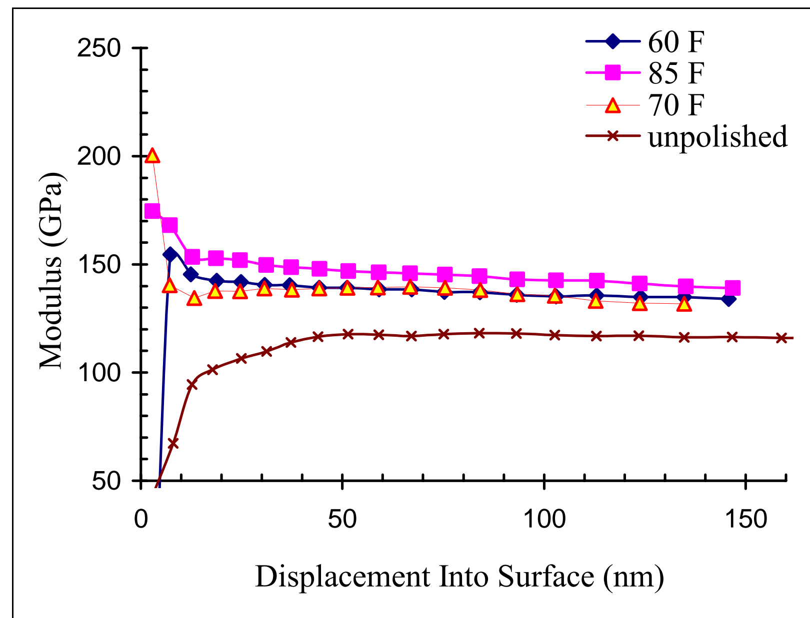


Figure 3.17 Modulus versus displacement for polished and unpolished copper samples



المنارة للاستشارات
www.manaraa.com

This confirms that the state of the copper surface does not change much during polishing at different temperatures [78]. This suggests that the changes in coefficient of friction are not concerned with the wafer surface characteristics, but mainly due to the mechanical properties of the pad and also some chemical interaction changes.

## 3.5 Conclusions

The effect of the interfacial temperature during the process of copper CMP was studied to better understand the polishing process. The role of the temperature on various aspects of CMP like the electrochemical behavior of the metal in the slurry, the surface modification of the metal during CMP, and the surface roughness has been investigated. An increase in the removal rate with an increase in interfacial temperature was observed. An increase in the coefficient of friction with rising interfacial temperature was attributed to larger area of contact at the interface due to pad softening. Electrochemical and XPS studies carried out at different temperatures indicate higher anodic reaction rates and higher dissolution rates of the formed surface oxides. The effect of temperature was not significant on the roughness of the copper surface post CMP. However, the scratch depths were deeper suggesting an increase in area of contact between pad and wafer at elevated temperatures. The With in Die Non-Uniformity (WIDNU) initially decreased from below room temperature to room temperature and then increased at elevated temperatures. The mechanical properties of the polished copper film however did not change with a change in temperature, suggesting no role of wafer surface in the observed change in tribology at the interface.



المنارة للاستشارات
www.manaraa.com

# CHAPTER 4: EFFECT OF TEMPERATURE ON TRIBOLOGY DURING CMP

## 4.1 Introduction

The tribology at the interface is dependent on a wide variety of aspects, such as the geometrical and material characteristics of the consumables involved in the polishing interface, the normal load, the sliding velocity, the interfacial temperature, etc. From the temperature study presented in the previous chapter it was learned that the coefficient of friction increases linearly with temperature. However, this result was deduced from experiments at a particular process parameter set. To deduce a comprehensive inference on overall dependence of friction on temperature, further experimental analysis at several process conditions is necessary. This forms the basis for the experimental investigation presented in this chapter. The following sub-sections, original contribution of this author, which were recently published as a section of a chapter in a text book [35], present a brief background on the effect of various consumable characteristics on CMP tribology.

### 4.1.1 Effect of polishing pad characteristics on CMP tribology

The grooves or perforations on the polishing pads have a significant impact on the polishing mechanism and outcome [79, 80]. Grooves or perforations on the pad allow for effective slurry flow under the wafer surface and thus are very crucial for an effective CMP process. Phillipossian et al. [37] carried out fundamental tribological studies during dielectric CMP on pads with different groove types at various slurry abrasive concentrations. The COF data was fitted as a function of Sommerfeld number and a



المنارة للاستشارات

www.manaraa.com

tribological mechanism indicator ' $\beta$ ' [37], an index to describe the change in coefficient of friction, was estimated. Preston's coefficient was calculated for each combination of pad type and slurry combination and was found to be correlating well with the coefficient of friction data. Stribeck curves were generated using the friction data for a variety of groove and pad types. From the shapes of individual curves, the authors deduced that some of the pads polished in partial lubrication regime, and some in boundary lubrication at lower Sommerfeld numbers and transitioned to partial lubrication regimes. Consistent removal rates and uniformity were observed as long as the polishing regime is in boundary lubrication regime. But polishing is aggressive in the boundary lubrication regime (where the particles abrade the wafer surface and a solid contact exists between pad and wafer) which might induce delamination during CMP for next generation ICs where mechanically weak low K dielectrics are integrated with copper. Analyses of Stribeck curves, Preston's coefficient, COF, and tribological mechanism indicator correlating each other helps to understand the polishing mechanisms. Such an analysis not only helps in the process development but also provides useful feedback to the pad development manufacturers.

### 4.1.2 Effect of slurry characteristics on CMP tribology

Abrasive particles in the slurry provide a majority of the mechanical component during CMP, whereas the slurry chemicals modify the exposed copper surface. Thus, both the slurry chemicals and the abrasive particles play a major role in the abrasion process and the interface tribology. Li et al [81] have studied the effects of slurry surfactant, abrasive size, and abrasive content on the tribology and kinetics of copper



المنارة للاستشارات
www.manaraa.com

CMP. They measured the friction coefficient at the interface during copper CMP using different slurry samples with varying chemical and abrasive characteristics, and generated Stribeck curves. From their results, it was concluded that the effect of slurry abrasive weight percentage had no effect on the tribological mechanisms of polishing, but the slurry particle size was shown to have a significant effect. They also concluded that the presence of surfactant significantly lowers the coefficient of friction. They stated that the removal rate during copper CMP correlated more with the variation of frictional forces (stick-slip) rather than the COF value itself. Investigations in the past also emphasized the effect of various additives of the slurry on the tribology during CMP [82, 83]. It was observed that the presence of a flocculent reduces the surface frictional force. Also, the ionic strength of the slurry has a significant impact on the frictional force. It can be seen from these works that the slurry characteristics in terms of abrasive content, particle characteristics, and the presence of surfactant used to provide better dispersion of particles, and ionic strengths of the slurries have an effect on friction. This is where the present research proves beneficial as it studies the effect of oxidizer and slurry pH (slurry buffer) on coefficient of friction, which deals with the electrochemical interaction of copper-slurry system.

### 4.1.3 Effect of wafer contour characteristics on CMP tribology

Besides process consumables like polishing pad and slurry characteristics, the geometrical shape of the wafer being polished also has an effect on the tribological interaction. The wafer contour determines the area of contact between the wafer and pad along with the abrasives. Thus, the amount of surface asperity interaction and the particle



المنارة للاستشارات
www.manaraa.com

wafer interaction depends also on the wafer contour. The fluid film that is in contact with the wafer surface also is dependent on the contour. Scarfo et al., [25] conducted polishing tests at different process conditions on different wafer samples with concave, convex and intermediate surface contours. It was seen that the change (due to process conditions) in coefficient of friction changes with the shape of the wafer. It was shown in their results that the pressure experienced by the wafer at different applied pressures and velocities changes with the shape of the surface. Pressure changes have been noted the most for concave shaped wafers. Also, it was shown that the coefficient of friction changes were quite significant with change in normal pressure for concave shaped and near flat surfaces. This explains the importance of the nature of the contact in the context of tribology and polishing mechanism.

Keeping in view the above mentioned effects of various process consumables, an in-depth study of the effect of the nature of the copper-slurry interaction and the effect of temperature on pad conditioning process on the interface tribology is performed as a part of this research work. The impact of a change in pad conditioning temperature on the subsequent copper CMP performance in terms of both interface tribology and post CMP surface characteristics is also presented. Thus, this chapter includes a detailed investigation on the influence of both process parameters and consumable characteristics on the CMP tribology.



المنارة للاستشارات
www.manaraa.com

### 4.2 Experimental methods and materials

Copper blanket thin films were polished at different slurry temperatures to determine the dependence of coefficient of friction on slurry temperature. Polishing experiments were carried out on the CETR bench top CMP tester. The contact interface is constituted of a 6” (15.25 cm) polishing pad coupon on a revolving platen and a 1” wafer coupon as the upper specimen. Cabot 5001 copper polishing slurry was continuously fed into the interface and the slurry temperature was varied from 18.3 $^{o}$C to 30 $^{o}$C, which simulates the increase in temperature at the interface. The slurry temperature was controlled for each experiment during the whole project by monitoring and maintaining the temperature at a specific value within a 0.1 $^{o}$C variation using a hot plate and temperature controller from Corning Inc.

Table 4.1 Process parameters for the study of effect of temperature.

| Parameter | Value |
|---|---|
| Polishing Pressure | 2, 3, and 4 psi |
| Platen velocity | 100 and 250 RPM |
| Slurry flow rate | 75 ml/min |
| Polishing Pad | IC 1000 K grove polishing pad |
| Slurry Temperatures | 18.3 $^{o}$C, 21.1 $^{o}$C, 23.8 $^{o}$C, 26.6 $^{o}$C, 29.4 $^{o}$C |

Further, various types of slurry combinations were employed to investigate the contributions of mechanical and chemical components of the CMP process on the coefficient of friction and surface interactions. The weight concentration of the abrasive



المنارة للاستشارات
www.manaraa.com

particles, peroxide percentage in the slurry, the slurry buffer (ammonium hydroxide in this case) present in the slurries was changed during the polishing experiments. The average size of the silica abrasive particle used in these slurries was 40 nm in diameter manufactured by Fuso Chemical Co., Ltd. Coefficient of friction data during polishing with various slurries was estimated at three different pressures keeping constant platen rotational speed. Coefficient of friction was determined *in-situ* by taking the ratios of the normal and the lateral loads monitored continuously during the polishing experiments. The detailed description of the polishing machine and the signals monitored during the process is provided elsewhere [69, 85]. The details of the process parameters used for the coefficient of friction experiments are given in Table 4.2 below.

Table 4.2 Process parameter conditions for slurry chemical experiments

| Parameter | Value |
|---|---|
| Peroxide concentrations | 0, 2.5 %, 5 % and 7.5 % by weight |
| Component for slurry pH | NH4OH – 5 % by weight<br>10 mM Acetic acid/Sodium Acetate |
| Pressures | 1, 2, and 3 psi |
| Platen velocity | 200 RPM |
| Slurry flow rate | 75 ml/min |
| Pad | IC 1000 K grove polishing pad |

The electrochemical cell for potentiodynamic polarization experiments, to study the effect of slurry buffer on the copper surface, consisted of an Ag/AgCl/KCl saturated



المنارة للاستشارات
www.manaraa.com

reference electrode with platinum strip as counter electrode and a diced strip of copper thin film coated silicon wafer as working electrode. The back and sides of the wafer were isolated from electrical and chemical contact by coating it with an insulating epoxy material. The electrodes were placed at least 50 mm apart from each other in the electrolyte. A PARSTAT 2263 model advanced electrochemical system manufactured by Princeton Applied Research was used for polarizing experiments of the copper sample. Current density data was collected for an applied potential range of -0.3 Volts to 0.9 Volts scanned at a speed of 0.166 mV/sec.

## 4.3 Results and discussion

### 4.3.1 Effect of process parameters and slurry temperature

Coefficient of friction (COF) is defined as a ratio of shear to normal force (COF= $\frac{F_s}{F_N}$; where $F_s$ is the shear force and $F_N$ is the normal force). COF data collected during polishing at different temperatures and different process conditions is plotted in the figures 4.1 and 4.2. It can be noted from the figures that the coefficient of friction decreases with increase in both pressure and the platen velocity. The observed decrease in COF with increase in pad velocity can be attributed to a thicker slurry film at the interface at higher velocities, thus resulting in effective lubrication at the interface. However, the decrease in COF with pressure is against the popular theory that the COF increases with increase in down force in boundary and partial lubrication regimes. The observed decrease in COF with increase in polishing pressure might be due to the elastic deformation of the pad surface asperities, in which case the coefficient of friction varies



المنارة للاستشارات
www.manaraa.com

as load$^{-1/3}$ or load$^{-1/4}$ according to the adhesion theory of friction [33, 86]. This behavior of coefficient of friction with down force is consistent with previous studies conducted on the bench-top tester [87, 88].

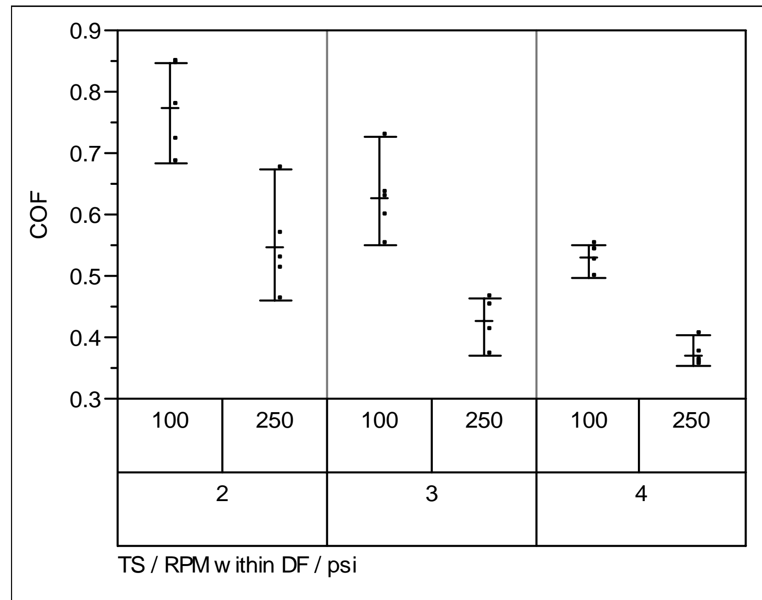


Figure 4.1 Effect of pressure and velocity on coefficient of friction during copper CMP

Also, according to the study by Scarfo et al. [25], the contour of the wafer surface, if it is concave or flat, results in a decrease of COF with increase in normal load. This was attributed to the suction of concave contours and development of positive pressures under the wafer at high pressures, resulting in decrease of COF. This suggests that the nature of area of contact during the polishing process might have influenced the friction characteristics to behave against the conventional trend.



المنارة للاستشارات
www.manaraa.com

Another plausible explanation for the decrease in COF with increase in down force is due to the viscoelastic nature of the polyurethane pad material. The second order normal reaction from the pad increases upon increase in applied down force. Also, the increase in shear force increases the second order normal reaction [7]. This increase in second order normal reaction adds up to the normal reaction (see equation 4.1) of applied force decreasing the coefficient of friction.

$$COF = \frac{F_{shear}}{F_{FN} + F_{SN}} \qquad [4.1]$$

Where, $F_{FN}$ is the first order elastic normal reaction (recovery) component of the normal force; $F_{SN}$ is the second order normal reaction; $F_{shear}$ is the shear force

According to the work published by Maria Ronay [89], the second order normal reaction increases with increase in both down force and shear force, thus making the denominator bigger than the numerator. This explains an overall decrease in the values of COF with the increase in the down pressure.

Upon plotting the coefficient of friction with P*V (see figure 4.2), a decreasing trend of COF with increasing P*V was noted. This was consistent at different slurry temperatures. This unconventional trend is attributed purely to the nature of pad surface asperity deformation without any role of slurry chemistry or abrasive particle characteristics. This was confirmed when the exact behavior was observed (see figure 4.3) when a glass piece was polished using de-ionized water using the same polishing pad and process conditions at the same flow rate. This decreasing COF with P*V suggests an inverse relation between coefficient of friction and removal rate.



المنارة للاستشارات
www.manaraa.com

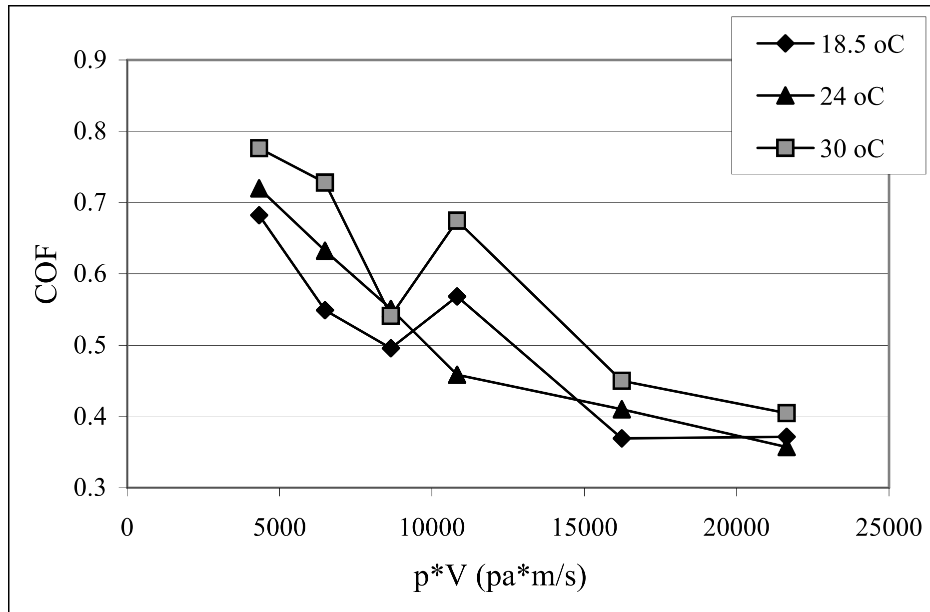


Figure 4.2 COF versus p*v during copper CMP using commercial copper slurry

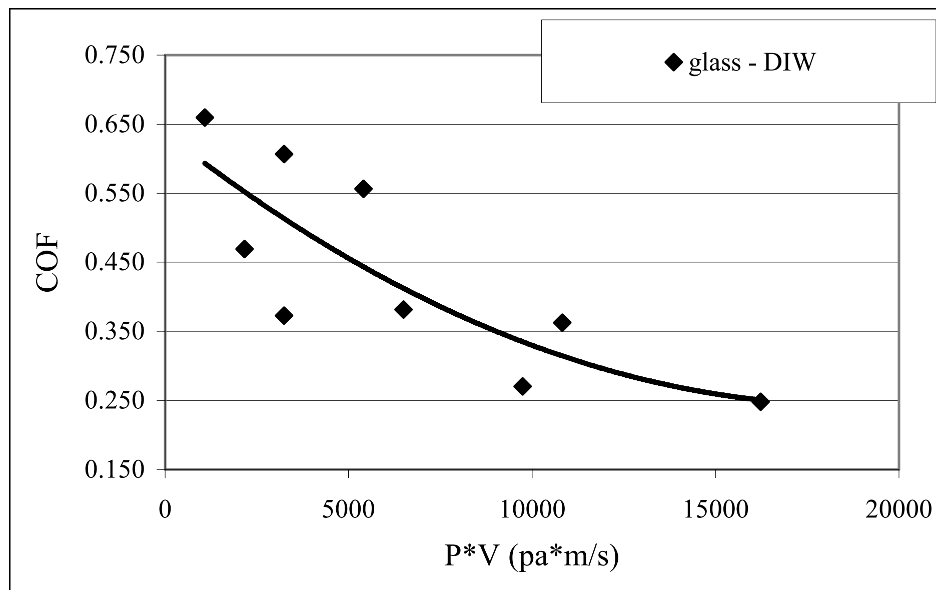


Figure 4.3 COF versus p*v during glass polishing using de-ionized water.

The coefficient of friction data was plotted as a variability chart to explain the role of process parameters more effectively. Figure 4.4 shows the dependence of COF on



المنارة للاستشارات
www.manaraa.com

slurry temperature at different process conditions. From the figure it can be seen that the effect of temperature on COF was observed only under certain process conditions. Figure 4.4 suggests there exist three regimes – namely scattered, monotonic increase, and ineffective [90]. The effect of temperature on COF seems to be scattered (not correlated) at low pressure regime, monotonic increase during medium pressure, and absent during high pressure regime. However, from the statistical (ANOVA) analysis of the data, it was found that platen velocity had the major effect as compared to down force and slurry temperature. This proves that process parameters like pressure and platen velocity dictate the effect of temperature on the coefficient of friction.

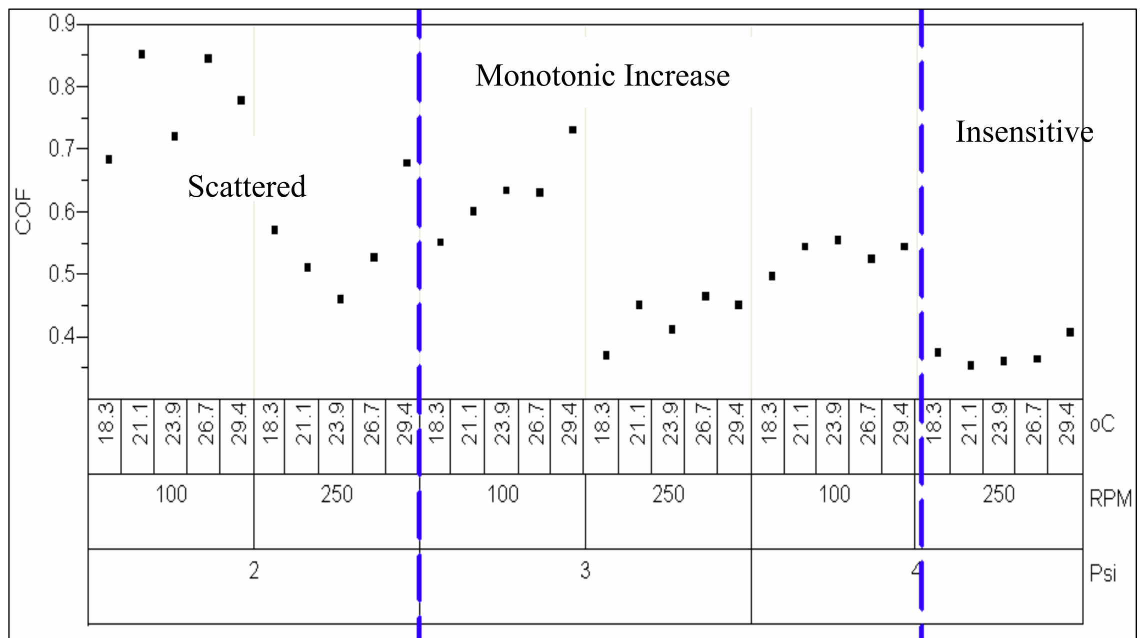


Figure 4.4 Dependence of coefficient of friction with slurry temperature at different process conditions.

The increase in coefficient of friction with temperature in the monotonic regime can be attributed to various factors. Firstly, the change in mechanical component (pad



المنارة للاستشارات
www.manaraa.com

property) being one of the factors due to an increase in tan (delta) of the pad with temperature [67]. Secondly, copper oxidation reaction is known to be sensitive to temperature due to its lower activation energy [44, 91], which suggests that another factor that influenced the COF could be the increase in surface oxidation and dissolution due to increase in temperature [84]. This hypothesis leads to further study of dependence of coefficient of friction with varying oxidizer concentrations and slurry chemistries.

### 4.3.2 Effect of oxidizer on CMP tribology

Further experimentation was carried out to study the effect of changes in slurry chemistry on COF during copper CMP process. In this regard, the concentration of hydrogen peroxide in the slurry was changed and its effect on COF was studied. COF values obtained from these experiments are presented in figure 4.5.

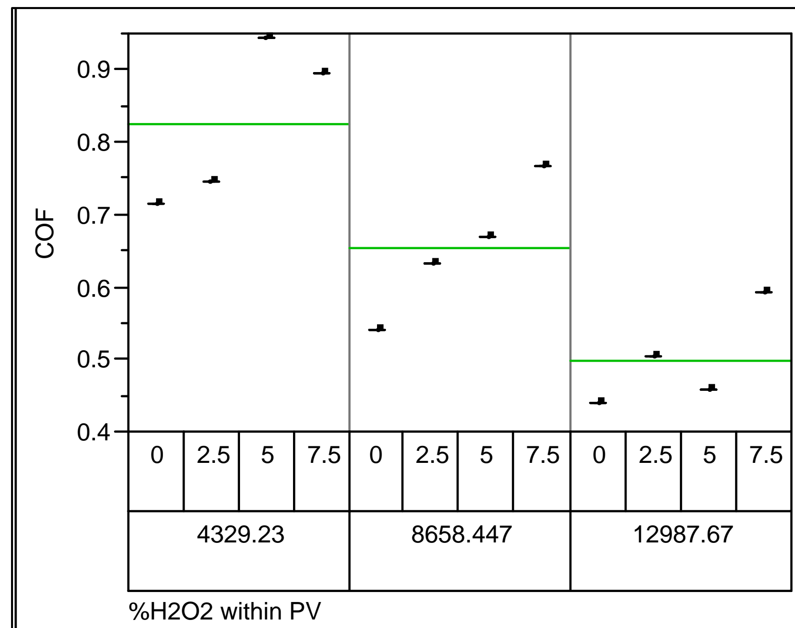


Figure 4.5 Effect of % concentration of hydrogen peroxide on coefficient of friction at different p*v values.



www.manaraa.com

The results indicate that COF increases with increasing peroxide concentration in the slurry. The surface oxidation of copper is least in the absence of hydrogen peroxide. It has been reported in the past that the surface oxide layer increases as the peroxide concentration in the slurry increases [63, 92].

The surface oxide layer is not totally disrupted by the abrasive particles at higher concentrations of peroxide, and dynamic repassivation of copper layer occurs. Thus, a surface oxide layer is always present at higher concentrations as compared to the exposed metallic copper surface at lower concentrations. The increase in the coefficient of friction could thus be attributed to such a change in the nature of surface layer at the interface. Another reason for the increase in coefficient of friction, which is related more to the consumable development than the process mechanism itself is the surface chemical decomposition of polyurethane material as reported by Obeng et al [93]. According to their study, it was concluded that the polyurethane material was decomposed at higher concentrations of peroxide and the change in pad properties were noted from DMA of the as received and slurry soaked pads.

From the above discussion it is conclusive that chemical interaction at the copper-slurry interface plays a significant role in the magnitude of coefficient of friction at the interface. This conclusion leads the way for a further detailed study of the chemical component on the coefficient of friction. The effect of slurry pH on coefficient of friction using acidic, basic and neutral slurries is studied and the results are correlated with the electrochemical interaction of the copper with slurry at different pH conditions.



المنارة للاستشارات
www.manaraa.com

### 4.3.3 Effect of slurry chemistry on CMP tribology

Polishing experiments to study the effect of the slurry component that maintains pH and its interaction with the wafer surface on the COF were conducted. Cu CMP employing slurries with and without the slurry buffer was carried out. Thermally grown oxide ($SiO_2$) film was also polished using the slurry containing ammonium hydroxide as slurry component formulated for copper CMP. From the results of these experiments (see figure 4.6), it was observed that the trend of coefficient of friction was independent of the pH of the slurry, indicating that the majority of the contribution is from the mechanical component of polishing. However, the individual magnitudes differed significantly with the change in chemical nature of the slurry, including presence and absence of a buffer and oxidizer and the acidic or basic nature of the slurry.

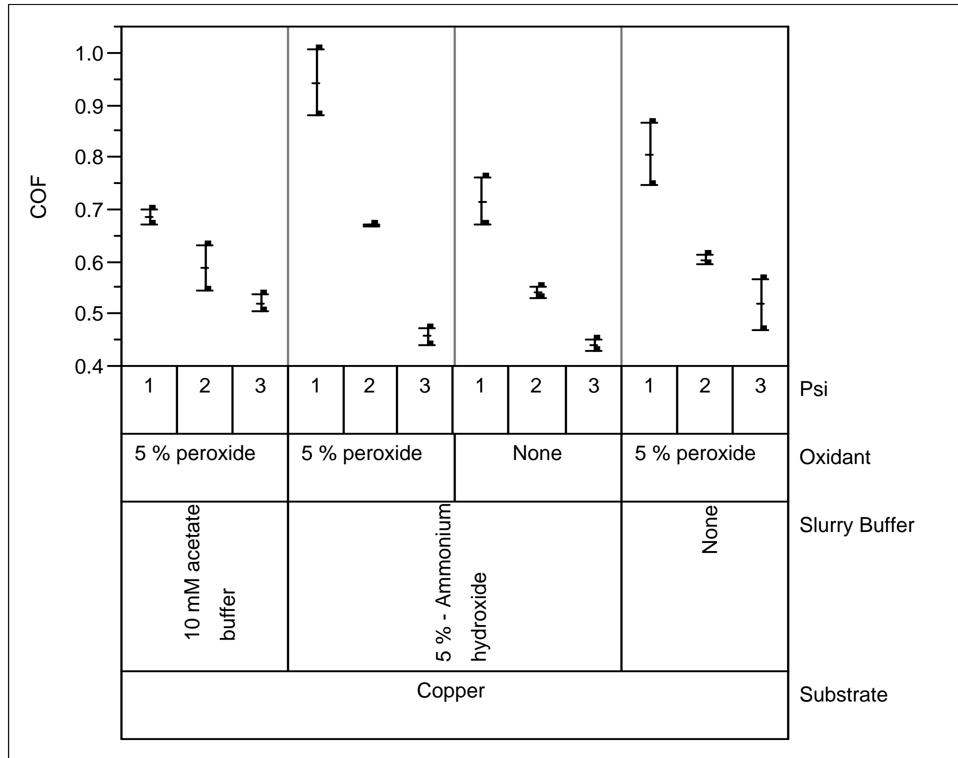


Figure 4.6 Effect of slurry chemistry on the coefficient of friction during CMP



المنارة للاستشارات
www.manaraa.com

These results were correlated with the potentiodynamic polarization measurements, which show the surface electrochemical interactions of copper in various chemical environments (see figure 4.7). The corrosion potential and current densities from the potentiodynamic polarization curves are presented in Table 4.3. From the table it could be seen that the corrosion potential becomes nobler when acidic or no buffer is used as compared to the ammonium hydroxide buffer. The corrosion potential data correlates well with the coefficient of friction data. Also, from the polarization experiments it was observed that the corrosion current density is higher for ammonia based slurry. This suggests that formation and dissolution of oxide layer is significantly higher for the ammonia based slurry, where s the passivated oxide layer does not dissolve into the slurry in acidic or no buffer systems.

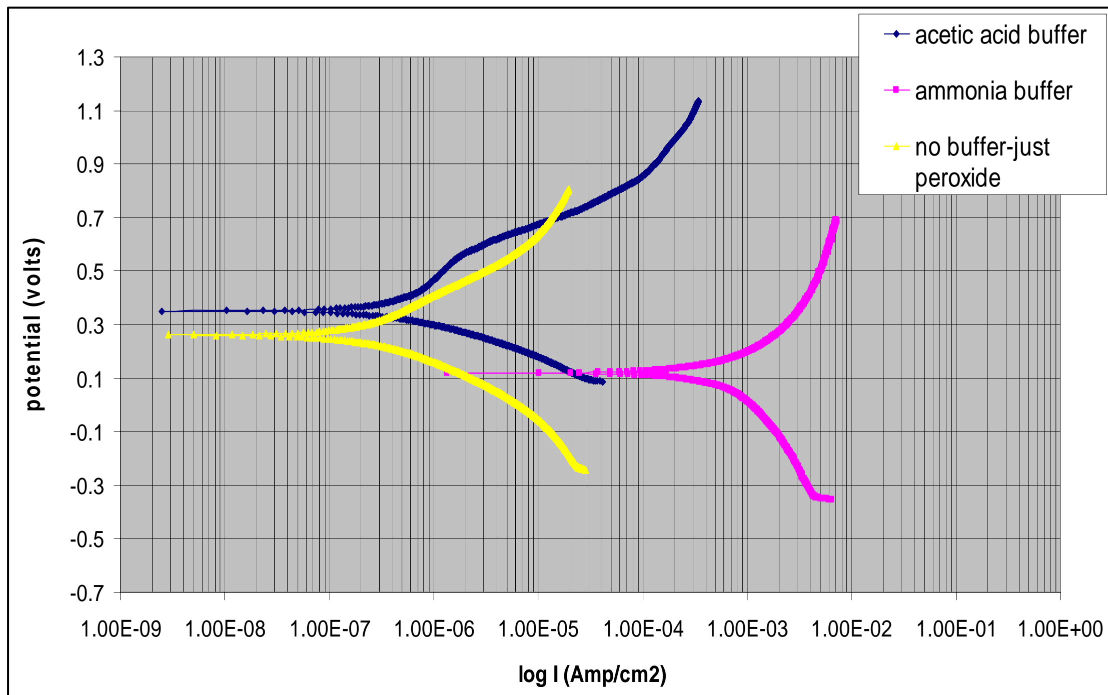


Figure 4.7 Potentiodynamic polarization scans for copper-slurry systems using various slurry chemistries.



المنارة للاستشارات
www.manaraa.com

Table 4.3 Corrosion potential and current density from polzarization experiments.

| Slurry chemical | Ecorr (mV) | Estimated Icorr (mA/cm2) |
|---|---|---|
| 5% $NH_4OH$ | 120 | 1.5 |
| No buffer (just 5% $H_2O_2$) | 261 | 1.50E-03 |
| Acetic acid buffer | 351 | 2.50E-03 |

Thus, it could be seen that the change in surface oxidation phenomenon plays an important role on surface tribology. To further confirm this, we studied the effect of oxidation of the wafer surface on the coefficient of friction. Copper and thermal oxide wafers were polished with copper oxidizing slurry. Thermal oxide wafer polished using copper chemistry exhibited a higher coefficient of friction as compared to the copper wafer (see figure 4.8).

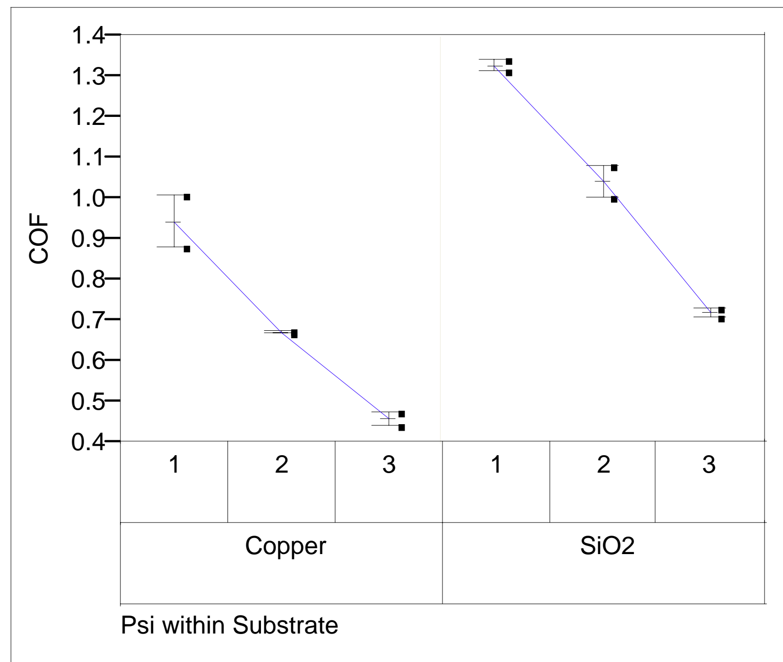


Figure 4.8 Effect of substrate (polished with 5 % $NH_4OH$ + 5 % $H_2O_2$ + 5 mM BTA) on COF during CMP



المنارة للاستشارات
www.manaraa.com

This is attributed to the absence of any surface modified layer in the case of silicon dioxide film and the formation of a softer oxide layer in the case of copper wafer.

### 4.3.4 Effect of temperature on pad conditioning process

From the above results, it was seen that the pad surface asperities are highly sensitive to temperature. In such a case, since pad conditioning process is concerned with the pad surface asperities, it is hypothesized that the change in conditioning temperature will have a pronounced effect on the conditioning process end point (effectiveness of pad conditioning) and at the same time will impact the pad wear rate (aggressiveness of pad conditioning). Before going further with the experimentation, the following discussion original contribution of this author, recently published as a section in a chapter of a text book [35] will provide a necessary introduction to the pad conditioning process and its significance to CMP process.

#### 4.3.4.1 Pad conditioning process

As the surface of a new (unconditioned) polishing pad is in general smooth and wets poorly, it does not provide good slurry transport to the pad/wafer interface. Pad conditioning is therefore necessary to open up the closed cells in the polyurethane pad to provide a consistent polishing surface throughout the pad's lifetime. Under-conditioned pads are prone to have a glazing effect on their surfaces, resulting in reduction of surface roughness. Such a reduction in surface roughness reduces the removal rate and increases non-uniformity. Over-conditioned pads result in excessive loss of pad material, which dramatically reduces the pad lifetime. Pad replacement becomes necessary due to two



المنارة للاستشارات
www.manaraa.com

reasons: changes in physical properties of the pad, and changes in grove dimensions because of pad wear. Replacing the pad prematurely would increase the cost of consumables and the machine down time, which affect the throughput of CMP process and overall process operational costs and thus the productivity index of a manufacturing process. Hence, it is crucial to understand the governing factors of an effective conditioning process. Pad conditioning has been proven to have a significant effect on the removal rate during CMP processes. Pad conditioning process can be optimized by monitoring the tribological aspects during the process. Coefficient of friction between the conditioner and the pad surface and the pad material removal rate (wear) are two critical parameters, which upon monitoring will provide sufficient information regarding the process. Many aspects such as pad conditioner performance, optimization of the conditioning process variables, etc., can be achieved with the help of tribometrology.

An important aspect of pad conditioning which has not been studied is the role of temperature. As both conditioning and polishing processes are by nature abrasion processes, heat energy is dissipated at the interface, which elevates the temperature at interface. CMP pads are highly sensitive to the temperature changes as pad is a polymer material whose properties change significantly with temperature, and chemical kinetics during polishing are well known to be affected by temperature. Understanding the effect of temperature on pad conditioning process is possible by monitoring the tribological aspects of the process. In the present study, the effect of pad conditioning temperature on the effectiveness and aggressiveness of conditioning process and on dishing and erosion during subsequent CMP process was investigated. Long pad conditioning experiments



المنارة للاستشارات
www.manaraa.com

using water at different temperatures were carried out and subsequent copper CMP was performed.

#### 4.3.4.2 Pad conditioning experiments

The second series of experiments with pad conditioning at different temperatures was carried out with subsequent copper polishing. The temperatures during conditioning were maintained constant (~ 0.5$^o$C) by constant monitoring of the water temperature in the beaker and subsequent adding of cold or hot water whenever necessary. Patterned copper polishing was conducted soon after the conditioning to study the effects of changes in the conditioning process on CMP performance in regard to dishing and non-uniformity. During the short period of time between the conditioning and polishing process, the polishing pad surface was maintained at the conditioning temperature by continuous dispense of water at that particular temperature. The process parameters for the pad conditioning experiments are tabulated in Table 4.4.

Table 4.4 Consumables and process parameters in polishing experiments

| Description | Value |
|---|---|
| Conditioning pressure and Pad RPM | 4 psi and 150 RPM |
| Polishing Pad | IC 1000 perforated/ Suba IV sub pad |
| Water Flow Rate during conditioning | 200 ml/min |
| Pad conditioning temperatures | 10$^o$C, 20$^o$C, 24$^o$C, 28$^o$C |
| Hard conditioner (Outer dia – 4" and inner dia - 3") for Ex-situ condition | Ring Conditioner by TBW industries – 200 grit size. |



المنارة للاستشارات
www.manaraa.com

#### 4.3.4.3 Results and discussion

The pad surface temperature transients associated with conditioning experiments are presented in Figure 4.9. From the figure, different levels of conditioning temperature can be noted. Coefficient of friction between conditioner and pad surface was continuously measured during the pad conditioning experiments.

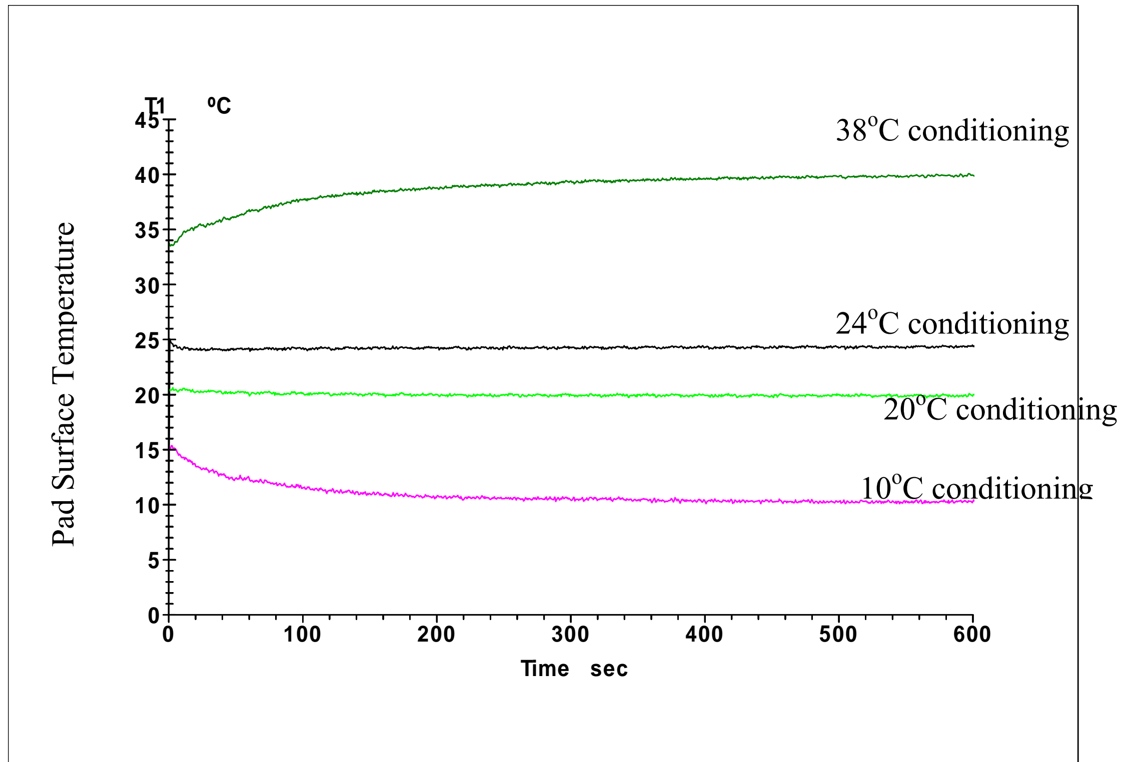


Figure 4.9 Pad surface temperature during conditioning at different temperatures.

The mean values of the coefficient of friction, along with standard deviation, are plotted against the pad conditioning temperature in Figure 4.10. It can be seen that friction between the pad and conditioner increased with increase in temperature during conditioning. The observed increase in pad coefficient of friction might be due to increase in surface contact area between the conditioner and the pad. This increase in contact area results in reduction of overall load experienced by the pad. It is the nature of



المنارة للاستشارات
www.manaraa.com

polymer materials that the coefficient of friction when in contact with a hard inelastic material increases with reduction in applied load. This justifies the increase in coefficient of friction with increase in temperature.

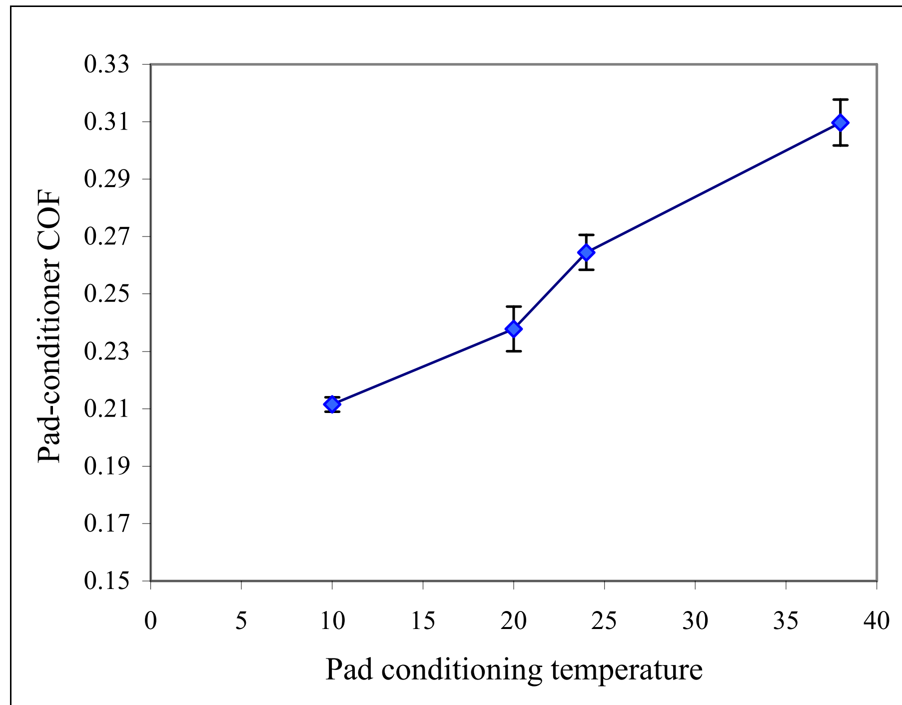


Figure 4.10 Pad coefficient of friction measured in-situ during pad conditioning at different temperatures

The pad-conditioner coefficient of friction curves plotted versus time obtained during conditioning are presented in Figure 4.11. The coefficient of friction stabilized faster during conditioning at lower temperatures than at higher temperatures. The pad wear and resulting exposure fresh pad surface during conditioning was easy at lower temperatures. This is the reason for faster stabilization of COF at lower temperatures. At elevated temperatures, the pad surface asperities become soft and get elastically deformed. As the pad surface asperities do not undergo plastically deformation (generation of rough



المنارة للاستشارات
www.manaraa.com

surface) easily at higher temperature it takes a longer time to stabilize the COF and completion of the conditioning process.

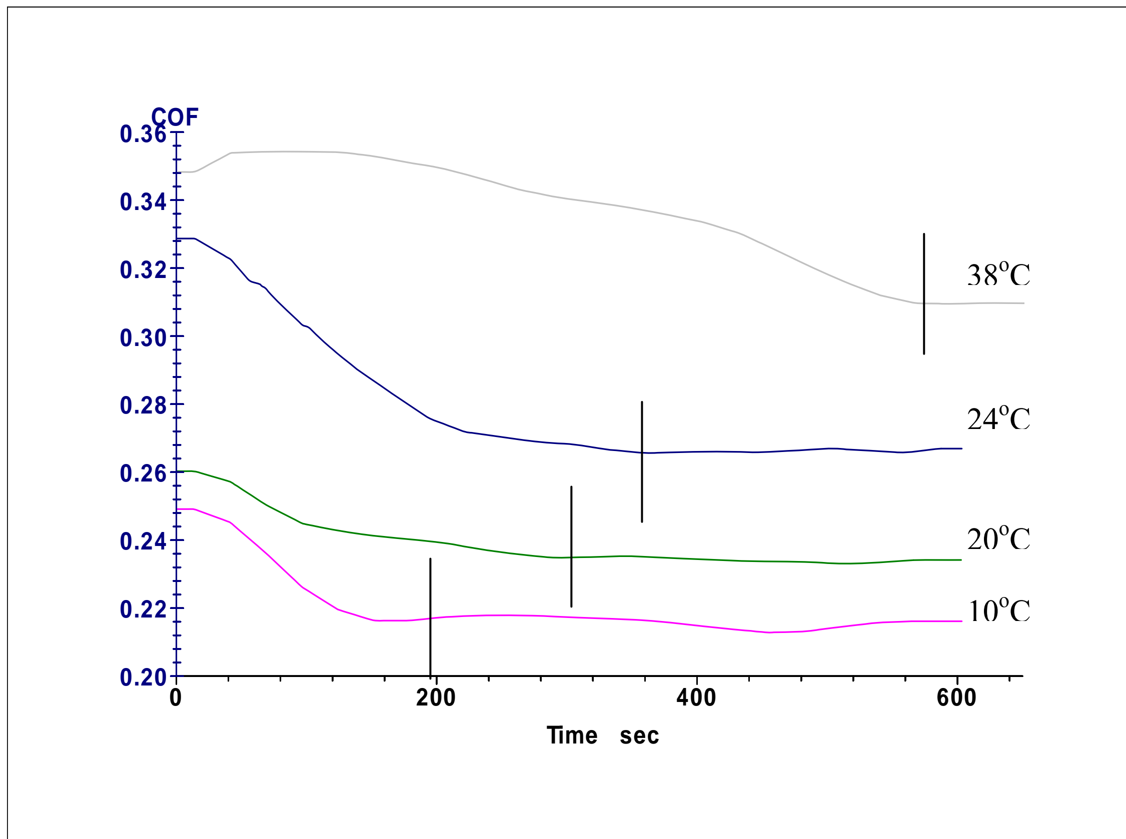


Figure 4.11 Coefficient of friction curves during pad conditioning at different temperatures

This observation can be mainly attributed to typical sensitivity of viscoelsatic pad material towards temperature change. The stabilization of the coefficient of friction is a measure of the end of the conditioning process [94]. Thus, longer conditioning was required for full pad conditioning at higher temperatures.



المنارة للاستشارات
www.manaraa.com

Loss of pad material during conditioning is another aspect which affects the pad lifetime and also polishing performance. As the pad loss increases along with a variation in polishing performance pad lifetime decreases, and so, pads need to be replaced more often. This increases the cost of consumables and the machine down time, which in turn negatively affects the throughput of CMP process and overall process operational costs.

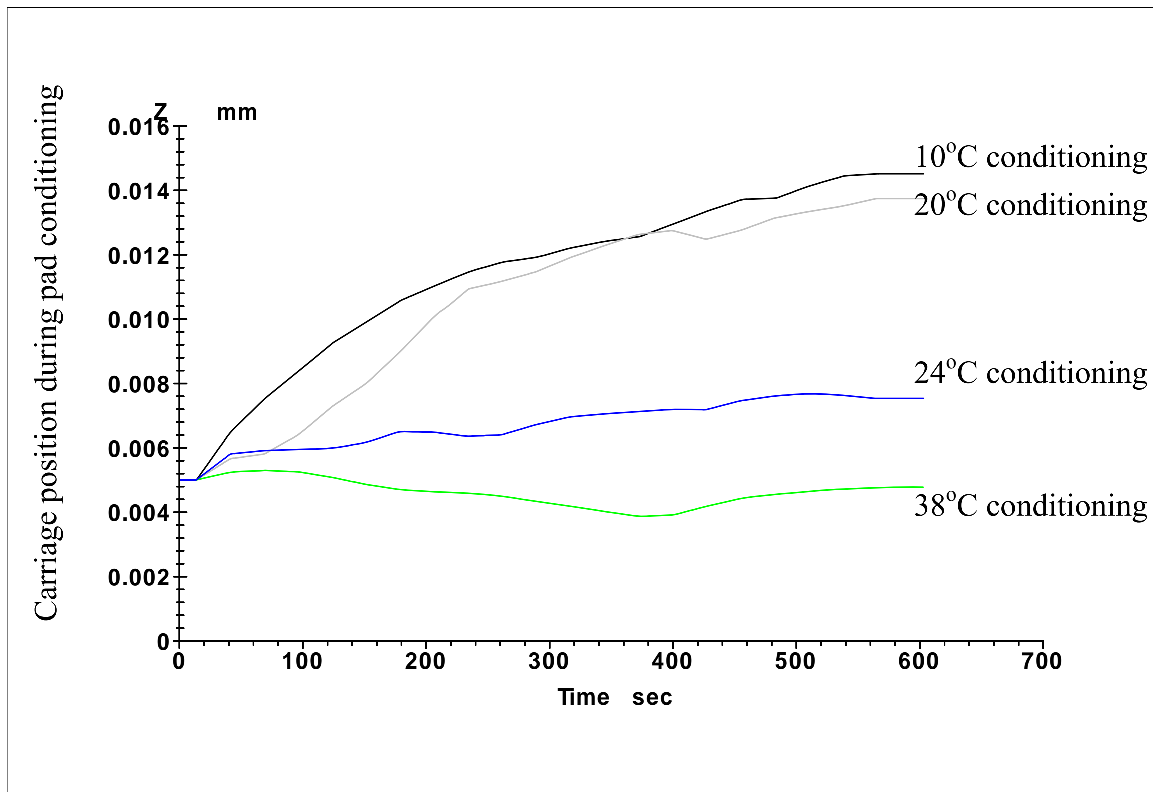


Figure 4.12 Carriage position during conditioning tests plotted versus time

Hence, it is crucial to monitor the pad loss during conditioning process. The real-time change in pad thickness and the pad cut rate during conditioning at different temperatures are presented in figures 4.12 and 4.13. The pad loss was high at lowest temperature and decreased thereafter with increase in water temperature. At elevated



المنارة للاستشارات
www.manaraa.com

temperature the pad cut rate was lower due to lower actual conditioning pressure resulting from higher surface contact area [85]. Also, the pad surface asperities deform elastically when they are soft at elevated temperatures. This prevents active abrasion and surface roughening process. This effect of softer pad surface asperities is indisputably evident from figure 4.12. The loss in pad thickness at 38°C was almost negligible compared to pad loss for conditioning process at 10°C. These observations indicate an aggressive conditioning process at lower temperatures, as compared to the elevated temperatures.

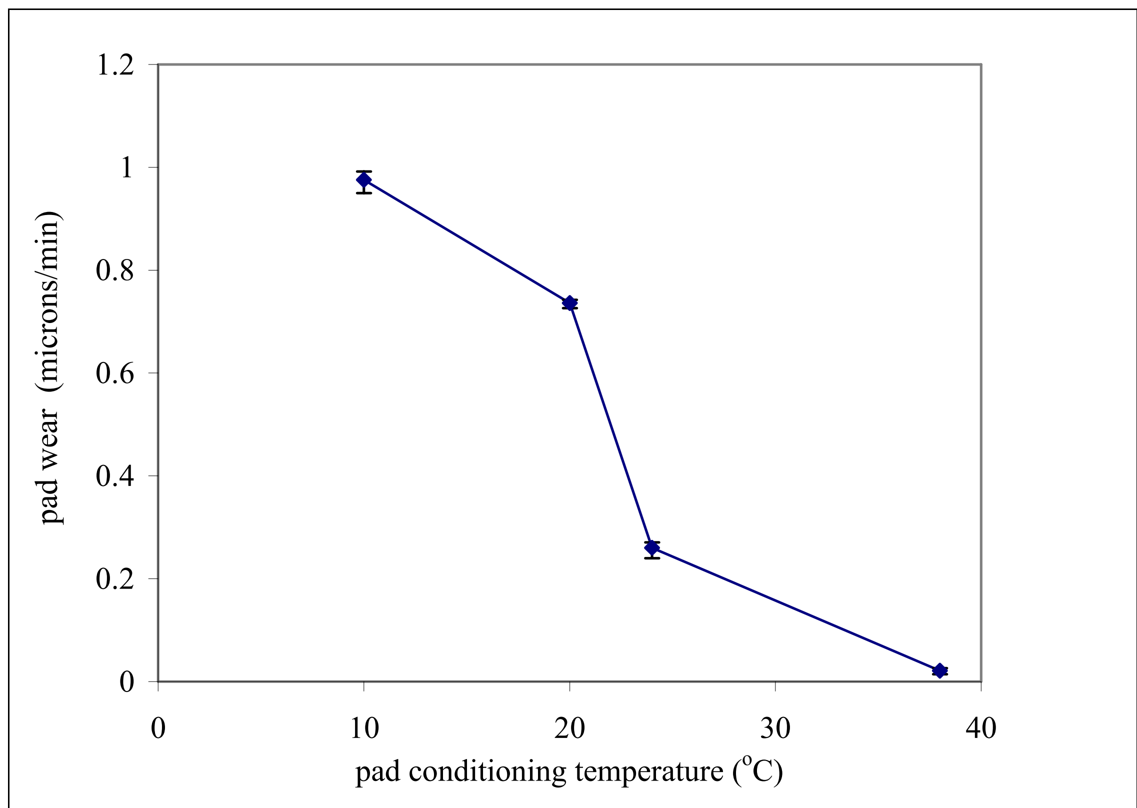


Figure 4.13 Pad wear rate versus temperature during conditioning.

To study the effect of the change in pad conditioning on CMP performance, patterned copper samples were subsequently polished. The process conditions for the



المنارة للاستشارات
www.manaraa.com

CMP experiments are tabulated in Table 4.5. Post CMP samples were accordingly analyzed for their dishing characteristics.

Table 4.5. Process parameter set for patterned CMP experiments.

| Description | Value |
|---|---|
| Wafer coupons 2” | 10,000 Å copper over patterned low-K dielectric |
| Slurry | I-cue 5001 copper slurry |
| Polishing Pressure | 4 psi |
| Polishing Velocity | wafer carrier – 95 RPM; polishing pad – 100 RPM |

The removal rate and coefficient of friction from these tests are plotted versus pad conditioning temperature as shown in figure 4.14. The coefficient of friction and removal rate values were higher when the pad was conditioned at temperatures below the room temperature. The removal rate and coefficient of friction values were the lowest at the room temperature and they rose as the temperature was elevated above the ambient temperature. The higher removal rate and coefficient of friction at lower temperature is attributed to the hardening of polishing pad surface asperities due to lower temperature. The pad surface asperities become hard and also they are less flexible at low temperatures due to the dependence of physical properties of polymer material on temperature. This will result in enhanced abrasion of thin film surface due to abrasive particles.



المنارة للاستشارات
www.manaraa.com

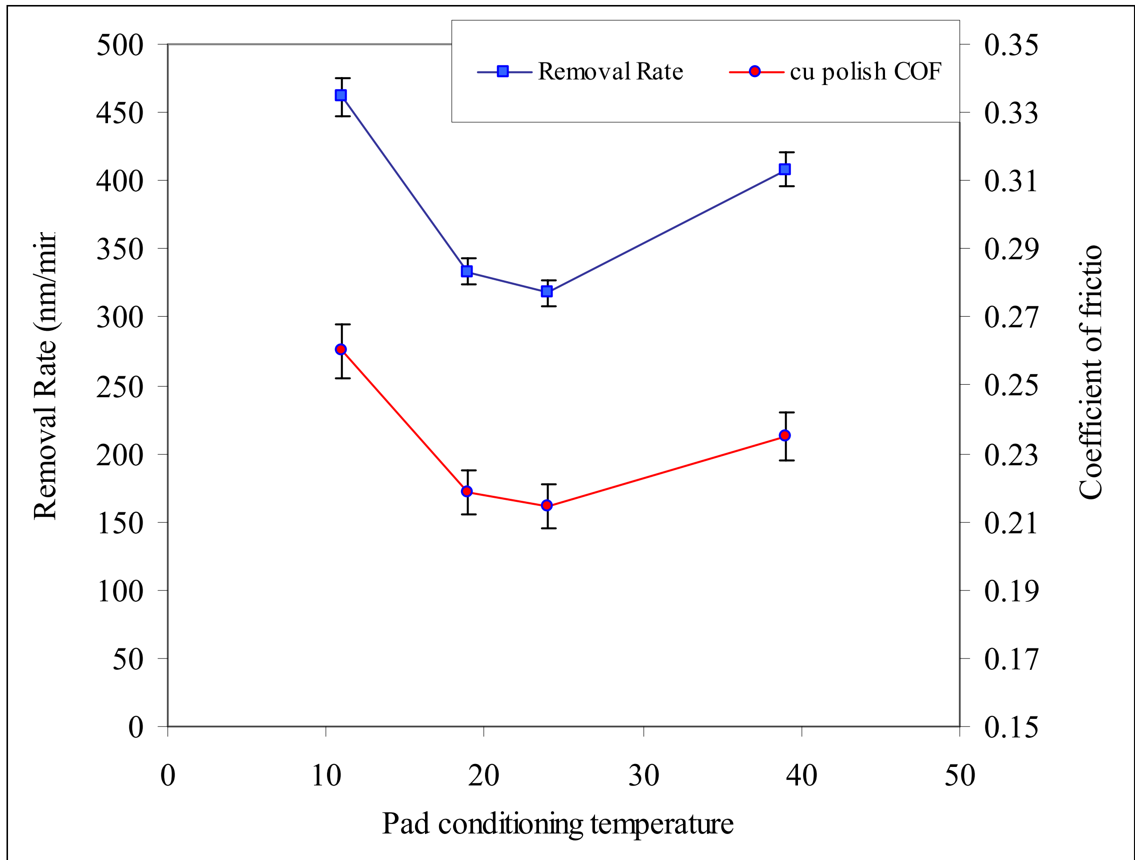


Figure 4.14 Removal rate and coefficient of friction measured during copper polishing after pad conditioning at different temperatures

Thus, pad-abrasive-wafer interaction at lower temperature is more effective, which dominates over the chemical reaction rate, which is expected to be slow at low temperature [45, 84]. On the other hand, at higher temperature the reactionkinetics of the slurry chemicals is high in accordance with Arrhenius relation [45] and hence a high polishing rate was observed. Even though the mechanism at higher temperatures is predominantly chemical kinetics dependent, there could also be a minor effect of increased area of contact due to softening of the pad surface asperities at higher



المنارة للاستشارات
www.manaraa.com

temperatures [41]. This increase in contact area results in increased shear force adding to increase in removal rate.

The dishing values on these samples were measured and found to be increasing with increase in pad temperature as shown in figure 4.15. It can also be noticed that the deviation from mean value decreased with increase in pad temperature. The standard deviation in figure 4.15 signifies the variation of dishing depths at different locations on the sample.

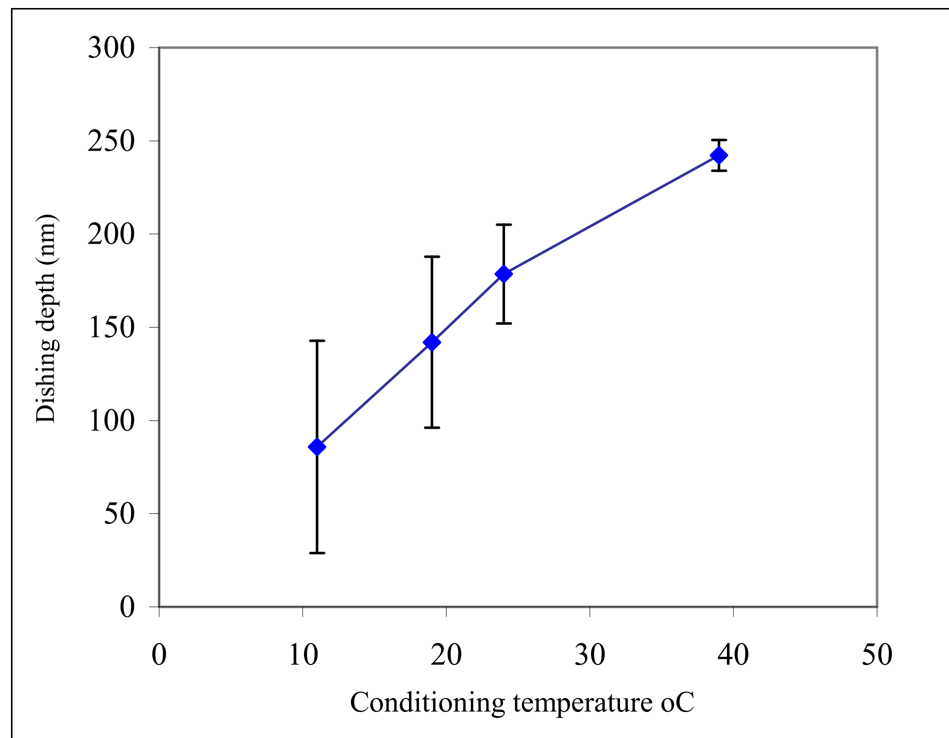


Figure 4.15 Dishing depth measured at 50 µm features for samples polished after pad conditioning at different temperatures



المنارة للاستشارات
www.manaraa.com

This indicates that the level of non-uniformity in the polishing process decreased considerably for the wafers polished after conditioning the pad at elevated temperatures. The fact that the absolute values of dishing increased with increase in pad temperature even with improved polishing uniformity, supports the earlier result that greater amount of dishing occurs when the increase in pad temperature is high.

## 4.4 Summary

Dependence of coefficient of friction on slurry temperature and slurry chemistry during copper CMP has been studied. From the results it was found that coefficient of friction during copper CMP decreases with increase in load and platen speed counter intuitive to the popular theory. This trend also indicates that the coefficient of friction and removal rate are inversely related. The effect of slurry temperature on coefficient of friction is observed only under certain specific process conditions. Kinematic parameters during CMP dictate the effect of temperature on surface tribology. Also from the results it was found that the chemical nature of the exposed surface layer affects the frictional properties during CMP. Friction at the interface increases with increase in peroxide content in the slurry. This result suggests that the increase in surface oxidation results in higher coefficient of friction. This could be one of the underlying reasons for an increase in coefficient of friction seen with an increase in slurry temperature. The slurry attack on the polishing pad surface could also be a reason for the change in tribology during CMP. The surface tribology is found to be influenced by the surface oxidation but not by the pH of the slurry medium. In summary, the coefficient of friction during copper CMP is



المنارة للاستشارات
www.manaraa.com

affected by slurry chemistry along with the mechanical component such as polishing pad and abrasive particle concentration.

During ex-situ pad conditioning, friction reached steady-state faster at lower temperatures comparing to the elevated temperatures, thus, full-conditioning at higher temperatures was longer. Higher removal rates and coefficient of friction between pad and wafer surface were noted at both very low and very high temperatures of conditioning. Post-CMP dishing increased with increase in the pad temperature. Pad temperatures during both conditioning and polishing play a major role in the generation of wafer defects like dishing and erosion during copper CMP process.



المنارة للاستشارات
www.manaraa.com

# CHAPTER 5: THERMAL MODEL-STEADY STATE HEAT CONDUCTION

## 5.1 Introduction

Chemical Mechanical Planarization (CMP) process needs to be optimized not only in regard to removal rate, pad conditioning and coefficient of friction but also in several other aspects such as defects during CMP as seen in the pad conditioning results of chapter 4. Process induced defects mainly related to pattern on the wafer surface such as dishing, erosion and metal loss need to be reduced in order to get good yields, which result in lower operational costs. The above mentioned defects are caused largely due to non-uniform pressure distribution and inconsistent material removal rates. Improving wafer-scale and die scale uniformity in polishing would reduce several defects concerned with wafer pattern densities and feature size. The thermal aspect of CMP, even though a significant factor affecting the process output, has not been researched as extensively as parameters like pressure, velocity, slurry flow rate, and other chemical aspects. The effect of temperature or heat dissipation at the interface could affect the polishing pad surface and the contact area during CMP, which thereby could induce polishing non-uniformities as observed in the pad conditioning studies presented in the previous chapter. Thus, studying the heat transfer mechanism at the interface and the subsequent rise of temperature on wafer surface is hypothesized to provide valuable insight into improving with-in wafer non-uniformity to a great extent.

Research work on temperature rise on the surface of polishing pad during interlayer dielectric and metal polishing, removal rate dependence on temperature and its



المنارة للاستشارات
www.manaraa.com

modeling, effect of slurry flow rate on pad temperature rise etc., has been carried out in the recent past to understand the role of temperature at interface on CMP performance. However, in all these research works, the reported temperature rise is either the average temperature on the pad surface or a predicted average temperature on the wafer surface or temperature rise at three isolated locations on the wafer. These works report the overall temperature rise but do not provide the information about the temperature distribution on the wafer surface. An analysis of the temperature distribution on the wafer surface after the polishing process reaches a steady state has not been researched till date. The temperature profile on the wafer surface as a function of radius and thickness will provide valuable insight into the extent of temperature rise at different locations on the wafer. Since the material removal rate during copper CMP is so sensitive to temperature, the temperature distribution over the entire wafer will significantly affect the uniformity of material removal over the entire wafer. Understanding the temperature profile will decrease the with-in-wafer non uniformity and thus improves yield by minimizing the number of faulty dies.

In this research, we model the conduction heat transfer mechanism at the interface after a steady state has been achieved by the polishing process. By solving the model, we present the temperature profile on the wafer surface as a function of wafer radius and thickness. The analytical modeling effort is supported with the finite element analysis using FIDAP package which can handle both conduction and convection heat transfer environments effectively. The coefficient of friction values at different pressures and velocities required to calculate the heat dissipation at the interface are obtained from copper polishing experiments conducted on a bench top tester.



المنارة للاستشارات
www.manaraa.com

## 5.2 Thermal model development

In this section, the thermal response of the wafer to a uniform heat flux at one boundary is examined as a non-homogenous steady state heat conduction problem. An exact analysis is performed using the method of separation of variables in a cylindrical coordinate system. The transformation of the heat conduction problem with non-homogeneous boundary conditions into one with homogeneous boundary conditions is essential for the analytical investigation.

Obtaining an expression for the steady state temperature distribution T(r, z) along the wafer surface undergoing polish and temperature distribution along its thickness is the most critical part of this research. With a substitution of $\theta(r,z) = T(r,z) - T_{atm}$, $\overline{q} = \frac{q}{k_S}$, $H_1 = \frac{h_1}{k_S}$ and $H_2 = \frac{h_2}{k_S}$ the equation describing the conservation of energy inside the solid can be written as [95]:

$$\frac{\partial^2 \theta(r,z)}{\partial r^2} + \frac{1}{r}\frac{\partial \theta(r,z)}{\partial r} + \frac{\partial^2 \theta(r,z)}{\partial z^2} = 0 \qquad \text{in } 0 \le r \le r_d,\ 0 \le z \le b \qquad (1)$$

The following are the boundary conditions.

$$\text{At} \quad z = 0, \quad \frac{\partial \theta(r,z)}{\partial z} + H_1 \theta = \overline{q} \qquad (2)$$

$$\text{At} \quad z = b, \quad \frac{\partial \theta(r,z)}{\partial z} = 0 \qquad (3)$$

$$\text{At} \quad r = r_d, \quad \frac{\partial \theta(r,z)}{\partial r} + H_2 = 0 \qquad (4)$$

Where $T_{atm}$ = atmospheric temperature (K); q = heat flux ($W/m^2$); $r_d$ = radius of the wafer (m);b = thickness of the wafer (m); $h_{1,2}$ = convection heat transfer coefficient at the



المنارة للاستشارات
www.manaraa.com

interface and at the wafer edge ($W/m^2K$); r, z =coordinate directions; $k_s$ = thermal conductivity of the solid. (W/mK)

The above problem was solved analytically with the help of the principle of separation of variables, which involved Bessel functions. It was necessary to solve Eigenvalues $\beta_{m's}$ or all positive roots of the following equation:

$\beta_m J_0^{'}(\beta_m, r_d) + H_2 J_0(\beta_m, r_d) = 0$ where $J_0$ is the Bessel function of zeroth order (5)

The final solution for the temperature distribution was derived with initial substitution

$$T(r,z) = T_\infty + \frac{2\bar{q}}{r_d^{\,2}} \sum_{m=0}^{7} \frac{\beta_m^2 J_0(\beta_m, r)\sinh\beta_m(b-z)}{J_0^2(\beta_m b)\cdot(H_2^2 + \beta_m^2)[H_1\cosh\beta_m b - \beta_m \sinh\beta_m b]} \cdot \int_{r=0}^{r_d} r \cdot J_0(\beta_m, r)dr \quad (6)$$

where $\beta_{m's}$ the eigen values; for m = 0 to 7 are β = [162.82, 380.20, 609.03, 844.39, 1083.86, 1325.76, 1813.57, 2058.62]

The experiments necessary for the coefficient of friction values and also for the validation of the model predictions were carried out on the bench top CMP tester. The tester holds a 6 inch polishing pad and a 2 inch silicon wafer. Real time coefficient of friction was measured using a dual force sensor which measures lateral and normal forces. Features of the bench top tester are provided in detail in previous publication [69, 85]. Before actual polishing of copper wafers, the Rodel IC1000 polyurethane perforated pad was conditioned for 20 minutes and a couple of dummy samples were polished to bring the pad surface condition to a steady state and thereafter the pad was conditioned for 5 minutes in between each polishing experiment. Pad conditioning was carried out using DI water at 1 psi and 100 rpm pad rotation keeping the conditioner stationary.



المنارة للاستشارات
www.manaraa.com

99.99 % pure copper disk of 2 inches in diameter from Sigma-Aldrich chemical company was then polished for 3 minutes using Icue 5001™ copper slurry from Cabot Microelectronics Corporation. The slurry flow rate was kept at 75 ml/min and the polishing parameters were set at 2 – 4 psi and 100 – 200 RPM pad rotation, which translates to 0.314 m/s to 0.628 m/s linear velocity.

The convective heat transfer coefficient necessary to compute the numerical values for the temperature was obtained from a finite element analysis. Finite element analysis was done using FIDAP package by Mr. Jorge Lallave under the guidance of Dr. Rahman, Associate Professor in Mechanical Engineering department. Four node quadrilateral elements were used in constructing a finite element model of the polishing interface in presence of a liquid medium. In each element, the velocity, pressure, and temperature fields were approximated which led to a set of equations that defined the continuum. Due to a non-linear nature of the governing transport equations, the Newton-Raphson procedure was used to arrive at the solution for the velocity and temperature fields. The solution was considered converged when the sum of the residuals in all the degrees of freedom was less than a predefine tolerance value; in this case, 1E-05. Once the convective heat transfer coefficients are obtained, the conduction heat transfer problem is modeled in the finite element analysis and the temperature distribution is obtained. The laminar slurry flow during the CMP process is controlled by three major physical parameters: the volumetric flow rate of the slurry (Q = 30 to 100 mL/min), the spinning rate of the wafer disk in conjunction with the top insulated plate at a uniform angular velocity (Ω) of 10.47 to 31.41 radians/sec or 100 to 300 rpm and machine



المنارة للاستشارات
www.manaraa.com

pressure of 0.5 to 3 psi. An absolute pressure that controls the heat flux is defined as $q = \mu_{frict}PV$. It ranged from 455 to 10,600 $W/m^2$. The wafer was modeled to have a diameter 2.54 cm and its thickness was kept at a value of 0.75 mm. The wafer material used in the present study was predominantly silicon with a thin layer of cooper. The solid material property was acquired from Bejan [96] and was assumed to remain uniform and isotropic for the temperature range encountered in the investigation.

## 5.3 Temperature contours on wafer surface

Figure 1 shows the variation of the interface temperature for different slurry flow rates under a rotational rate of 100 rpm. The surface temperature has a maximum value at the center and decreases towards the edge. As the copper removal rate is greatly affected by the temperature, this could be one of the main reasons for non-uniformity during CMP process.

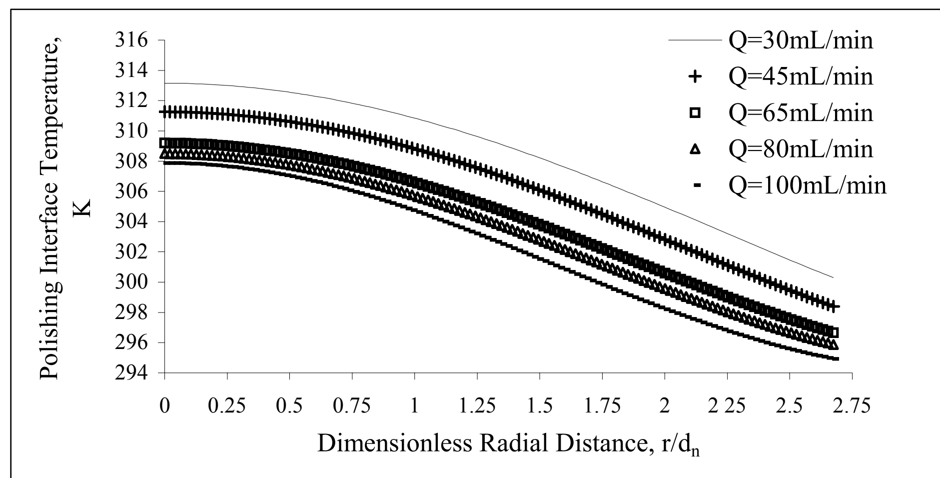


Figure 5.1 Local polishing interface temperature for a silicon wafer at different flow rates of alumina as the slurry (b=0.075mm, $\Omega$=100 rpm, q=455$W/m^2$)



المنارة للاستشارات
www.manaraa.com

The plots in figure 5.1 reveal that interface temperature decreases with slurry flow rate. Figure 5.1 confirms to us how an increasing slurry flow rate contributes to a more effective cooling.

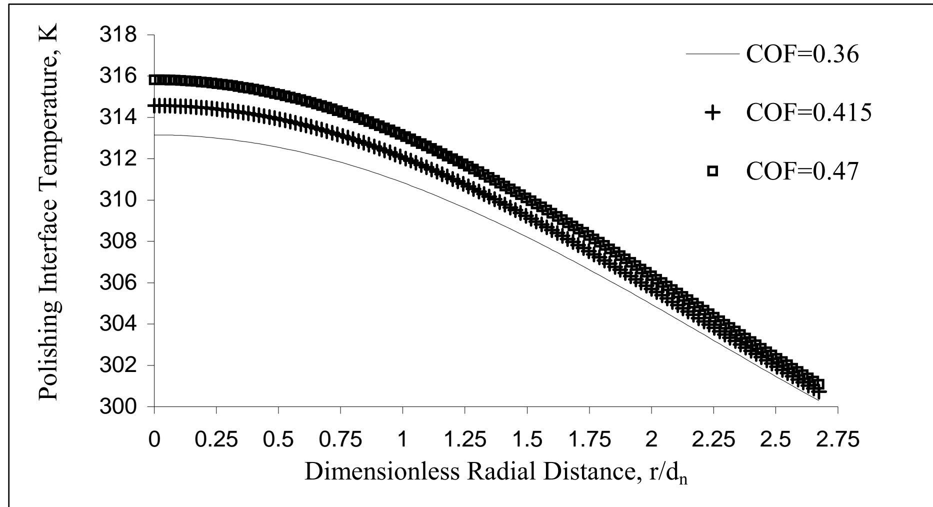


Figure 5.2 Polishing interface temperature for a silicon wafer at different coefficient of friction ($q = 455$ to $593 W/m^2$, $b = 0.075mm$, $\Omega = 100$ rpm)

From the solution of the analytical model, surface temperature curves were obtained for different coefficient of friction values. From figure 5.2 it can be noted that the coefficient of friction has a significant effect on the temperature increase on the wafer surface. The increase in friction resulted in higher temperature on the wafer surface. This is attributed to generation of higher amount of heat at the interface due to higher friction. Effect of wafer rotation on temperature at the polishing interface is illustrated as a function of dimensionless radial distance in figure 5.3. It can be noted from figure 5.3 that the effect of wafer rotational speed is statistically insignificant.



www.manaraa.com

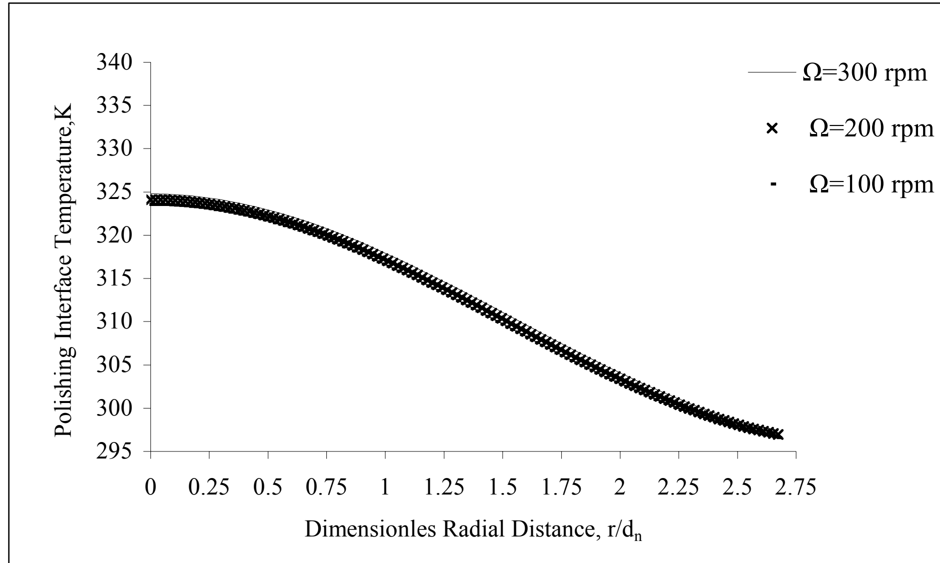


Figure 5.3 Local polishing interface temperature for a silicon wafer at different (Ω) spinning rates and alumina as the slurry (Q=65 mL/min, b= 0.075mm, q =1364W/m$^2$)

The temperature across the thickness of the wafer is also estimated at various radial locations. The cross sectional temperature distributions within the wafer are plotted as shown in figure 5. 4. It can be seen from the figure that the temperature distribution inside the wafer decreases linearly as we move towards the non polishing side of the wafer. As the wafer consisted of predominantly single material, the temperature distribution is completely based on conduction heat transfer mechanism which changes linearly within the solid. From these temperature contours on the wafer surface as a function of thickness and radius, it was concluded that apart from process parameters that gave different coefficient of friction values, slurry flow rate had a major influence on the wafer surface temperature. This can be attributed to the ability of the slurry film to transfer heat from the interface using convection heat transfer mechanism.



المنارة للاستشارات
www.manaraa.com

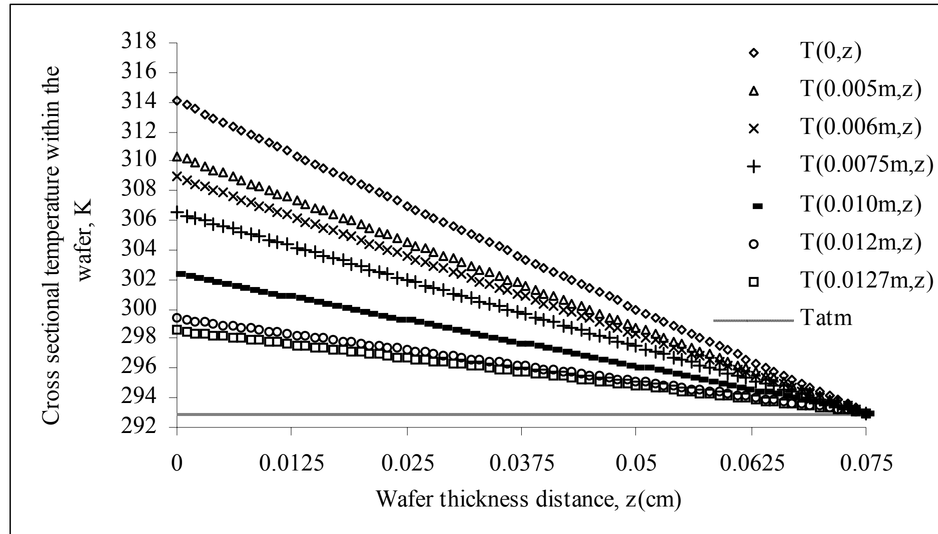


Figure 5.4 Cross sectional temperature within the wafer during CMP at a rotation speed of $\Omega$=200 rpm (Q = 65 mL/min, b = 0.075 mm, q=1049W/$m^2$)

This led the way to study the effect of slurry flow rate on CMP in terms of interfacial temperature rise, interface tribology and post CMP surface characteristics.

## 5.4 Slurry flow rate experiments

Slurry acts as a lubricant and coolant at the interface during polishing. From the results obtained by solving the thermal model, it was seen that the increase in slurry flow decreases the temperature rise. The lubricant film separates the sliding surfaces and thus reduces friction between them resulting in lesser amount of heat dissipation and hence low temperature rise. Even though the slurry acts as a lubricant medium during CMP, besides modifying the wafer surface it even dissolves or etches the formed surface compounds in several cases and the abrasives present in the slurry abrade the chemically modified surface. Thus, the effect of slurry on the tribology is beyond the simple



المنارة للاستشارات
www.manaraa.com

mechanism of lubrication offered by a fluid film. Lu *et al* [97] investigated the effect of normal force and pad velocity on the slurry film thickness at the interface and correlated it to the friction coefficient data. Their data indicated that the thickness of the slurry film at the interface decreases with increase in the applied normal force and decrease in pad velocity. The slurry film thickness data was correlated to the measured coefficient of friction data collected during their experiments. According to their findings, coefficient of friction increased with an increase in force and decrease in pad speed. An inverse relation was thus observed between the slurry film thickness and the coefficient of friction, emphasizing the role of slurry as an effective lubricating medium. As per the study by Runnels et al [98], it was concluded that the pressure applied during CMP is partially supported by the slurry film at the interface. Thus we understand that slurry film thickness and slurry flow pattern significantly impact the frictional characteristics at the interface, which needs to be studied in much more detail to fully understand the mechanism during copper CMP.

Along with the effect of slurry flow on friction characteristics, dependence of post CMP surface characteristics on slurry flow is an aspect of interest to this study. Due to the pattern density variations across the wafer, there is a difference in individual removal rates and step height reductions of patterns mainly depending on the density and width of the pattern lines. Due to this difference in removal rate, global planarization faces issues such as non-uniformity across the wafer of within a single die subsequently leading to defects such as dishing and erosion of the interconnect materials. Dishing is the loss of the copper from the copper lines resulting in a deviation from the desired flatness of the metallization layer [7, 8]. Erosion is the loss of dielectric material due to its removal



المنارة للاستشارات
www.manaraa.com

during over polishing step (practiced in order to remove even the final trace of copper between the metal lines). There are many factors that influence the generation of these anomalies on the surface. Some of such factors are width of the lines, pattern density, down force, and physical properties of the polishing pads. Even though models and investigations on dishing have been done in the past [27, 50-52] to investigate the effect of down force, slurry chemistry and pattern dependencies, very little effort has been put into studying in depth the sources of generation of dishing and erosion. From the above mentioned past investigations, down-force and pattern line width have a substantial influence on dishing depth. This indicates a predominant role of the mechanical aspect of polishing on the generation of dishing. Since, the slurry film at the interface is found to significantly influence the mechanical intensity of abrasion during CMP [98], slurry flow rate is hypothesized to have a direct impact on the dishing and erosion characteristics. Also, the slurry being delivered at the interface of the pad and wafer contact, takes away major part of the heat from the interface through convective heat transfer [41, 67]. Thus, slurry flow affects heat transfer at the interface, which in turn influences the physical properties of the polishing pad. As discussed earlier, the polishing pad softens due to the temperature increase, and so the area of contact at the interface increases, which would again impact the post CMP surface planarity. Understanding the effects of slurry flow rate and related pad surface temperature during copper CMP process on the generation of dishing and erosion thus proves highly beneficial to optimize the CMP process and to minimize defects.



المنارة للاستشارات
www.manaraa.com

### 5.4.1 Materials and techniques

The polishing experiments were conducted on an upgrade bench-top CMP machine model CP-4, manufactured by CETR Inc. (refer figure 5.5). This polisher provides a fully controlled CMP process, which imitates closely any large-wafer fab production processes. The polisher can accommodate 2" to 4" wafers, the platen can hold up to a 9" pad, which imitates the CMP process more closely and with greater control than the previous version explained in Chapter 3.

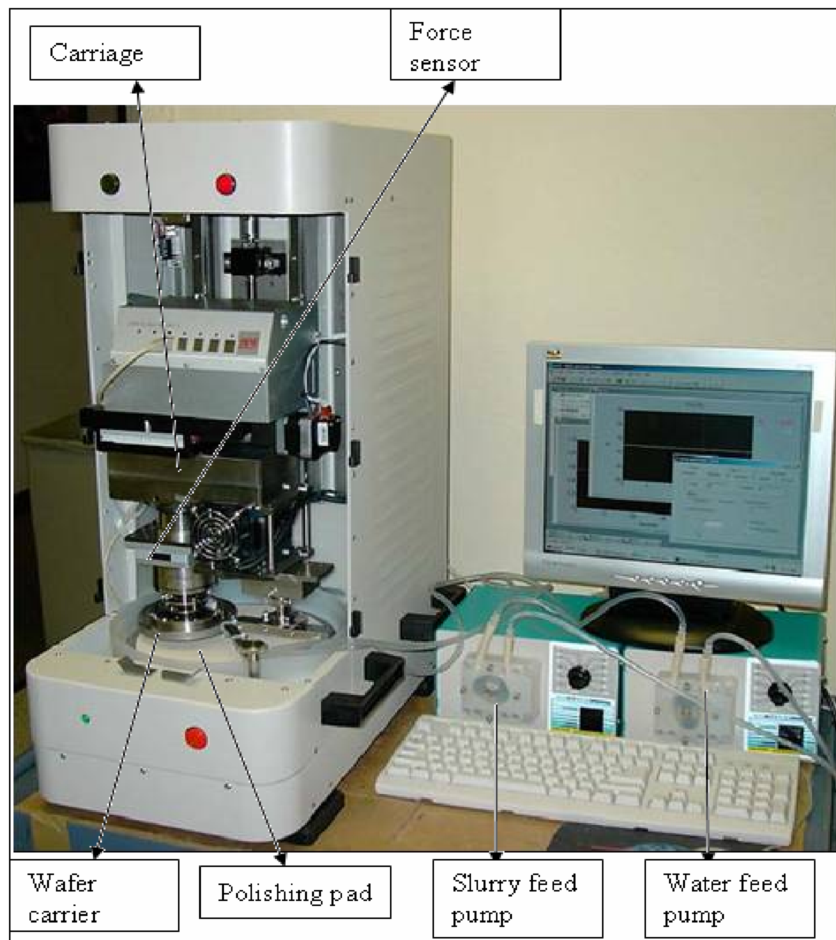


Figure 5.5 Bench top CMP tester mod. CP-4

Post-CMP surface characterization was carried out using both KLA-Tencor surface profiler and Pacific Nanotechnology (PNI) atomic force microscope integrated



المنارة للاستشارات
www.manaraa.com

with the Universal Nano+Micro Tester (UNMT-1), manufactured by CETR Inc. The instrument has a “move-n-scan” procedure, which facilitates imaging at several locations on the wafer in a single operation. The UNMT-1 with AFM head is used for large-area automated multi-scanning and facilitates imaging of multiple locations on wafers up to 8” in diameter. Its large sample stage can rotate with a sub-micron angular positioning resolution, while the AFM head on the lateral slider has a long translational motion to provide precision positioning on various wafer radii. The co-ordinates of the features on the wafers were pre-determined to be used as inputs to the “move-n-scan” procedure. The AFM was operated in the contact mode imaging, scanning in the direction perpendicular to the direction of cantilever holding the tip. Scan size was set at 80 µm, frequency of the cantilever was set at 1 Hz. The post processing on the images is performed in the Nanorule® software. Upon processing, a line analysis was performed and an average of 10 dishing depth measurements on every image was taken to obtain statistically meaningful data. The measurements of metal loss and erosion were performed on the KLA-Tencor surface profiler, as imaging of the total pattern width of 1500 µm is not possible on AFM due to scan size limits. Similar to the AFM measurements, 10 measurements at each feature were taken on the profiler.

### 5.4.2 Experimental procedures and samples

In the present research, the effects of slurry flow rate were studied in the first series of experiments, the effects of pad temperature and conditioning on the generation of wafer defects during polishing were studied in the second series of experiments. The consumables and the polishing parameters employed for the experimentation are presented in Table 5.1.



المنارة للاستشارات
www.manaraa.com

Table 5.1 Consumables and process parameters in slurry flow rate experiments

| Description | Value |
|---|---|
| Wafer coupons 2” | 10,000 Å copper over patterned low-K dielectric |
| Polishing Pad | IC 1000 perforated/ Suba IV sub pad |
| Slurry | I-cue 5001 copper slurry |
| Oxidizer | 30% hydrogen peroxide |
| Slurry Flow rates | 20, 30, 45, 55 and 75 ml/min |
| Polishing Pressure | 4 psi |
| Velocity | Wafer carrier – 95 RPM; Polishing pad – 100 RPM |
| In-situ conditioning pressure | 4 psi |
| Water Flow Rate during conditioning | 200 ml/min |
| Soft conditioner ( 4” diameter disk) for in-situ condition | Disk conditioner by 3M™ – 400 grit size. |

The chosen slurry flow rates scale up to the range of 100 ml/min – 375 ml/min on an 8” wafer polishing system. The polishing experiments constituted of preliminary tests for removal rate determination and main tests for dishing and erosion characteristics. The preliminary tests for removal rate were conducted with varying slurry flow rate. The end-point of copper planarization was determined from the coefficient of friction changes during polishing, which shows a characteristic transition at the time of copper removal as the underlying barrier layer is exposed (see figure 5.6). Thus, removal times and removal



المنارة للاستشارات
www.manaraa.com

rates were estimated. The main experiments for dishing and erosion characteristics were then carried out at varying slurry flow rate with a 20% over-polish time to fully expose the underlying barrier layer.

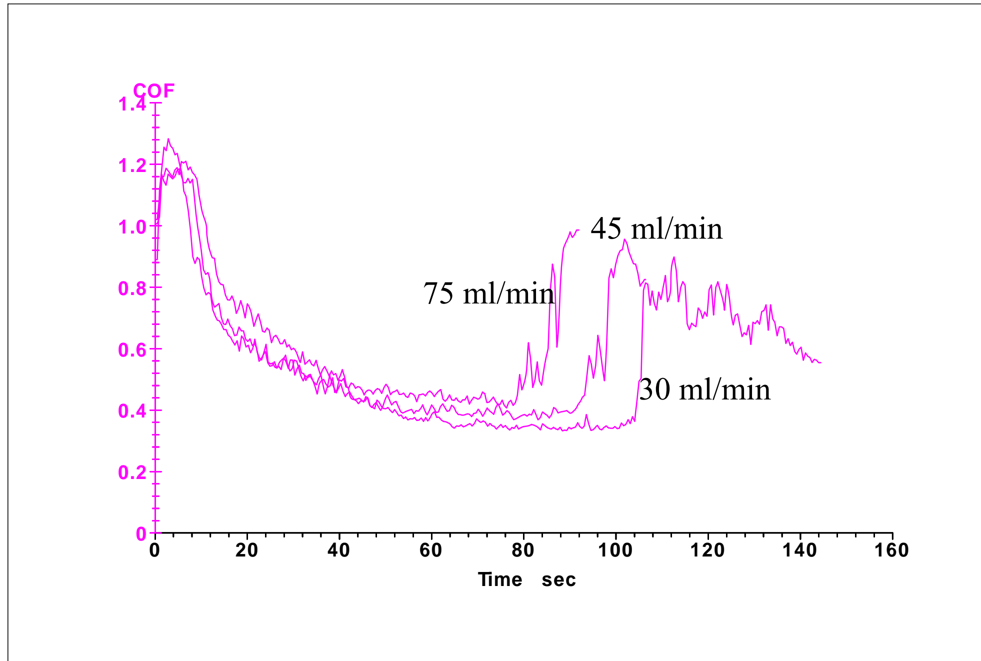


Figure 5.6 Coefficient of friction real-time graphs for three slurry flow rates

Patterned 2” wafers with 10 kÅ electroplated copper layers and an MIT 854 pattern were used for our experiments [70]. Isolated lines of 50 µm wide at two locations from a single die were chosen for dishing depth measurements. Two wide metal line patterns, 50 µm line width with 98% density and 100 µm line width with 99% density, were chosen from each die for metal loss data. Two thin metal line patterns, 10 µm line with 50% density and 1.5 µm line with 67% density were chosen from each die for erosion data. Thus, 8 locations per wafer were available for dishing, erosion and metal loss measurements.



المنارة للاستشارات
www.manaraa.com

### 5.4.3 Results and discussion for flow rate experiments

Coefficient of friction at the interface is a function of various factors such as surface characteristics, nature of interacting materials, kinematic aspects of polishing etc. It also determines the regime of lubrication at the interface [40]. The coefficient of friction also gives a measure of polishing intensity at the interface which would result in heat dissipation (generation of thermal energy from mechanical interaction). Thus the measure of the coefficient of friction at the interface during CMP gives vital information about the polishing and removal mechanism. The coefficient of friction between the pad and wafer surface during polishing and removal rate data from the first series of slurry flow rate experiments are presented in figure 5.7.

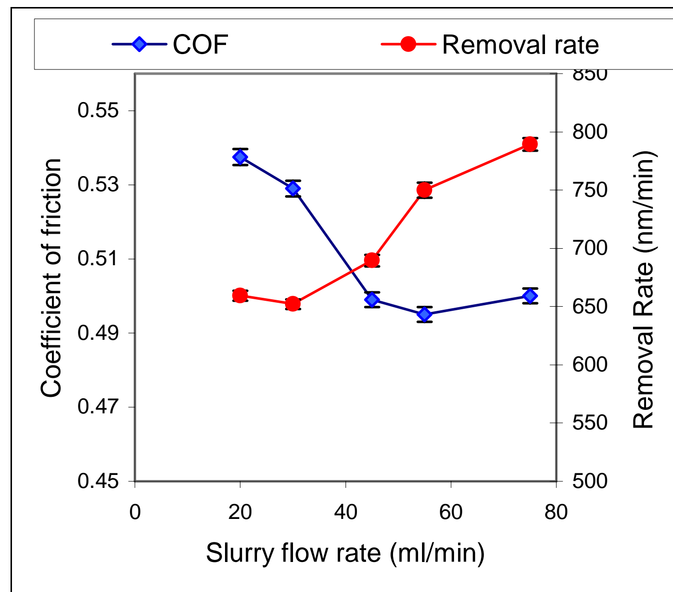


Figure 5.7 Coefficient of friction and copper removal rate versus slurry flow rate

The numerical values in figure 5.7 are averages of data collected from four samples polished at each slurry flow rate. Y-axis error bars represent the standard deviation of the data about the average values.



المنارة للاستشارات
www.manaraa.com

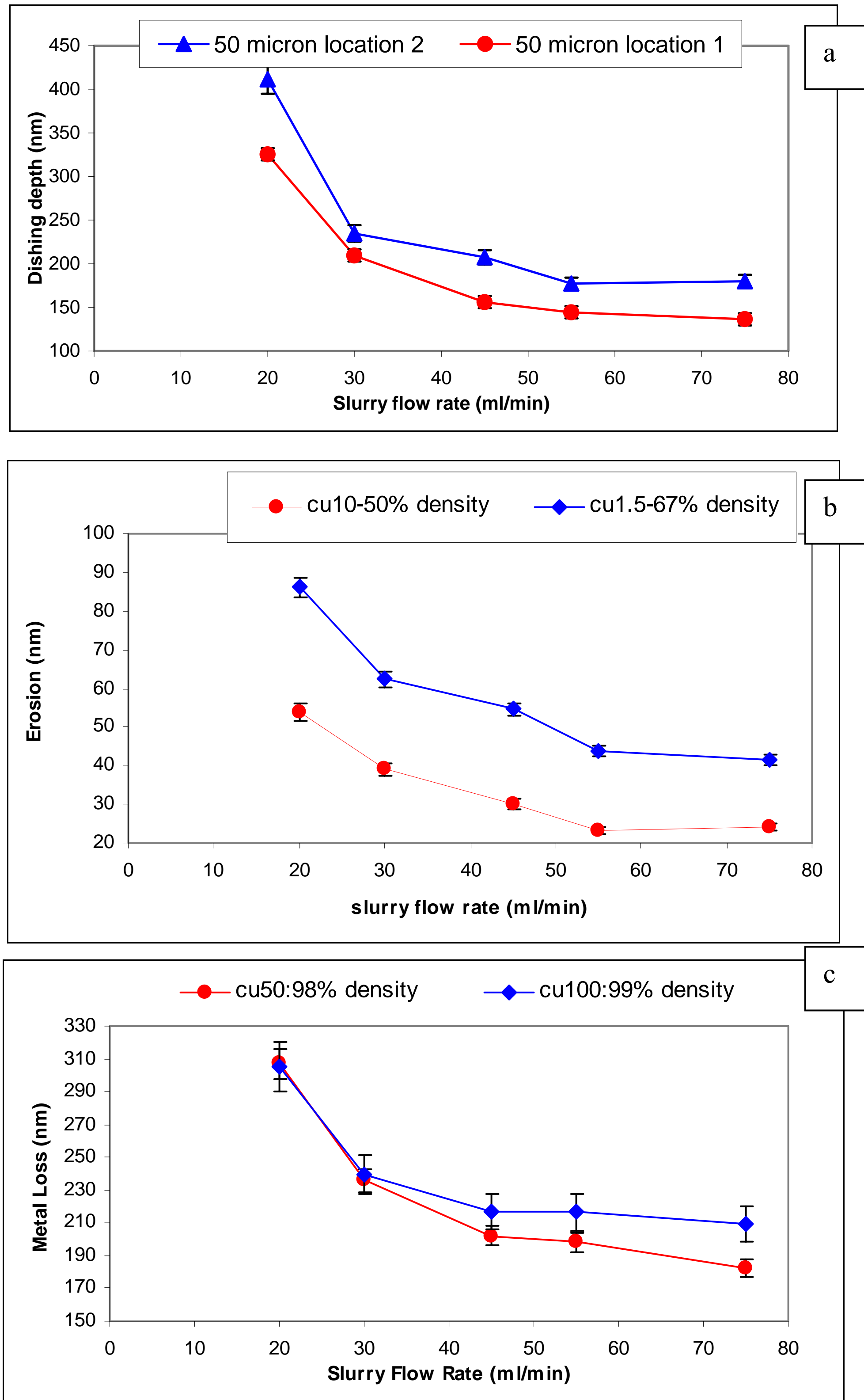


Figure 5.8 Effects of slurry flow rate on (a) dishing, (b) erosion and (c) metal loss



المنارة للاستشارات
www.manaraa.com

From the figure 5.7 it can be seen that coefficient of friction decreased and removal rate increased with an increase in slurry flow rate. As the higher flow rate decreases the temperature at the interface, the observed decrease in coefficient of friction is in agreement with the results from other investigations [40, 84]. The observed trend of the removal rate can be attributed to the inadequate chemical component during polishing at lower slurry flow rates. During CMP process, slurry should act as both a surface oxidant and dissolver of the fragments of copper detached from the wafer surface. If the amount of slurry available on the pad is not sufficient to carry out these chemical activities, the removal rates decrease. The dishing, metal loss and erosion data, plotted versus slurry flow rate, are presented in figure 5.8. Polishing was repeated 4 times at each condition to confirm data reproducibility. From figure 5.8 it can be seen that all the three levels of dishing, erosion and metal loss decreased with an increase in slurry flow rate.

High amounts of dishing, erosion and metal loss at lower slurry flow rates may be due to a combination of two reasons: a) relatively high temperatures at the interface at low slurry flow rates, causing local softening of the pad. Resulting softer asperities of the pad reach deeper into the trenches compared to the stiffer pad asperities, resulting in increase of dishing, erosion and metal loss; b) the second reason might be due to increased chemical activity between the copper and the slurry at elevated temperatures. Figure 5.9 shows AFM images of dishing profiles of 50 µm features at different slurry flow rates.



المنارة للاستشارات

www.manaraa.com

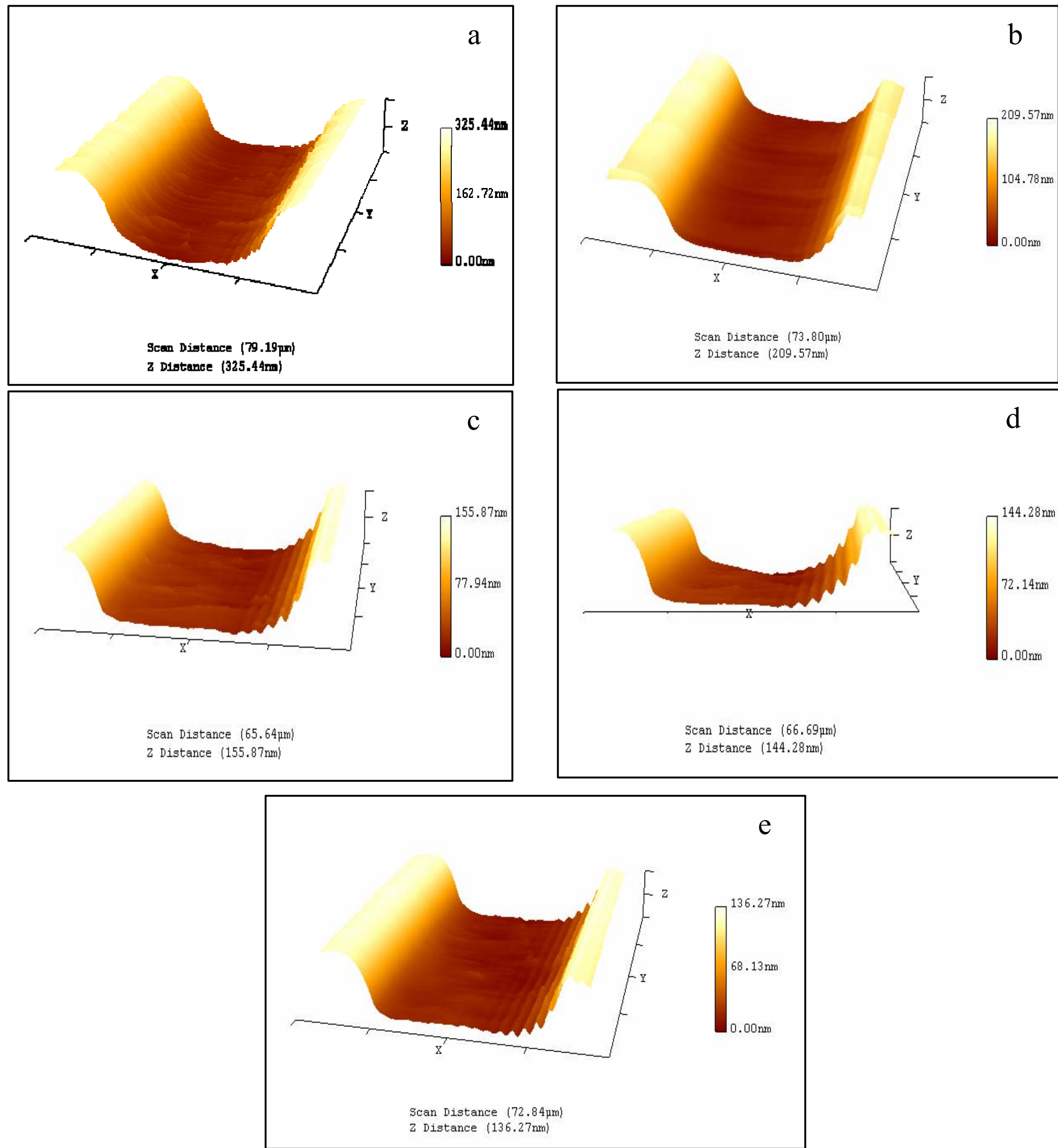


Figure 5.9 AFM images of dishing profiles of a 50 µm wafer feature at a) 20 ml/min b) 30 ml/min c) 45 ml/min d) 55 ml/min and e) 75 ml/min slurry flow rates.



المنارة للاستشارات
www.manaraa.com

The rise in the pad surface temperature during polishing experiments at different slurry flow rates is shown in figure 5.10. From the figure 5.10 it could be seen that the amount of rise in pad surface temperature decreased with increase in slurry flow rate.

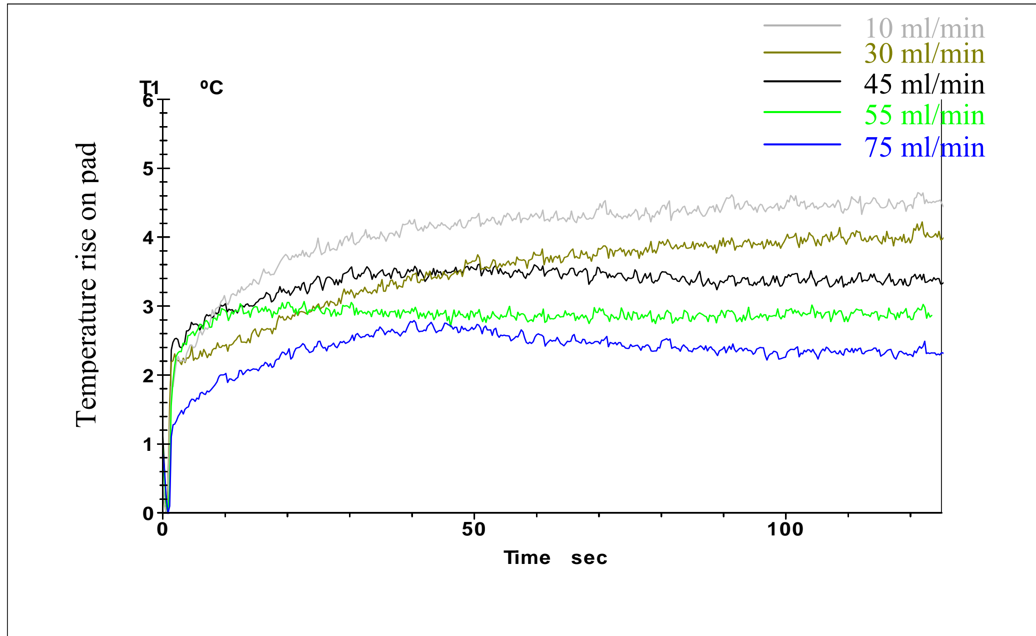


Figure 5.10 Measured temperature rise on the pad surface during copper polish at different slurry flow rates

## 5.5 Summary

The steady state conduction heat transfer model is developed and is solved analytically to obtain the surface temperature on the wafer as a function of its radius and thickness. The polishing interface temperature and local heat transfer coefficient are significantly affected by slurry flow rate and tribology at the interface. Increase in the slurry flow rate and decrease in friction coefficient results in lower wafer surface temperature. The surface temperature is highest at the center and decreases towards the edge. This steady state surface temperature profile could be one of the reasons for non-uniformity within wafer during CMP process. The temperature across the cross section of



المنارة للاستشارات
www.manaraa.com

the wafer decreases linearly reaching room temperature on the back side of the wafer. The effects of slurry flow rate, pad temperature and conditioning temperature on the copper CMP performance have been studied. During copper CMP process, higher slurry flow rates resulted in decreased levels of friction, dishing, erosion and metal loss, while increased copper removal rate.



المنارة للاستشارات
www.manaraa.com

# CHAPTER 6: NOVEL SLURRY DEVELOPMENT TO REDUCE CMP DEFECTS

## 6.1 Introduction

Besides global planarization and high polish rate, the CMP process should also achieve high material selectivity (high polishing rate of one material compared to the other), high-quality surface finish, which is devoid of scratches, pattern related defects, pits, delamination and particle contamination [99-104]. Oxide CMP is conducted during shallow trench isolation (STI) in logic device fabrication and also in many other novel applications. Achieving a superior surface quality includes fewer scratches, with minimal oxide dishing and nitride erosion, particularly in case of STI CMP. CMP defects can be due to contamination issues from slurry chemicals, particle contamination (residue) from abrasive, scratches during polishing due to agglomerated abrasive particles, pattern related defects like dishing and erosion, delamination and dielectric crushing due to mechanical damage of dielectrics [105]. Such defects during CMP hamper the device yield and reducing the defects is thus highly important. These defects result in nullifying the advantages of using CMP as a global planarization technique.

The quality of the post CMP wafer surface is significantly dependent on the characteristics of the abrasive particles present in the slurry. The polishing process involves active abrasion of the wafer surfaces using abrasive particles present in the slurry. Such an abrasion results in generating surface scratches on the wafer being polished. The generation of surface scratches depends on a wide variety of factors such as



المنارة للاستشارات
www.manaraa.com

the process conditions, characteristics of the abrasive particles, their content in the slurry, hardness of the pad, chemistry of the slurry etc. Of particular interest in the present research are the characteristics of the abrasive particles. Abrasive particles at times agglomerate in the slurry and the effective size of the particles can be much higher than the specification of the slurry. Such agglomerated particles cause deep scratches in the surface and result defects that cannot be removed by any other post processing techniques. Commonly used ceramic abrasive particles are much harder than the low dielectric constant materials and copper. These particles can easily scratch the surface and if agglomerated can result in permanent scratch defects. Thus, the inherent nature of the particle plays a significant role. These surface scratches in turn result in formation of puddles in further layers of metallization causing an electrical short circuit [106]. Also, the abrasive particles that result in low friction at the interface are beneficial to the process as lower friction helps reduce surface damage during CMP [83]. Another aspect of polishing related to slurry abrasives that needs to be countered in order to improve the yield and effectiveness of polish is particle residue on the wafer surface after CMP [105].

Researchers in the recent past have studied mixed or modified abrasive particles in order to reduce defects during CMP (107-111). These studies mostly use abrasives of different inorganic oxides and of different sizes or use micelles etc. Minimal success has been achieved in reducing both surface scratches and particle residue at the same time as the inherent material characteristics of the abrasive particle that meets the wafer surface is still hard and has the same surface properties.



المنارة للاستشارات
www.manaraa.com

The focus of this research is to reduce surface defects during polishing by developing slurries using novel inorganic-organic composite particles. These particles consist of polymer, surface of which is mostly modified using silica functional groups and ceria nanoparticles. Presence of ceria nanoparticles is proven to be highly beneficial for oxide CMP, both in terms of removal rate and selectivity [112]. The developed composite particles are inherently soft due to the presence of polymer. These particles exhibit controllable surface hardness and chemical nature and hence are hypothesized to prevent aggressive scratching, leave particle residue, or apply high mechanical stress during polishing. The incorporation of functional groups onto polymer latex surfaces to form new hybrid materials represents an emerging discipline for the synthesis of novel materials with diverse architectures. Particle synthesis and characterization was conducted by Mr. Cecil Coutinho under the guidance of Dr. Vinay Gupta in the Department of Chemical Engineering.

## 6.2 Silica hybrid particles

### 6.2.1 Hybrid particle synthesis

Unless otherwise noted, all chemicals were purchased from Sigma-Aldrich (WI) and used without further purification. The monomer NIPAM (TCI), was recrystallized from hexane before use. With the goal of developing novel slurry for CMP applications, polymer-siloxane (hybrid) microgels were formed by the surfactant free precipitation polymerization of NIPAM (5g) in aqueous media (800 ml) using N,N'-methylenebisacrylamide (0.2g) as the cross-linker. Following purging with $N_2$ for 1h, the reaction mixture was heated in an oil bath to 75°C and the ionic initiator potassium



www.manaraa.com

persulfate (0.1g) was added to instigate polymerization. After an initial polymerization of 2 hours, 3-(trimethoxysilyl)propyl methacrylate (1g) was added to the reaction mixture and the polymerization continued for a further 90 minutes. The microgels formed were collected and purified by repeated centrifugation (7800g, 30minutes) and re-dispersed with deionized water.

### 6.2.2 Particle characterization

Microgel sizes and polydispersities were determined via dynamic light scattering (DLS) using a Zetasizer Nano-S (Malvern, PA). Samples were sonicated prior to analysis. A 1ml of the microgel solution was placed into a cuvette and allowed to thermally equilibrate to a certain temperature for 10 mins before each measurement. Data fitting was done using a multi-modal algorithm supplied by Malvern. The collected correlelograms were fitted to diffusion co-efficients and converted to a hydrodynamic diameter using the Einstein-Stokes equation. The polymer-$CeO_2$ composites were examined using TEM to visually determine the extent of $CeO_2$ loading and dispersion within the polymer matrix. A drop of the sample solution was placed on a Formvar-coated Cu TEM grid that was examined using a FEI Morgagni 268D. Bulk FTIR spectrum of the microgels was measured using a Nicolet Magna-IR 860 spectrometer by pelletizing a small amount of dried gel with KBr.

### 6.2.3 Post CMP surface characterization

Qualitatively, surface quality of the oxide surface post CMP was examined by optical microscopy using a Leitz Ergolux Optical Microscope. Quantitatively, the surface



المنارة للاستشارات
www.manaraa.com

roughness was measured using a Digital Instruments Dimension 3100 Atomic Force Microscope. The bench top CMP tester provided real-time measurements of the friction coefficient during polishing and the average value after the process has reached the steady state has been reported. Removal rates of the silica film were measured using a home-built ellipsometer. 633 nm wavelength light from a helium-neon laser was polarized by a Glan-Thompson polarizer both manufactured by Melles Griot. The polarization of the light was subsequently modulated using a liquid-crystal (LC) variable phase retarder (by Meadowlark Optics) and directed onto the silicon dioxide film of the wafer surface at an incident angle of 64°. The laser spot measured approximately 1mm - 2mm at the surface. Reflected light was analyzed using another Glan-Thompson polarizer, and the intensity was measured using a Si photodiode manufactured by Thor Labs. Control of the variable LC retarder and the data acquisition from the detector was performed using a HP-VEE (version 4.0) program. Thickness measurements were made at a minimum of six different spots on each substrate, and the average value is reported.

### 6.2.4 Experimental conditions for silica hybrid particle slurry testing

Upon synthesis and re-dispersion of the hybrid particles in water, the pH of the solution was adjusted to 12 using KOH solution. Conventional silica particles of 50 nm and 150 nm were used to make silica slurries for comparison with the hybrid particles. The details of the slurry samples made using these particles have been tabulated in Table 6.1. All the slurries were formulated to have equal amount of weight percentage of abrasive particles.



المنارة للاستشارات
www.manaraa.com

Table 6.1 Details of the slurry samples made out of hybrid and silica particles

| Slurry Name | Particle Type | Particle size (nm) | Wt % |
|---|---|---|---|
| Slurry 1 | Hybrid polymer-oxide particle | 500 (Less surface Oxide) | 1.5 |
| Slurry 2 | Hybrid polymer-oxide particle | 300 (More surface Oxide) | 1.5 |
| Slurry 3 | Pure silica - NEI corp. | 150 | 1.5 |
| Slurry 4 | Pure silica -Fuso chemical co. | 50 | 1.5 |

The slurries were then employed for performing CMP of 1” thermal oxide wafers on the bench top CMP tester. The testing of the slurry samples was carried out at the process conditions as summarized in Table 6.2

Table 6.2 Experimental conditions for slurry testing

| Parameter | Value |
|---|---|
| Pressure | 4 Psi |
| Pad RPM | 200 RPM |
| Slurry flow rate | 75 ml/min |
| Pad | IC 1000 K grove polishing pad |
| Slider stroke and velocity | 7 mm and 3mm/sec respectively |

### 6.2.5 Results and discussion – silica hybrid particles

Hybrid particles synthesized using precipitation polymerization were characterized using TEM and the average size of the particles was noted to be approximately 500 nm. The TEM image of the hybrid particles is presented in the figure 6.1 along with the 50



المنارة للاستشارات
www.manaraa.com

nm silica particles. The patchy surface of the particle can be clearly seen from the image, which indicates the presence of silica functional groups on the surface

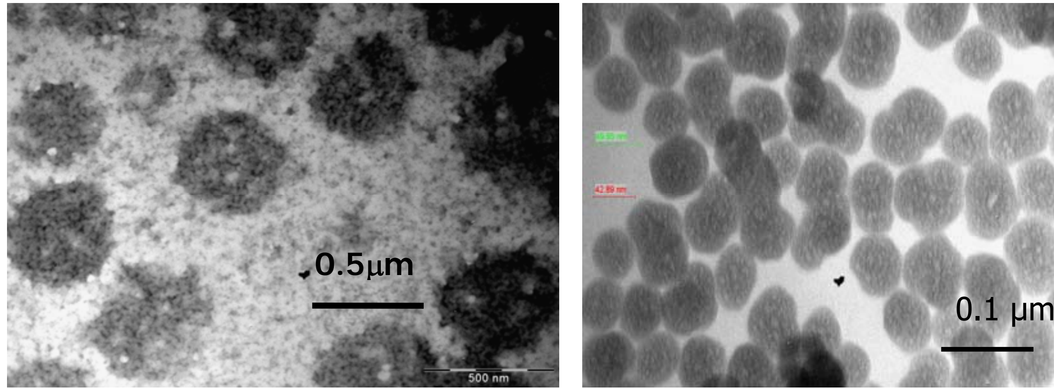


Figure 6.1 TEM images of the Hybrid particles and silica particles

The coefficient of friction data measured in-situ by the polisher is presented in Figure 6.2. The removal rate measurements as presented in Figure 6.3 were obtained by using a Rudolph AutoEL III ellipsometer. From the removal rate data, it can be noticed that the hybrid particles performed similar to the silica particles.

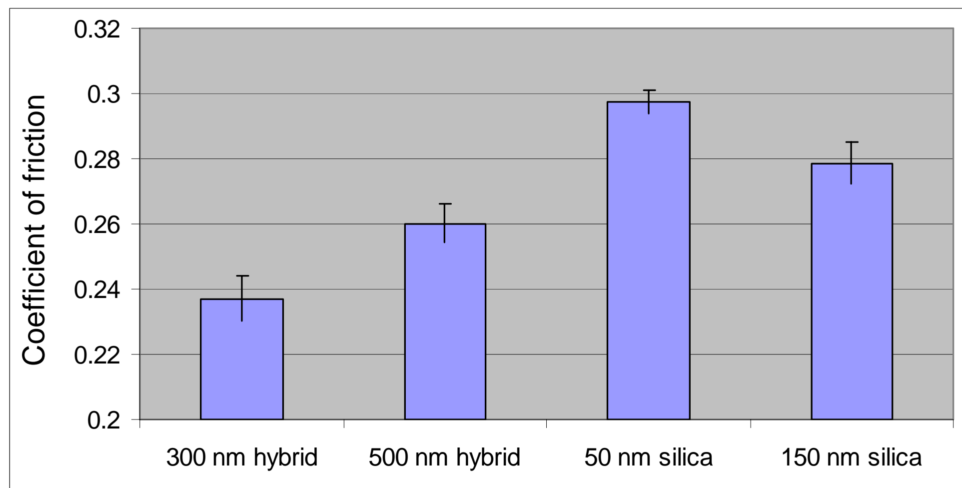


Figure 6.2 COF data measured in-situ during CMP of thermal oxide wafers using various kinds of abrasive particles.



المنارة للاستشارات
www.manaraa.com

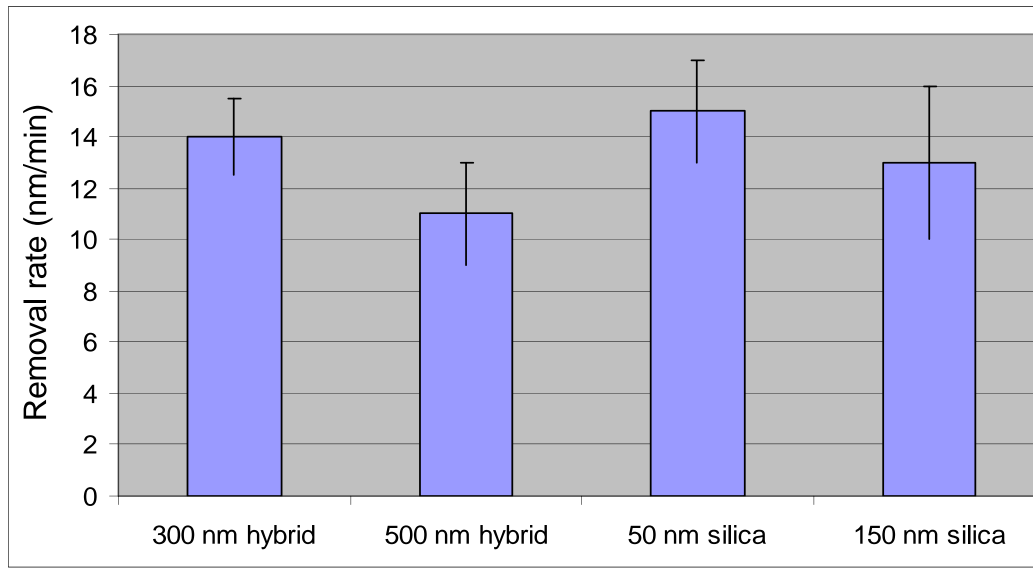


Figure 6.3 Removal rate measurements during CMP of thermal oxide wafers using various kinds of abrasive particles.

Friction data suggested that the hybrid particles demonstrated better frictional characteristics as compared to the 50 nm and 150 nm silica particles. This indicates that the hybrid particles perform much better than the traditional silica particles resulting in higher removal rate and having less friction at the interface. The 300 nm hybrid particles resulted in lower coefficient of friction and higher removal rate as compared to the 500 nm hybrid particles. This result could be due to the increased hardness of the 300 nm particle as compared to the 500nm particle. The thermal oxide wafer surface was characterized before and after CMP using Fourier Transform Infrared (FTIR) Spectroscopy to ensure any deposition of the polymer material onto the wafer surface during polishing. From the FTIR spectrum (see figure 6.4), it can be seen that polishing



المنارة للاستشارات
www.manaraa.com

with the hybrid or silica particles did not result in any change in the surface properties of the thermal oxide wafer.

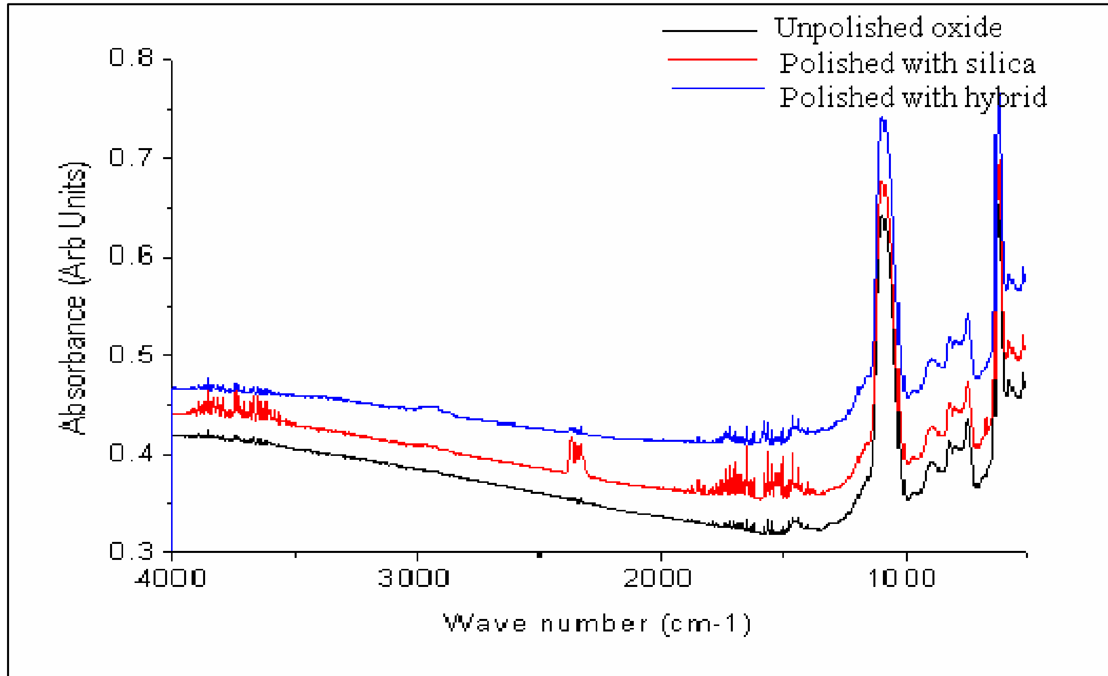


Figure 6.4 FTIR spectroscopy on thermal oxide wafer before and after CMP.

Surface roughness imaging using Atomic Force Microscopy (AFM) was conducted to probe the surface quality and roughness. Also an estimate of particle residue was obtained from the AFM images (10 X 10 μm images at 200 nm data scale) as shown in Fig 6.5 (a-d). From the AFM images and the numerical data, it could be seen that the hybrid particles performed much better than the pure silica particles both in terms of achieving lower surface roughness and more importantly lowering the particle residue, which helps eliminate rigorous post CMP clean steps [113]. The numerical values of the surface roughness are presented in the table 6.3.



المنارة للاستشارات
www.manaraa.com

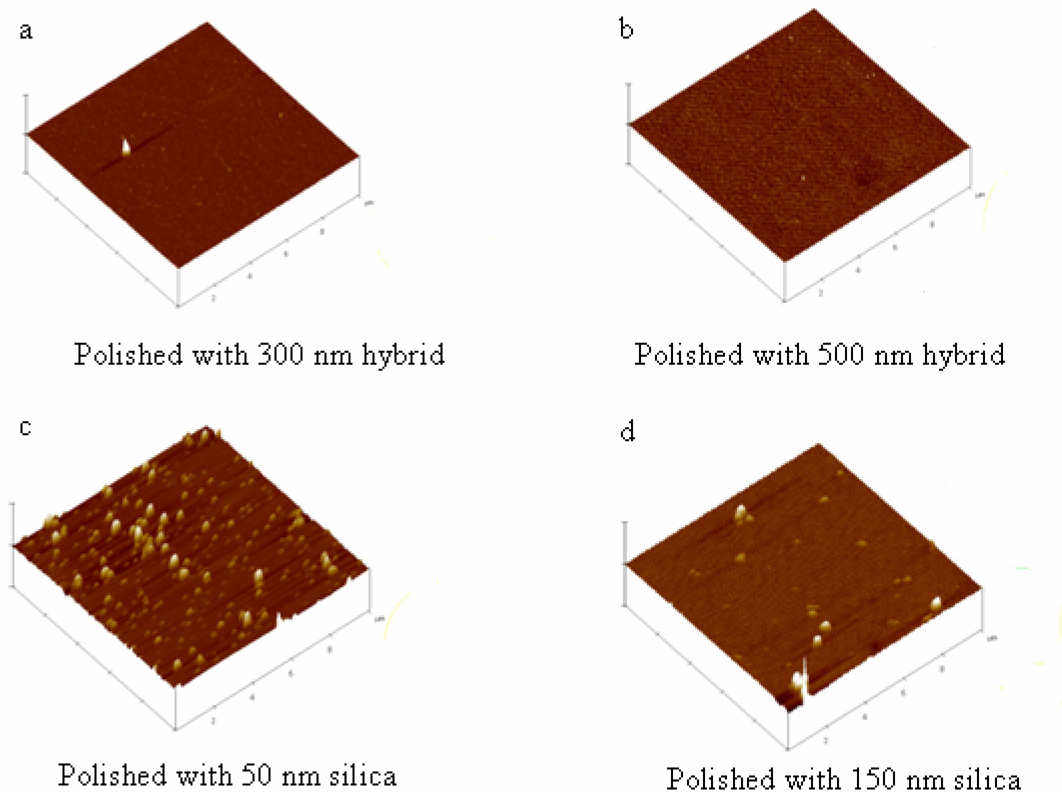


Figure 6.5 AFM images of the thermal oxide wafer surfaces polished with (a) 300 nm hybrid (b) 500 nm hybrid (c) 50 nm silica and (d) 150 nm silica

Table 6.3 Surface roughness of wafer after CMP using various abrasive particles

| Abrasive particle | Abrasive particle size | Surface roughness (nm) rms roughness |
|---|---|---|
| Hybrid polymer particle | 500 | 0.86 |
| | 300 | 1.26 |
| Pure silica particle | 150 | 2.86 |
| | 50 | 5.32 |



المنارة للاستشارات
www.manaraa.com

From the above results and discussion, it can be noted that the hybrid particles exhibit superior performance as compared to the conventional silica particles in regard to surface finish after CMP. Moreover, the amount of particle residue on the polished wafers is minimal in the case of hybrid particles when compared to the silica particles. However, the oxide removal rates during CMP upon using the slurries made of hybrid particles are negligible. Even though the observed negligible removal rate can be attributed to the absence of any additives and dispersants that are used in commercial slurries, the inclusion of ceria particles on the surface of the hybrid particle along with silica functional groups is hypothesized to improve the oxide removal rate during CMP. This hypothesis led us into the modification of the surface chemical nature of the hybrid particles making them into 'Interpenetrating hybrid ceria composite' particles.

### 6.3 Ceria composite particles

In previous work, we have reported the performance of hybrid microgels consisting of soft polymeric networks containing hard inorganic siloxane segments. Although the slurries made from these hybrids produced a superior surface finish compared to traditional silica slurries, the low removal rates of silica from the wafer surface hinders its potential for commercial CMP applications. As an extension to the above study, in order to improve oxide removal rates during CMP, we chose to incorporate ceria on the surface of the microgel. Traditionally ceria particles are well known for achieving significant removal rate during oxide CMP and moreover, they enhance the selectivity of the slurry thereby avoiding dishing during STI CMP [114-116]. However, these ceria particles produce both major and minor scratches on the wafer



المنارة للاستشارات
www.manaraa.com

surface during polishing. In our approach, ceria nanoparticles on the surface of a polymeric microgel (hybrid composites) will conceivably prevent aggressive abrasion of the ceria on the wafer surface resulting in smoother surfaces with reduced surface damage. These hybrid composite particles are hypothesized to provide a cushioning effect to the wafer being polished due to the soft nature of the polymer and at the same time achieve appreciable oxide layer removal rate due to the chemical nature of the surface silica and ceria particles. Since the polishing is not suspected to be aggressive, the coefficient of friction while polishing with the slurries containing hybrid particles is also expected to be lower than during polishing with slurries containing conventional abrasive particles.

### 6.3.1 Composite particle synthesis

Hybrid microgels were formed similar to the procedure described in silica hybrid particle synthesis but in addition poly(acrylic acid) sodium salt (~10g, $M_W$ ~15000 g/mol) was added during initial polymerization to achieve interpenetrating chains of poly (acrylic acid) within the hybrid microgel, thus forming IP-hybrid microgels [117-119]. These IP-hybrid microgels enhance the incorporation of ceria nanoparticles. Nanoparticles of $CeO_2$ suspended in deionized water, were mixed with the IP-hybrid microgel solution in a desired loading ratio (50wt %) at a pH 5. The resulting composite settled to the bottom and the supernatant was removed. The composite slurry was homogenized by washing three times with deionized water. All pH adjustments were done using 0.1M NaOH and 0.1M HCl.



المنارة للاستشارات
www.manaraa.com

### 6.3.2 Experimental conditions for composite particle slurry testing

The planarization of 1.5" square PECVD oxide wafers was carried out on the CMP bench top polisher using slurries consisting of (a) 0.5wt% composite particles, (b) 0.5wt% of ceria (same weight fraction of the composite) and (c) 0.25wt% of ceria (same number fraction of ceria as in composites). All slurries were dispersed in deionized water at a pH of 5 to maintain a slight positive charge on the $CeO_2$ (Iso-Electric Point (IEP) ~ pH 6.0) that helps disperse the ceria more evenly and aids in abrading the negatively charged silica surface (IEP ~ pH 2.3). All the slurries were well agitated during experimentation to prevent sedimentation of the abrasive particles. The planarization was conducted for 3min at room temperature and all CMP experiments were repeated to ensure reproducibility. The process conditions for the polishing experiments were the same as tabulated in the Table. 6.1 except that 7psi down pressure was used instead of 4psi.

### 6.3.3 Results and discussion – composite particles

Upon controlling the mixing ratios of the microgel and ceria solutions precisely, the mass fraction of ceria within the composite can be easily tailored. The composite particles prepared contain approximately 50wt% ceria and is shown in the TEM image in figure 6.6. The dark spots indicate ceria (~20nm) that is well dispersed and unaggregated within the polymer microgel. The synthesis and development of the slurry with these hybrid composites is under the process of patenting (Ref # 06B115PR).



المنارة للاستشارات
www.manaraa.com

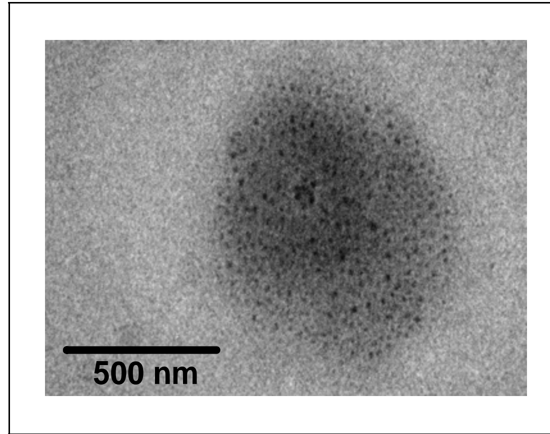


Figure 6.6. TEM image of the composite particle - dark spots indicate $CeO_2$

As mentioned earlier, PNIPAM has become one of the best studied responsive polymers. A hydrophilic-hydrophobic balance that exists between the amide and isopropyl side chains [120] causes the polymer microgel to phase separate out of solution above the transition temperature (~32°C). The co-polymerization of NIPAM with MPS and the presence of interpenetrating chains of PAAc do not significantly alter the temperature response behavior of the IP-hybrid microgel.

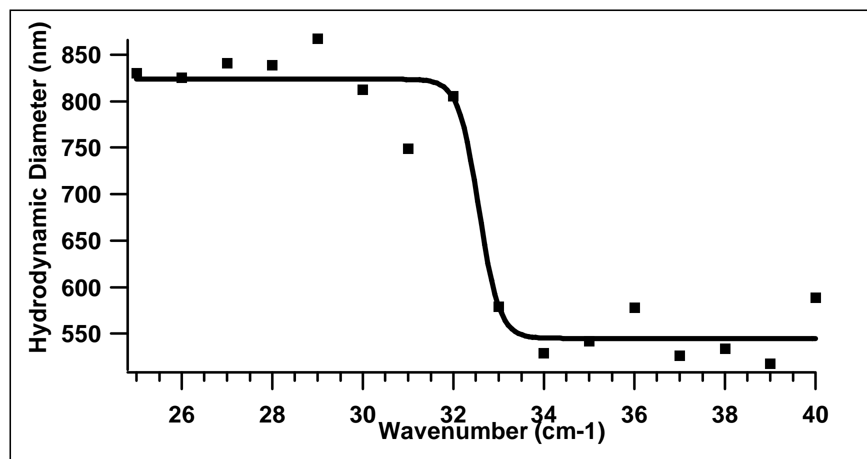


Figure 6.7 DLS of microgels where the particle phase separates at nearly 32°C



المنارة للاستشارات
www.manaraa.com

The phase separation of the IP-hybrid microgel is described by the DLS data in figure 6.7 where the transition results in a 70% decrease in the volume of the microgel. Hence, by controlling the temperature, the hardness of the particle can be easily manipulated to create harder or softer abrasive particles when desired.

To examine the removal rates of the silica from the wafer surface and test for organic residue on the polished surface (data not shown), we used infrared spectroscopy. FTIR characterization of the wafer surface before and after CMP confirmed that there was no polymer deposition onto the wafer surface during CMP. The intensity of the absorption peak of Si-O-Si at 1075cm$^{-1}$ was evaluated and this showed substantial removal of the oxide layer by the ceria and composite slurry as seen in figure 6.8. Qualitatively, it can be seen that the 0.25wt% ceria slurry and 0.5wt% composite slurry achieve nearly identical removal while the slurry consisting of 0.5wt% ceria achieves about double that removal.

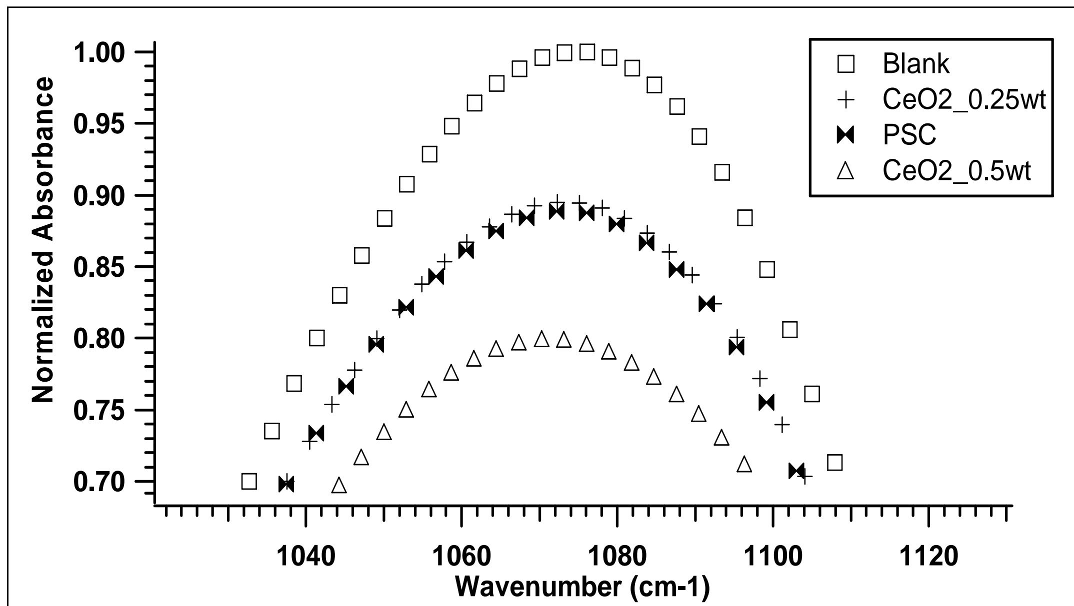


Figure 6.8 FTIR characterization of silica removal from the wafer surface.



www.manaraa.com

Thereby, it can be concluded that the ceria is the primary factor responsible for removal of silica, while the polymer microgel is the entity that ensures a planar surface. Quantitative thickness measurements of the wafer were measured very accurately using ellipsometry.

The coefficient of friction during polishing was obtained from the ratio of lateral and normal forces measured in-situ using a dual force sensor installed to the upper carriage of the machine carrying the wafer carrier. The average coefficient of friction after the process has reached the steady state has been noted. The numerical values of the average coefficient of friction along with the standard deviation are tabulated in the table 6.4. The numerical values for removal rate were obtained from Ellipsometry measurements.

Table 6.4. Numerical values for coefficient of friction, surface roughness and removal rate

| | COF | Surface Roughness (nm) | Removal Rate (nm/min) |
|---|---|---|---|
| Composite | 0.16 ± 0.01 | 1.06 ± 0.44 | 104 ± 4.24 |
| 0.5wt% CeO2 | 0.22 ± 0.01 | 2.31 ± 0.84 | 241 ± 28.28 |
| 0.25wt% CeO2 | 0.11 ± 0.01 | 4.4 ± 2.2 | 125 ± 0.71 |

From the average values it can be seen that the slurry containing 0.5 wt % ceria composite particles resulted in lower coefficient of friction as compared to the slurry



المنارة للاستشارات
www.manaraa.com

containing 0.5 wt % conventional ceria particles. This shows that the composite particles aid in reducing the friction at the polishing interface. This could be attributed to their relative softness and the resulting cushioning effect. However, it was noted that 0.25 wt % ceria resulted in lower coefficient of friction than the 0.5 wt % conventional ceria and also the 0.5 wt % ceria composite particles. This observation can be attributed to the fact that slurry with 0.25 wt % ceria will have a fewer number of particles of same size as compared to 0.5 wt % ceria, thus resulting in milder abrasion and hence lower coefficient of friction. 0.25 wt % ceria will have much smaller volume fraction in comparison with the composite particles, which could be the plausible reason for the lower coefficient of friction observed.

### 6.3.4 Post CMP surface characterization

Even though from the removal rate and coefficient of friction measurements it appears as if 0.25 wt % conventional ceria would be beneficial due to their low friction characteristics, it is crucial to study the post CMP surface characteristics to draw any conclusions regarding the performance of ceria composite particles. Optical microscopy images of the post CMP oxide surface at 5X magnification are shown in figure 6. As revealed from figure 6.9, slurries with conventional ceria particles resulted in severe scratches on the wafer surface. Conversely, slurries consisting of the composites resulted in relatively much less surface defects.



المنارة للاستشارات
www.manaraa.com

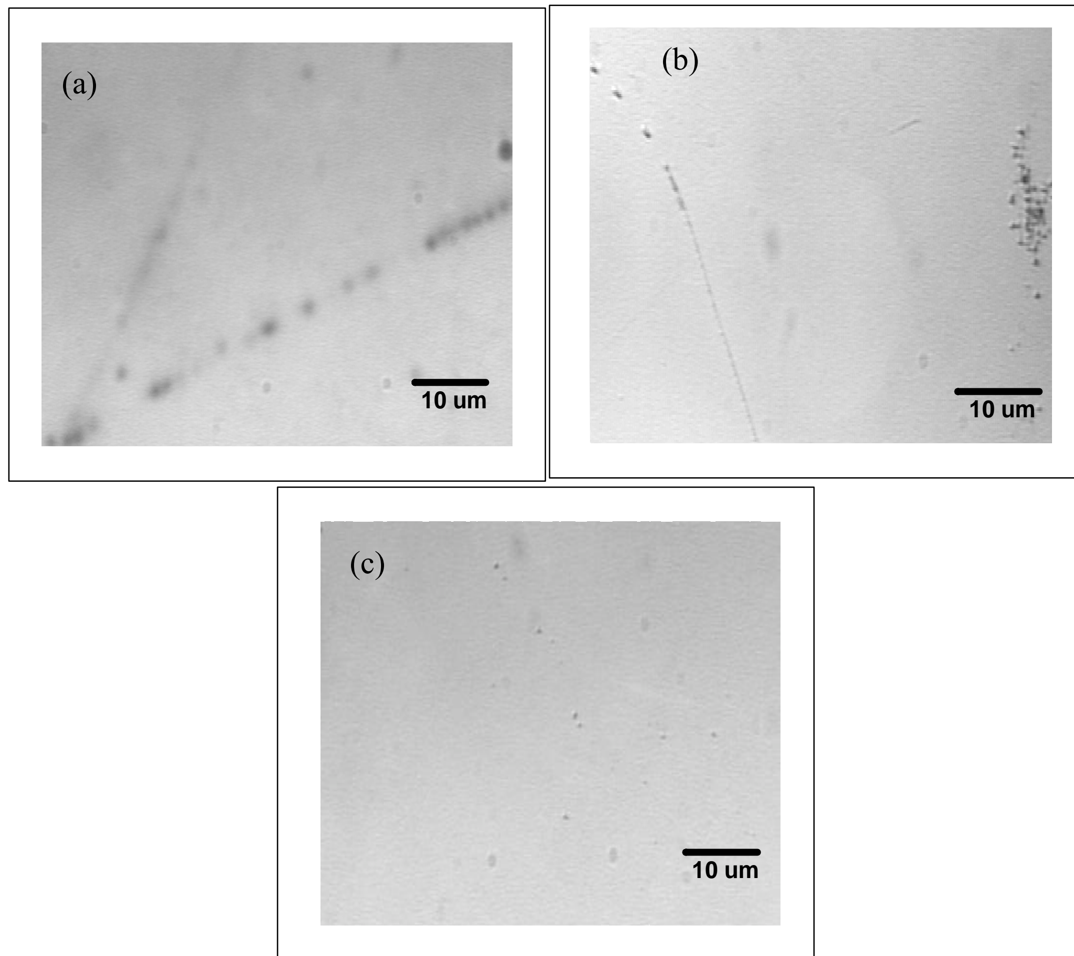


Figure 6.9 Optical microscopy (5X magnification) images of wafers polished with (a) ceria composite particles, (b) 0.5wt% $CeO_2$, (c) 0.25wt% $CeO_2$ nanoparticles

This reduction in surface scratches can be plausibly attributed to polymer microgels maintaining an even dispersion of the ceria nanoparticles and preventing aggregate formation during the duress planarization. Further, the cushioning effect of the polymer particles helps in reducing the aggressiveness of polishing thereby resulting in reduced surface damage.



المنارة للاستشارات
www.manaraa.com

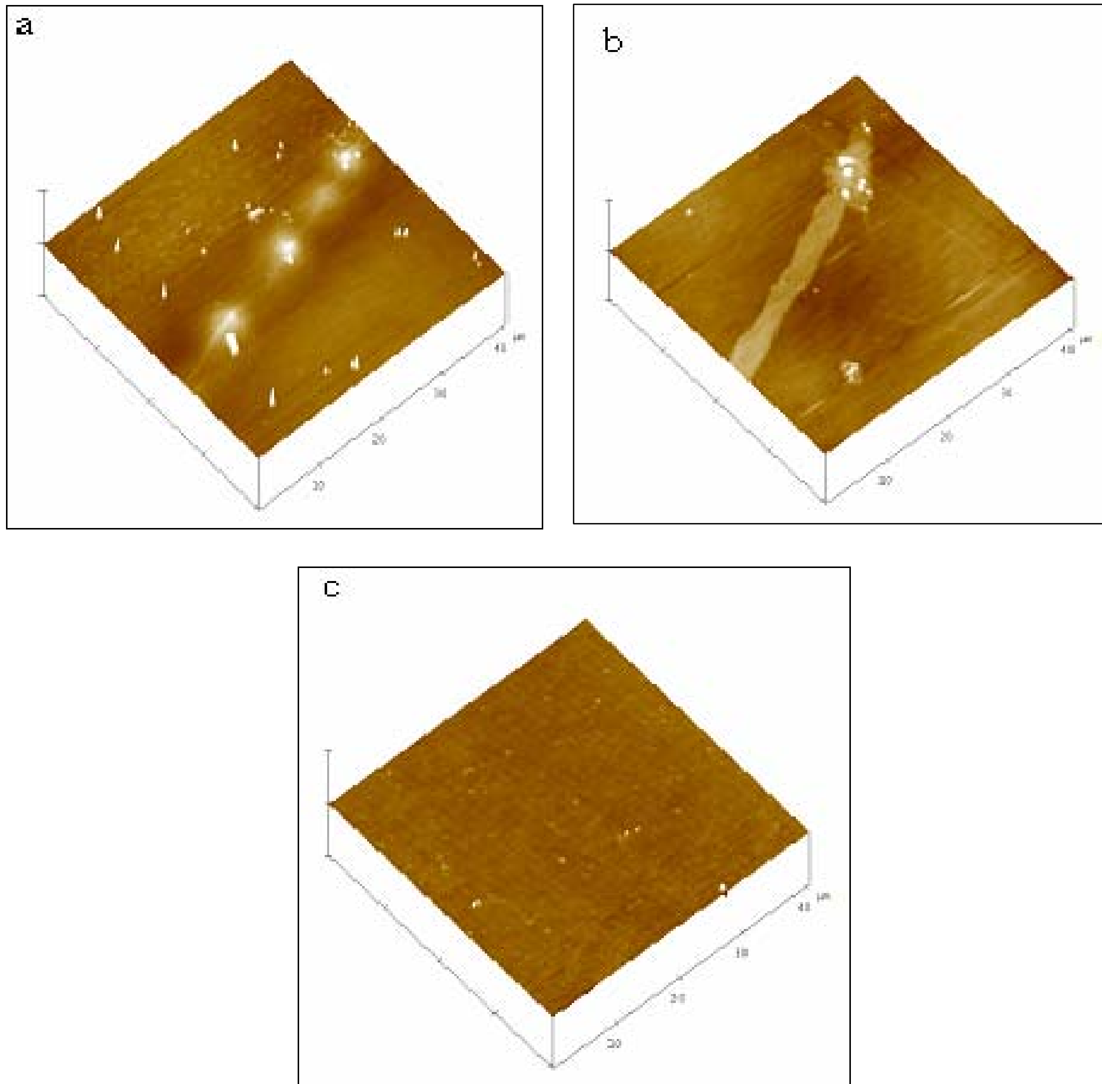


Figure 6.10 AFM images of wafers polished with (a) 0.25wt% $CeO_2$ (b) 0.5wt% $CeO_2$ nanoparticles and (c) composite particles

Additionally, AFM images in figure 6.10 show particle contamination on wafer surfaces polished with only ceria nanoparticles. The wafer polished with the composite is devoid of pitting and minor scratches. The above results clearly indicate that the composite particles with controlled softness/hardness can be potentially beneficial and



للاستشارات المنارة
www.manaraa.com

can be successfully implemented for polishing in the final stage of CMP process where only moderate amounts of material needs to be removed but superior surface quality is required.

## 6.4 Summary

Novel slurries based on hybrid particles consisting of polymer with inorganic component on the surface are successfully developed. The hybrid silica microgels resulted in superior surface finish as compared to the conventional silica particles. The hybrid particles resulted in lower coefficient of friction and lower particle residue as compared to the conventional silica particles. However, the oxide removal rates during CMP upon using the slurries made of hybrid particles are negligible. Improved surface finish, lower COF make these particles potential candidates for next generation stringent polishing requirements.

In order to improve the removal rate during oxide CMP, ceria particles were embedded into the hybrid microgels and also were incorporated onto the surface of the hybrid particles to form ceria hybrid composites. These hybrid composite particles resulted in moderate removal rates but at the same time did not compromise the surface quality. The oxide surface polished with the hybrid composites was superior when compared to the surface polished with conventional ceria particles. Such performance makes these particles potential candidates for CMP slurries to be used for next generation CMP processes.



المنارة للاستشارات
www.manaraa.com

# CHAPTER 7: SUMMARY AND FUTURE WORK

A detailed investigation of effect of temperature on Cu CMP process has been conducted in this dissertation. The effect of temperature not only on CMP process but also on the electrochemical, surface chemical analysis, coefficient of friction and pad conditioning process has been explored. Besides temperature, the effect of slurry flow rate on CMP process has also been studied. Finally, novel slurries are developed to reduce post CMP surface damage and friction during CMP process. All the above mentioned studies are summarized below.

## 7.1 Effect of temperature on CMP process

The effect of temperature on CMP process and interface tribology has been studied. This research demonstrated that the increase in removal rate during CMP due to an increase in temperature is not only due to increase in oxidation rate but also an increase in dissolution rate of the dissolvable surface copper oxides and hydroxides in to the slurry. It was noted that the increase in temperature did affect the surface quality as the scratch depth increased with increase in slurry temperature above room temperature. The temperature study on the patterned copper samples revealed that the non-uniformity in polish decreases from below room temperature to room temperature and then increases with increase in temperature. This along with surface quality shows that the polish was predominantly mechanical at lower temperatures. The surface mechanical properties did



المنارة للاستشارات
www.manaraa.com

not change due to polishing at different temperatures which suggests that the increase in coefficient of friction is mainly due to the change in contact area and pad surface asperity deformations. The study of coefficient of friction plotted as stribeck curves indicated no change in the polishing regime with a change in temperature. Further, the effect of temperature on coefficient of friction was studied at different process conditions, which revealed the existence of three distinct regimes of the effect of temperature, determined by the process parameters pressure and velocity. Thus, it was concluded that the change in coefficient of friction is mainly due to the change in pad surface asperity deformation and the change in contact area.

The effect of temperature was further studied on pad conditioning process which indicated an aggressive conditioning process at low temperatures but a rather ineffective conditioning process at elevated temperatures. However, the pad loss was found to be the most during conditioning at low temperatures and minimal pad loss was noted during conditioning at elevated temperatures. Thus, it was shown that temperature has a pronounced effect of pad conditioning process and an optimized setting of temperature is needed for each specific case depending on the process requirements. Also, the dishing on the post CMP surface after subsequent polishing at different pad conditioning temperatures was measured. It was found that the dishing increased with increase in pad surface temperature but the with-in wafer uniformity increased at the same time. This shows a significant difference in the area of contact at various pad surface temperatures.



المنارة للاستشارات
www.manaraa.com

## 7.2 Effect of slurry flow rate on CMP process

Thermal model to estimate wafer temperature as a function of thickness and radius of the wafer has been developed and the temperature on the wafer surface as a function of radius and thickness of the wafer has been estimated. From the finite element analysis of the model, slurry flow was shown to reduce the temperature rise on the surface, which in turn would reduce pattern effects on post CMP wafer surface.

A study of the effect of slurry flow rate on tribology during Cu CMP has been conducted. It was seen that the coefficient of friction decreases with increasing slurry flow rate and at the same time, the removal rate increases with increase in slurry flow rate. Post CMP surface characteristics indicated a decrease in dishing, erosion and metal loss with increasing slurry flow rate. Also, a smaller rise in pad surface temperature was noted at higher slurry flow rates. The above mentioned two results confirm the finding from pad conditioning studies that dishing increases with an increase in pad surface temperatures. These results suggest that maintaining the pad surface asperities at a constant temperature, dishing and erosion can be reduced to a considerable extent.

## 7.3 Novel slurry development for reduced surface defects

Also, low defect slurries using novel polymer based hybrid particles have been developed. The proposed slurries result in superior surface finish as compared to the surface finish obtained using the slurries containing conventional abrasive particles. Slurries containing polymer-silica hybrid particles even though gave a superior surface finish, they did not result in a substantial removal rate. Ceria particles were then



المنارة للاستشارات
www.manaraa.com

embedded onto the polymer silica hybrid particles. These particles resulted in generating a superior surface quality as compared to the conventional ceria particles and at the same time resulted in lower coefficient of friction. The removal rate obtained using the slurry consisting of polymer-silica-ceria particles even though was not as much when compared to the conventional ceria slurries, the coefficient of friction, surface damage and scratches following CMP were found to be much less. Thus, the slurries containing polymer particles prove to be potential slurries for the generating a superior surface after polishing sans any defects. Thus, these slurries provide a valuable solution for the next generation stringent CMP output requirements.

## 7.4 Future Work

There are several aspects of this research that could be extended to gain valuable in-sight into the process mechanisms and several methods of detecting defects *in-situ* can be improved. Slurry viscosity and its importance to CMP could be studied drawing the analogy of the working of a journal bearing to the CMP polishing interface.

### 7.4.1 Thermal model

Thermal model of the wafer along with carrier assembly needs to be developed to simulate the industry set up and to estimate the temperatures on the wafer which are more representative of the actual process temperature profiles. In the same context, steady state heat transfer thermal model of the polishing pad can also be developed, which can improvise the design and manufacturing of the polishing pad. Analytical model improvised by more realistic geometrical model along with pad model



المنارة للاستشارات
www.manaraa.com

supported by thermal imaging data on the wafer carrier and polishing pad could be extremely helpful.

### 7.4.2 Electrochemistry and impedance spectroscopy

Electrochemistry (potentiodynamic polarization) and Electrochemical Impedance Spectroscopy (EIS) studies can be conducted at different temperatures and for varying chemistries. The electrochemical study of different slurry chemistries at different temperatures will provide information about the dependence of oxidation and dissolution rates of various chemistries on slurry temperature. Such a study could be highly complimentary to the present research work.

### 7.4.3 Low defect slurry development

The novel low defect slurry developed using hybrid composite abrasives could be improved for its particle dispersion characteristics by adding appropriate additives and thereby improving the shelf life and possibly the removal rates of oxide CMP further. Thus developed slurries could be tested on STI (patterned) oxide wafers for their selectivity with the underlying nitride layer on STI wafers. A study on dishing and erosion during STI CMP could be conducted and the performance of hybrid abrasives be evaluated in comparison with conventional ceria particles. The applicability of these abrasive particles for copper CMP could also be evaluated as they provide relatively lower coefficient of friction as compared to the conventional particles, which could prove highly beneficial for next generation low pressure sensitive CMP of Copper/Low-K metallization stacks.



المنارة للاستشارات
www.manaraa.com

## REFERENCES


1. Gordon E. Moore, Cramming more components onto integrated circuits, Electronics, Volume 38, Number 8, April 19, (1965)

2. Internet website: http://www.itrs.net/Links/2006Update/FinalToPost/09_Interconnect2006Update.pdf © International Technology Roadmap for Semiconductors, Interconnects update, (2006).

3. Gordon Moore; Solid-State Circuits Conference, Digest of Technical Papers. ISSCC., IEEE International, vol.1, 20 – 23, (2003).

4. S.M. Sze, VLSI Technology, McGraw-Hill, (1983).

5. J.W. Mayer and S.S. Lau, Electronic Materials Science: For Integrated Circuits in Si and GaAs, Macmillan, (1990).

6. S. Thompson, M. Alavi, M. Hussein, P. Jacob, C. Kenyon, P. Moon, M. Prince, S. Sivakumar, S. Tyagi, M. Bohr, Intel Technology Journal Vol. 6 Issue 2, 5-13 (2002).

7. P B Zantye, Ph.D. dissertation, University of South Florida, (2005).

8. J.M. Steigerwald, S.P. Murarka, and R. J. Gutmann, Chemical Mechanical Planarization of Microelectronic Materials, Wiley, New York (1997).

9. Robert L. Rhoades, Evolution of CMP for New Applications and Materials, 210th ECS meeting, Cancun, Mexico (2006).

10. M Bakli, L Baud, H M'Saad, D Pique, P Rabinzohn, Microelectronic Engineering, 33, 175-188, (1997).

11. Z. Stavreva, D. Zeidler, M. P1otner, G. Grasshoff, K. Drescher, Microelectronic Engineering, 33, 249-257, (1997).

12. Intenet website, http://www.semiconductor.net/article/CA440787.html, L.V. Trotha, G. Mörsch and G Zwicker, Advanced MEMS Fabrication Using CMP, ©Semiconductor International, (2004).




المنارة للاستشارات

www.manaraa.com

13. Yong-Jin Seo, Woo-Sun Lee, Microelectronic Engineering, 75, 149–154, (2004).

14. International Technology Roadmap for Semiconductors, (2001).

15. J.M. Steigerwald, S.P. Murarka, R.J. Gutmann, D.J. Duquette, *Mater. Chem. Phys.,* 41, 217, (1995).

16. P. B. Zantye, A. Kumar and A. K. Sikder, *Mat. Sci. Eng. R,* 45, 3-6, 89, (2004).

17. Q. Luo, D.R. Campbell, S.V. Babu, *Thin Solid Films* , 311, 177–182, (1997).

18. Y Li and S. V. Babu, *Electrochemical and Solid-State Letters*, 4 (2) G20-G22 (2001).

19. Y. Ein-Eli, E. Abelev, E. Rabkin, and D. Starosvetsky, *Journal of The Electrochemical Society*, 150 (9) C646-C652 (2003).

20. R. Carpio, J. Farkas and R. Jairath, Thin Solid Films, 266, 238 – 244, (1995).

21. M.R.Oliver, Chemical-Mechanical Planarization of Semiconductor Materials, Springer series in Materials Science, Vol.69, (2003).

22. F. Preston, *J. Soc. Glass Tech*. 11, 214 (1927).

23. R. Stribeck. Zeit. Ver. Deut. Ing., Vol 46, pp 1341-1348, 1432-1438, 1463-1470, (1902).

24. Sharath Hosali and Eric Busch, Materials Research Society Symposium Proceedings, Spring (2005).

25. Scarfo, V. Manno, C. Rogers, S. Anjur and M. Moinpour, The Journal of Electrochemical Society, 152, (6), G477-G481, (2005).

26. J. Luo, PhD thesis, University of California, Berkeley, (2003).

27. N. Elbel et al, *J. Electrochem. Soc.*, Vol. 145, ( 5), May (1998).

28. W. Li, D.W. Shin, M. Tomozawa, S. P. Murarka, Thin solid films, 270, 601 – 606, (1995).

29. T. Nishioka, K. Sekine, Y. Tateyama, Proceedings of IEEE International Interconnect Technology Conference, IITC 99 – 89, (1999).

30. D. Castillo-Mejia, J. Kelchner and S. Beaudoin, Journal of The Electrochemical Society, 151 (4), G271-G278, (2004).




المنارة للاستشارات

www.manaraa.com

31. D. Castillo-Mejia, S. Gold, V. Burrows, and S. Beaudoin, Journal of The Electrochemical Society, 150, (2), G76-G82, (2003).

32. Gregory P. Muldowney and David B. James, Material Research Society Symposium Proceedings, Vol. 816, K5.2.1, (2004).

33. K. Ludema, Friction, Wear and Lubrication: A Textbook in Tribology. CRC Press, Inc.; (1996).

34. B. Bhushan, Introduction to Tribology. John Wiley & sons, Inc.; (2002).

35. Yuzhuo Li (edt), Microelectronic Applications of Chemical Mechanical Planarization. Wiley-Interscience publishers, ISBN: 9780471719199, (2007).

36. D. DeNardis, J. Sorooshian, M. Habiro, C. Rogers and A. Philipossian, Jpn. J. Appl. Phys. Vol. 42, 6809–6814, (2003).

37. Philipposian and S. Olsen, Japan Journal of Applied Physics, 42, 6371-6379, (2003).

38. T. Das, R. Ganesan, A. Sikder, and A. Kumar, IEEE Transactions on Semiconductor Manufacturing, 18, (3), 440-447, (2005).

39. N. Gitis. Tribology Issues in CMP, Semiconductor Fabtech, 18th Edition., 125-128, (2003).

40. Z. Li, L. Borucki, I. Koshiyama, and A. Philipossian, *J. Electrochem. Soc.*, 151, 7, G482-G487, (2004).

41. J. Sorooshian, D. DeNardis, L. Charns, Z. Li, F. Shadman, D. Boning, D. Hetherington, and A. Philipossian, Journal of The Electrochemical Society, 151, G85, (2004).

42. P. Renteln and T. Ninh, Materials Research Society Symposium Proceedings, 566, 155, (1999).

43. L. Borucki, L. Charns, and A. Philipossian, Abstract 918, The Electrochemical Society Meeting Abstracts, Vol. 2003-2, Orlando, FL, Oct 12-16, (2003).

44. L. Borucki, Z. Li, and A. Philipossian, Journal of The Electrochemical Society, 151, G559 (2004).

45. D. White, J. Melvin, and D. Boning, Journal of The Electrochemical Society, 150, G271, (2003).



المنارة للاستشارات
www.manaraa.com

46. Y. L. Wang, C. Liu, M. S. Feng and W. T. Tseng, Materials Chemistry and Physics, 52, 17-22, (1998).

47. H Hocheng, Y-L Huang, and L-J Chenb, Journal of The Electrochemical Society, 146, (11), 4236-4239, (1999).

48. J Cornely, C Rogers, V Manno and A Philipossian, Materials Research Society Symposium. Proceedings, Vol. 767, F1.6.1, (2003).

49. Y Sampurno, L Borucki, Y Zhuang, D Boning, and A Philipossian, Journal of The Electrochemical Society, 152, (7), G537-G541, (2005).

50. V. Nguyen et al, *Microelec. Eng.,* 50, 403–410, (2000)

51. Shih-Hsiang Chang, *Microelec. Eng*., 77, 76–84,(2005)

52. Internet Website: http://www.semiconductor.net/article/CA456650.html, Peter Singer, © Semiconductor International, (2004).

53. Muthukkumar Kadavasal, Sutee Eamkajornsiri, Abhijit Chandra and Ashraf Bastawros, Materials Research Society Symposium Proceedings, Spring (2005).

54. C.L. Borst, W.N. Gill and R.J. Gutmann, Chemical–Mechanical Polishing of Low Dielectric Constant Polymers and Organosilicate Glasses: Fundamental Mechanisms and Application to IC Interconnect Technology, Kluwer Academic Publishers, Boston (2002).

55. Alex A. Volinsky, William W. Gerberich, Microelectronic Engineering, 69, 519–527, (2003).

56. L.Y. Yang, D.H. Zhang, C.Y. Li, R. Liu, A.T.S. Wee, P.D. Foo, Thin Solid Films, 462–463, 182– 185, (2004).

57. Shou-Yi Chang , Hui-Lin Chang , Yung-Cheng Lu , Syun-Ming Jang, Su-Jien Lin, Mong-Song Liang, Thin Solid Films, 460, 167–174, (2004).

58. S. Balakumar, X.T. Chen, Y.W. Chen, T. Selvaraj, B.F. Lin, R. Kumar, T. Hara, M. Fujimoto, Y. Shimura, Thin Solid Films, 462–463, 161– 167, (2004).

59. Lu Shen, Kaiyang Zeng, Microelectronic Engineering, 71, 221–228, (2004).

60. Y.H. Wang, M.R. Moitreyee, R. Kumar, S.Y. Wu, J.L. Xie, P. Yew, B. Subramanian, L. Shen, K.Y. Zeng, Thin Solid Films, 462–463, 227– 230, (2004).

61. Jeff lee from zantye's , J.A. Lee, M. Moinpour, H.-C. Liou and T. Abell, Proceedings of Materials Research Society San Francisco, CA, p. F7.4. (2003).



المنارة للاستشارات

www.manaraa.com

62. D. Zeidler, Z. Stavreva, M. Plotner, and K.Drescher, *Microelectron. Eng.,* 33, 259, (1997).

63. T. Du., A. Vijayakumar, V. Desai, *Electrochim. Acta*, 49, 4505, (2004).

64. Y. Ein-Eli, E. Abelev, and D. Starosvetsky, *J. Electrochem. Soc.*, 151 (4), G236, (2004).

65. A.Nishi, M.Sado, T.Miki and Y.Fukui, *Appl. Surf. Sci.,* 203-204, 470, (2003).

66. T. Du , D. Tamboli, V. Desai, *Microelectron. Eng.*, 69, 1, (2003).

67. J. Sorooshian, D. Hetherington and A. Philipossian, *Electrochem. Solid State Lett.*, 7 (10), G222, (2004).

68. N. Gitis and M. Vinogradov, *Proceedings of 2nd ICMI, Santa Clara*, CA (2001).

69. A. K. Sikder, F. Giglio, J. Wood, A. Kumar and M. Anthony, Journal of Electronic Materials, Vol. 30 (12), pp 1520-1526, (2001).

70. Internet website: www.atdf.com/waferservices/docs/854Doc.pdf, © International Sematech.

71. Kojima and M.Kurahashi, *J. Electron. Spectr. Rel. Phen*. 42, 177, (1987).

72. W. Li, D. W. Shin, M. Tomozawa, S. P. Murarka, *Thin Solid Films* 270, 601, (1995).

73. B. Mullany, G. Byrne, *J. Mater. Process. Technol.*, 132, 28, (2003).

74. H.J. Kim, H.Y. Kim, H.D. Jeong, E.S. Lee, Y.J. Shin, *J. Mater. Process. Technol.*, 130–131, 334, (2002).

75. S. Mudhivarthi, Parshuram Zantye, Ashok Kumar, and J Y Shim, Materials Research Society Symposium Proceedings, Vol. 867, W1.5.1 (2005).

76. W. C. Oliver, G. M. Pharr, MRS Bull. 17, 28-33 (1992).

77. G.M. Pharr, Mater. Sci. Eng. A253, 151, (1998)

78. S. Mudhivarthi, V. Kakireddy, J. Banerjee, and A. Kumar, Proceedings of ASME/STLE International Joint Tribology Conference, IJTC2006-12307, Texas (2006).

79. T. Doy, K. Seshimo, K. Suzuki, A. Philipossian and M. Kinoshita, Journal of The Electrochemical Society; 151 (3): G196-G199, (2004).



المنارة للاستشارات
www.manaraa.com

80. G. Muldowney, Material Research Society 2004; K5.3.1-k5.3.6.

81. Z. Li, K. Ina, P. Lefevre, I. Koshiyama and A. Philipossian, Journal of The Electrochemical Society, 152 (4): G299-G304, (2005)

82. G. Basim and B. Moudgil, Journal of Colloid and Interface Science 2002; 256: 137-142.

83. W. Choi, U. Mahajan, S. Lee, J. Abiade, and R. Singh, Journal of The Electrochemical Society, 151 (3), G185-G189, (2004).

84. S. Mudhivarthi, P. Zantye, A. Kumar, A. Kumar, M. Beerbom, and R. Schlaf. Electrochemistry and Solid-State Letters, 8, (9), G241-G245, (2005).

85. S. Mudhivarthi, N. Gitis, S. Kuiry, M. Vinogradov and A. Kumar, Journal of The Electrochemical Society, 153, 5, G372-G378, (2006).

86. Bowden and Tabor, The Friction and Lubrication of Solids, Oxford university press, (1964).

87. P. Zantye, A. Kumar and J. Yota, 207th ECS meeting, Quebec, Canada (2005).

88. P. Zantye, A. Kumar, W. Dallas, S. Ostapenko, A. Sikder, J. Vac. Sci. Technol. B, vol. 24, pp 1, (2006).

89. Maria Ronay, Journal of The Electrochemical Society, 151, (12), G847-G852, (2004).

90. S. Mudhivarthi, V. Kakireddy, A. Kumar, Y. Obeng, 210th ECS meeting transactions, E5-1155, Cancun, Mexico, (2006).

91. J. Sorooshian, D. DeNardis, L. Charns, Z. Li, D. Boning, F. Shadman, and A. Philipossian, in Proceedings of the 2003 CMP-MIC, IMIC, pp. 43-50, (2003).

92. S. Seal, S.C. Kuiry and B. Heinmen, Thin Solid Films, 423, 243–251, (2003).

93. Y. Obeng, J. Ramsdell, S Deshpande, S. Kuiry, K. Chamma, K. Richardson, and S. Seal, IEEE Transactions on Semiconductor Manufacturing, Vol. 18, No. 4, pp 688-694, (2005).

94. N. Gitis et al, US Patent 6,702,646 (2004).

95. M. Özisik, Heat Conduction, 2nd ed., Chapter 3: pp.99-153. John Wiley and Sons, N.Y., (1993).



المنارة للاستشارات

www.manaraa.com

96. Bejan, Convection Heat Transfer, 2nd ed., Append. B: pp.585-594, John Wiley and Sons, N.Y., (1995).

97. J. Lu, C. Rogers, V. Manno, A. Philipossian, S. Anjur and M. Moinpur, The journal of The Electrochemical Society, 151, (4), G241-G247, (2004).

98. S. Runnel and L. Eyman. The Journal of Electrochemical Society, 141, 1698, (1994).

99. A. K. Sikder, Swetha Thagella, Ashok Kumar, and Jiro Yota, J. Mater. Res., 19 (4), 996, (2004).

100. P. Zantye, S. Mudhivarthi, and A. Kumar, Y.S. Obeng, J. Vac. Sci. Technol.- A., 23 (5), 1892, (2005).

101. A. K. Sikder, I. M. Irfan, Ashok Kumar, A. Belyaev, S. Ostapenko, M. Calves, J. P. Harmon and J. M. Anthony, Mat. Res. Soc. Sym. Proc., 670, M1.8.1-7, (2001).

102. A. K. Sikder, P. Zantye, S. Thagella, Ashok Kumar, B. Michael Vinogradov, and Norm V. Gitis, Proc. 8$^{th}$ CMP-MIC Conf., 120, (2003).

103. A.K. Sikder, P. Zantye, S. Thagella and Ashok Kumar, Mat. Res. Soc. Sym. Proc. 767, F7.3 (2003).

104. R. Ganesan, T. K. Das, A. K. Sikder and A. Kumar, IEEE Trans. Semicond. Manuf., November, (2003).

105. L. Zhang, S. Raghavan, M. Weling, J. Vac. Sci. Technol. B 17.5., 2248, (1999).

106. T. Y. Teo, W. L. Goh, V. S. K. Lim, L. S. Leong, T. Y. Tse, and L. Chan, J. Vac. Sci. Technol. B 22.1., 65, (2004).

107. A. Jindal, S. Hegde, and S. V. Babu, Electrochemistry and Solid-State Letters, 5 (7), G48, (2002).

108. J.Song, Y Chen, S. Lee, W.C. Chiou, T.C. Tseng, H.H. Kuo, C. J. Chuang, K.C. Lin, S.M. Jang, and M.S. Liang, *Symposium of VLSl Technology. Digest of Technical Papers*, 9B-1, 123, (2003).

109. P. Wrschka, J. Hernandez, G S. Oehrlein, J. A. Negrych, G. Haag, P. Rau and J. E. Currie, *The Journal of Electrochemical Society*, 148, (6), G321, (2001).

110. K. Cheemalapati, A. Chowdhury, V. Duvvuru, Y. Lin, K. Tang, G. Bian, L. Yao, and Y. Li, *Materials Research Society Symposium Proceedings*, 816, K1.7.1., (2004).



المنارة للاستشارات
www.manaraa.com

111. Yong-Jin Seo, Woo-Sun Lee, Pochi Yeh, Microelectronic Engineering 75, 361–366, (2004)

112. D. Evans, *Materials Research Society Symposium Proceedings 816*, 245, (2004).

113. S. Mudhivarthi, C. Coutinho, A. Kumar, V. Gupta, 210th ECS meeting transactions, E5-1143, Cancun, Mexico, (2006).

114. J. Lee, B. Yoon, S. Hah, J. Moon, *Materials Research Society Symposium Proceedings, 671*, M5 3/1, (2001).

115. Y. Tateyama, T. Hirano, T. Ono, N. Miyashita and T. Yoda, *Proceedings - Electrochemical Society*, *2000-26*, 297, (2001).

116. N. Koyama, T. Ashisawa and M. Yoshida, *Application: JP Patent 98-2863562000109814*, (2000).

117. M. Das, N. Sanson, D. Fava and E. Kumacheva, *Langmuir, 23*, 196, *(*2007).

118. X. Xia and Z. Hu, *Langmuir, 20*, 2094, (2004).

119. C. Coutinho and V. Gupta, *Journal of Colloid and Interface Science, 315*, 116, (2007).

120. M-S. Kang and V. Gupta, *Journal of Physical Chemistry B, 106*, 4127, (2002).



www.manaraa.com

## ABOUT THE AUTHOR

Subrahmanya Mudhivarthi was born in 1980 in the state of Andhrapradesh located in Southern part of India. The author received his Bachelor's degree in Mechanical Engineering in 2001 from Sri Krishnadevaraya University, India. He then pursued his Master's studies in the field of Tribology under the guidance of Dr. Daniel Hess and received his Master of Science in Mechanical Engineering degree at University of South Florida, Tampa in the December of 2003. He then joined Dr. Ashok Kumar's group in 2004 to pursue doctoral studies in the area of Chemical Mechanical Planarization. During his doctoral studies the author has worked as a Graduate Intern at Center for tribology Inc. and Intel Corporation. The author is a member of the Tau Beta Pi honor society for engineers and American Society of Mechanical Engineers.



المنارة للاستشارات
www.manaraa.com